ROR1-TARGETED ADOPTIVE IMMUNOTHERAPIES

University College London

A Thesis Presented for the Degree of Doctorate in Philosophy

Micaela Harrasser

September 2019

Declaration

I, Micaela Harrasser, confirm that the work presented in this thesis is my own. Where information has been derived from other sources, I confirm that this has been indicated in the thesis.

Acknowledgements

First, I would like to thank Andrew. My rock throughout the whole journey. You have always been there for me, and still are! I cannot thank you enough for this. I would also thank my parents, endless source of support. It is to you three that I dedicate this milestone, as you have been essential for the completion of this PhD. To my best friends, or extended family (Fede, Elly, micia, Eli, Leila, Ila, Shiori): thank you so much for your help, support, advice, laughter and drinks, all very much needed.

I would like to thank my supervisor Amit, for giving me the chance to undertake this challenging yet rewarding experience. To my colleagues, current and former, for the vital help and support: Sat, Marco, Rachel, Doyoung, Vincent, Sol, Su. To my fellow PhD student gal pals, thank you for the chats and drinks, you made this journey much more fun! Also, to everyone in the Cancer Institute who have helped me with experiments, scientific discussions and chats.

Abstract

The tumour antigen ROR1 plays a critical role in tumorigenesis and is overexpressed in several haematological and solid malignancies including triple negative breast cancer (TNBC) and non-small cell lung cancer (NSCLC). Its absence on most of healthy tissues makes it an attractive target for cancer immunotherapy.

Cancer immunotherapy has opened a new era of cancer treatments. Successful examples include therapeutic antibodies (e.g. Rituximab, and immune checkpoint inhibitors) and adoptive cell therapy with engineered T cells expressing a Chimeric Antigen Receptor (CAR), particularly against haematological malignancies.

CAR-T cells have so far had limited success against solid tumours. Overexpression of inhibitory receptor ligands such as PD-L1 by tumour cells is one of the main mechanisms that makes the anti-tumour immune response ineffective.

We developed a second generation ROR1-41BB-CD3ζ CAR targeting ROR1. These CAR-T cells rapidly acquired a phenotype associated with increased expression of programmed death receptor 1 (PD-1) following exposure to ROR1-expressing tumour targets. To bolsters potency, we engineered the lentiviral CAR construct to enable IL-2 mediated, NFAT-induced secretion of anti-PD-1 single-chain variable fragments (scFv) within the tumour environment following CAR T-cell activation. Local secretion of anti-PD1 scFv led to increased anti-tumour activity against TNBC and NSCLC tumour cell lines in *in vitro* co-culture studies. In a murine xenograft model of TNBC, tumour growth was significantly decreased and associated with a significant survival benefit compared to parental ROR1 CAR-T cells and to combination therapy with ROR1 CAR-T cells and anti-PD1 monoclonal antibody. Thus, second-generation CAR T cells engineered to secrete anti-PD-1 scFv shows promise and represents a clinically relevant approach to improving potency of CAR-T cells against solid tumours whilst limiting toxicities associated with systemic administration of monoclonal antibody-mediated checkpoint inhibition.

Impact Statement

Adoptive cell therapy with engineered T cells expressing a Chimeric Antigen Receptor (CAR) have shown unparalleled therapeutic results, particularly against haematological malignancies in patients that were relapsed or refractory to conventional treatments.

However, CAR-T cell therapy is still struggling to achieve the same results in the context of solid tumours. Overexpression of inhibitory receptor ligands (PD-L1) by tumour cells is one of the key mechanisms that hampers anti-tumour immune responses.

Breast cancer is the most common malignant disease in women in developed countries. The triple-negative breast cancer (TNBC) subtype is characterised by a highly aggressive and metastatic phenotype; this, combined with the lack of effective treatment, makes the prognosis dismal. The tumour antigen ROR1 plays a critical role in tumour growth and metastasis. Despite being expressed at low level on some healthy tissues, its overexpression on an array of tumours (including TNBC) make it a promising therapeutic target.

We developed a monotherapy approach where our second-generation ROR1-targeted CAR-T cells secrete checkpoint blockade molecules within the tumour environment following activation by ROR1-expressing tumours. The efficacy of these CAR T cells was better than that achieved by parental format and by combination therapy with ROR1 CAR-T cells and anti-PD1 monoclonal antibody.

We believe this strategy has great potential and can be tailored with the desired secreted molecule, including but not limited to other checkpoint inhibitors, to act directly on tumours or on bystander immune cells. Overall, we believe this strategy has the potential to improve the potency and specificity of the immune response against solid tumours with high unmet therapeutic need such as TNBC, making a meaningful impact on patient survival and quality of life.

Abbreviations

ACT Adoptive cell therapy
APC Antigen presenting cell
BiTE Bispecific T Cell Engager
BsAb Bispecific antibody
CAR Chimeric Antigen Receptor
CLL Chronic lymphocytic leukaemia
CRS Cytokine release syndrome
CTLA-4 Cytotoxic T-Lymphocyte Antigen 4
DLBCL Diffuse large B cell lymphoma
EGFR epidermal growth factor receptor
ELISA Enzyme linked immunosorbent assay
EMA European Medicine Agency
FACS Fluorescent activated cell sorting
Fab Fragment antigen-binding
FBS Foetal bovine serum
FDA US Food and Drug administration
GD2 Disialoganglioside
GvHD Graft versus host disease
GvL Graft versus leukaemia/lymphoma
HLA human leukocyte antigen
i-CAR CAR-T cells secreting anti-PD1 scFv
IFNγ Interferon γ
IHC Immunohistochemistry
IL-2 Interleukin 2
ip Intraperitoneal
IS Immunological synapse
iv Intravenous
kDa kilo Daltons
LAG-3 Lymphocyte-activation gene 3
MFI Mean fluorescent intensity
MHC Major Histocompatibility complex
mAb Monoclonal Antibody
NFAT Nuclear factor of activated T cells
NHL Non-Hodgkin's lymphoma
NK Natural killer (cells)
NSCLC Non-small cell lung cancer
NSG Nod SCID gamma
PBMCs Peripheral Blood mononuclear cells
PD-1 Programmed cell death receptor
PD-L1 Programmed cell death receptor-Ligand 1
PDX Patient derived xenograft
PGK Phosphoglycerate kinase
ROR1 Receptor tyrosine kinase like orphan receptor 1
scFv Single chain variable fragment
SPR Surface plasmon resonance
TAA Tumour associated antigen
TCR T cell receptor
TILs Tumour infiltrating lymphocytes
TIM-3 T-cell immunoglobulin and mucin-domain containing-3
TK Tyrosine kinase
TNBC Triple negative breast cancer
TNF Tumour necrosis factor
Treg Regulatory T cell
TSA Tumour specific antigen
VEGF Vascular endothelial growth factor

Table of Contents

Table of figures:

Table of tables:

Chapter 1 Introduction

The role of the immune cells is to detect and respond to deviations and pathologic insults in our body, a process defined as immunological surveillance. When immunological surveillance fails, many complex diseases such as autoimmunity and cancer arise (1).

Tumours are highly complex mixtures of normal and neoplastic cell types, including immune cells (2). In the context of solid tumours, the immune response arises in the early stages of tumorigenesis, where highly proliferating cells exhaust all nutrients and release chemokines such as vascular endothelial growth factor (VEGF) to promote angiogenesis. This usually attracts immature myeloid cells which start the process of tissue repair as if this was a wound. These myeloid cells could be either immunosuppressive (in the absence of immunogenic stimulus) or immunogenic, with the ability to phagocyte, process and present tumour proteins to T cells (3).

An insight into the physiology of the canonical T cell response will be described in the following section to provide the underlying mechanistic concepts that have supported the development of T-cell based immunotherapies, the subject of this project.

1.1 The T cell-mediated response

The maximal activation of naïve T cells via recognition of their cognate MHC:peptide complex requires both antigen presentation ('signal 1' through the T cell receptor (TCR)-CD3 complex) and a costimulatory signal sent through co-receptors ('signal 2') such as CD28 interacting with its ligands CD80 (B7-1) or CD86 (B7-2) on antigen presenting cells (APCs); to ensure T cell differentiation and survival, 'signal 3' is given via cytokine receptors on the T cell (Figure 1-1) (4). Signal 2 is essential to prevent T cell anergy (5-8). Given the fact that virtually every nucleated cell in the body expresses MHC class I (MHC-I) molecules, MHC-I-restricted T cells should theoretically be able to directly recognise many types of tumour cells. Alternatively, APCs

such as dendritic cells (DC) and macrophages can process exogenous peptides and present them to T cells within the lymph node via MHC class II molecules, or in the context of MHC-I molecules via cross-priming (9-11).

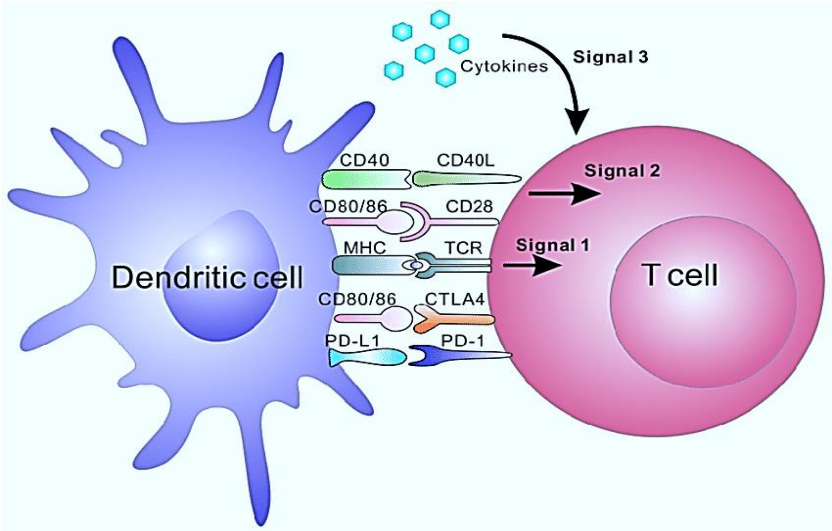

Figure 1-1 T cell activation via signal 1-3. Antigen presentation from a dendritic cell leads to multiple receptor-ligand interactions: MHC:peptide with the TCR, or signal 1, CD80/CD86 with CD28 for signal 2 (or co-stimulation) and cytokine signalling (signal 3).

At the molecular level, signal 1 starts several signalling events that lead to the activation of the mitogen-activated protein kinases (MAPKs) ERK and JNK (12) which play a role in several cellular processes such as proliferation, differentiation, motility, apoptosis and survival. In parallel, the release of calcium ions from the endoplasmic reticulum (ER) induces translocation of the transcription factors NFAT and CREB, which in turn increase IL-2 transcription to enhance proliferation and cytokine production. For signal 2, CD28 intracellular domain activates downstream kinases such as AKT which boosts proliferation and survival via mTOR pathway, and PKCθ which activates NF-κB and MKK7, required for IL-2 production. Activation of both AKT and PKCθ is essential to gain full proliferative and effector functions (Figure 1-2) (13).

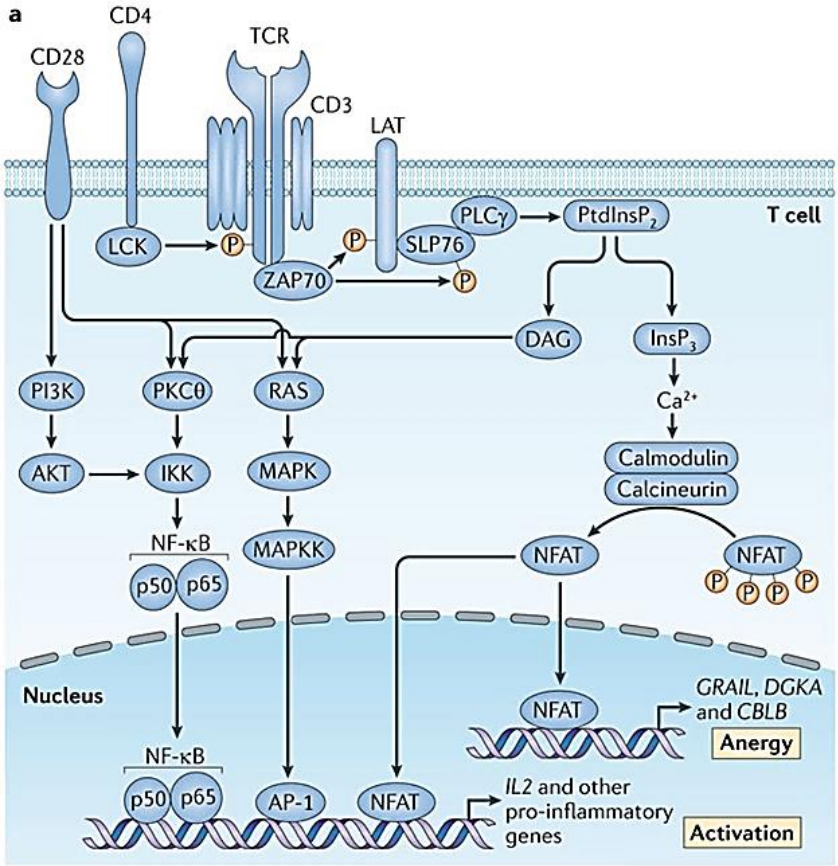

Figure 1-2 T cell activation signalling pathways. Schematic representation of key intracellular signalling molecules involved in canonical T cell activation. Adapted from: KN Pollizzi and JD Powell. Nature Reviews Immunology (2014)

Upon antigen recognition, activated T cells undergo clonal expansion in secondary lymphoid tissues then migrate towards the location of the recognised antigen (14) to perform their effector functions (direct, or by helping other immune cells) to eliminate the target cell (15). When successful, in the context of cancer, this leads to clearance of tumour subpopulations and a reduction in tumour burden (16). Against tumour cells, CD8+ cytotoxic T cells may exert direct cytotoxic responses either via expression of apoptosis-inducing molecules or by releasing cytotoxic granules such as perforin and granzyme. Mature CD8+ T cells and some CD4+ T cells produce interferon-γ (IFNγ) and tumour necrosis factor (TNF), which in turn enhance the anti-tumour response via upregulation of both MHC class I and II on both cancer cells and tumour-resident APCs (11). Pre-clinical and clinical data highlighted that the differentiation stage of CD8+ T cells is inversely related to their proliferative capacity and persistence following adoptive transfer. This

suggests that the CD8+ T cell stage at the time of the treatment appears to be crucial for the success of T cell-based therapies. Following antigenic stimulation, the T cell progresses from naïve cell to a terminally differentiated memory T cell, which is capable of eliciting a quick effector response with increased release of cytotoxic granules, but loses the ability to produce IL-2 (essential for T cell proliferation), to home lymph nodes and to resist apoptotic death (Figure1-3) (17-19). To note, the two late memory stages are reportedly very different for the anti-tumoral response, where central memory T cells (TCM) are more persistent and elicit better anti-tumour responses than effector memory (TEM) (20, 21).

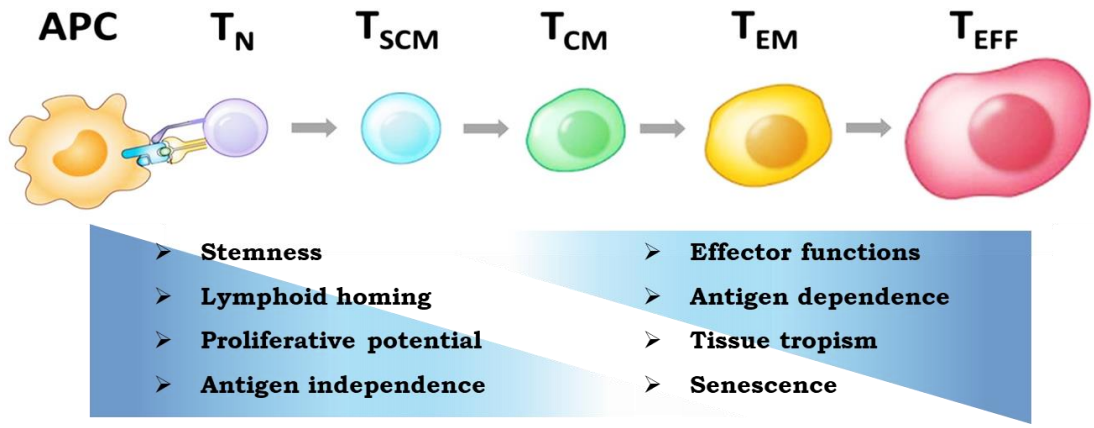

Figure 1-3 T cell differentiation stages. Upon antigen recognition, T cells undergo serial activation stages characterised by different features; these stages may be used for better design and characterisation of adoptive T cell therapies. T_N=naïve; T_{SCM}=T stem cell; T_{CM}=central memory T cell; T_{EM}=effector memory T cell; T_{EFF}=effector T cell. Adapted from Nicholas P. Restifo Blood 2014;124:476-477

In the context of chronic diseases like chronic viral infections and cancer, persistent antigen and chronic TCR stimulation can occur. These chronically stimulated T cells can undergo exhaustion (22).

Exhausted cells are hypofunctional and present altered effector functions, such as decreased proliferative potential and cytokine production, and sustained high expression of multiple inhibitory receptors (22, 23). In the context of chronic viral infections, the loss of effector functions usually starts from hampered IL-2 production, proliferative capacity, and ex vivo cytolytic

activity; this is then followed by impaired production of tumour necrosis factor (TNF)-α, interferon (IFN)-γ, and degranulation (24). In cancer, similar changes are observed but given the different tumour types, it is still unclear how the hierarchy of dysfunction evolves for exhausted TILs (24).

Importantly, these cells are not totally inert and can still mount an effector response against a pathogen (25). Moreover, exhausted T cells differ from dysfunctional primed T cells, lacking effector functions which makes them unable to control tumour growth, and from anergic naïve T cells (22).

Recent studies in murine and human cancers suggest that tumour infiltrating T cells display a broad spectrum of (dys-)functional states which are influenced by a range of immunosuppressive signals which include inhibitory ligands, inhibitory cell subsets like regulatory T cells (Tregs) and myeloid-derived suppressor cells, metabolic factors and suppressive soluble mediators (24, 26). One example of the latter is the release of immunoregulatory cytokines. Sawant et al described how Treg-derived IL-10 and IL-35 can cooperatively promote CD8+ T cell exhaustion by upregulating several inhibitory receptor expression (PD-1, TIM-3, LAG-3), limiting differentiation into a memory phenotype and downregulating effector functions (27). These inhibitory effects were reversed by co-targeting IL-10 or Treg cells with checkpoint blockade (27).

The second major group of T cells is made of CD4-expressing T cells. Naïve $CD4^+$ T cells undergo differentiation into various T cell subsets which are characterized by their ability to produce key cytokines to stimulate and regulate many aspects of innate and adaptive immune responses (28). The effector functions of CD4+ T helper cells crucially depend on their polarization which is under the control of key transcription factors (29). Examples of these functions include IFNγ and IL-2 production and the engagement and licensing of APCs which in turn can recruit additional CD8+ T cells to the tumour site (30-32). On the other hand, regulatory T cells (Tregs) have strong immunosuppressive functions and can contribute to T cell exhaustion and anergy in the tumour microenvironment (TME) by producing anti-inflammatory cytokines like IL-4 and IL-10 (33-35). There

is mounting evidence that considerable plasticity exists within T helper cell subsets *in vivo*, especially during responses to pathogens (36). Cytotoxic CD4+ T cells exert their effector functions by secreting granzyme B and perforin and can kill the targeted cells in an MHC class II-restricted manner.

Great advances in genetic engineering and synthetic biology combined with the feasibility of isolation, editing and transfer of immune cells, give us the skills and tools to reprogram and enhance the function of immune cells to generate effective immunotherapy-based strategies (1).

1.2 Cancer immunotherapy

In the past few years enormous progress has been made in understanding tumour biology and immunological responses, creating a new and promising cancer treatment named immune-based cancer therapy or cancer immunotherapy (37, 38). It can be defined as the manipulation of immune cells, particularly T cells, to generate a better anti-tumour response (39).

For the purpose of this thesis, adoptive T-cell therapy (ACT) and therapeutic antibodies (mainly as checkpoint inhibitors), which are two of the main forms of cancer immunotherapy, will be discussed in detail.

1.2.1 Adoptive Cell Therapy

Adoptive cell therapy (ACT) relies on the ability to generate *ex-vivo* large numbers of specific T cell populations for the treatment of malignant and infectious diseases, as well as autoimmunity. Preconditioning of the patient via lymphodepletion using chemotherapy with or without radiotherapy, has shown to facilitate persistence of the transferred T cells and to improve therapeutic responses (40). Pioneering research by Rosenberg and colleagues showed for the first time the potential of using the endogenous anti-tumour immunity for therapeutic purposes. They showed that tumour infiltrating lymphocytes (TILs) could be isolated from tumours, expanded and re-infused into the patient eliciting therapeutic effects in metastatic melanoma

resections, leading to objective clinical response rates up to 50% for refractory patients (41, 42).

Successful examples of ACT, either with naturally occurring or with gene edited T cells, include:

Ex vivo expansion of Tregs, which showed promising results against Crohn's disease (64) and is currently being investigated to treat type 1 diabetes (65).

Donor leukocyte infusions, which can be used to generate a graft-versus leukaemia (GvL) effect against certain haematological malignancies such as chronic myeloid leukaemia (43).

Administration of ex-vivo expanded TILs, which showed remarkable anti-tumoral effect against metastatic melanoma (44).

The main limitations of TIL therapy include: inaccessible or unresectable tumours, 'cold' malignancies with very poor immune cell infiltrate and the characteristic exhausted phenotype of terminally differentiated TILs (45, 46).

1.2.1.1 ACT side effect: GvHD

The ever evolving technologic and therapeutic advances in the field of cellular engineering offers multiple promising options for cancer immunotherapy, despite novel hazards that often arise at the same time. In the context of ACT, the main risks are dosage, target specificity, and the potential of undetected and uncontrolled expansion of therapeutic product. One of the most common ACT-derived toxicities is graft versus host disease or GvHD, which we will briefly describe in the context of T cell therapy.

GvHD is the most serious complication following graft of immunologically competent mediators such as T cells (47). GvHD is a sever multi-inflammatory reaction, involving several organs with apparent clinical manifestation to the skin, gastrointestinal tract and liver. Despite therapeutic

advances, it remains a potentially lethal toxicity as patients may be refractory to curative agents like corticosteroid or immunosuppressive cocktails, or may develop infections (48-50).

GvHD results from T cells recognising non-self MHC molecules (allorecognition). In case of transplants with mismatched human leukocyte antigen (HLA), T cell-mediated responses against both HLA-derived epitopes and peptide-HLA complexes may occur. Moreover, GvHD responses may also result from a matched donor transplant (51), for instance when the conformational structure generated by alternative epitopes is similar to another TCR-peptide-MHC interaction that would lead to activation (52). Several strategies have been designed to prevent progression of GvHD, including selective removal of alloreactive T cells (53), low dose of IL-2 to boost Treg activity (54), and ex-vivo induction of anergy of patient-responsive T cells (55).

1.2.1.2 TCR Engineered cells

The greatest and most promising advances in synthetic immunology come from the genetical engineering of a patient's own T cells to allow direct recognition of cancer cells. The two main approaches for redirecting T cells are TCR engineered cells and Chimeric Antigen Receptor (CAR) T cells (1).

Using viral transduction, T cells can be edited to express different TCR α and β chains to provide the desired specificity towards tumours expressing common tumour antigens and presented by appropriate MHCs. Proof of concept was first demonstrated with the isolation and transfer of the α and β chains from one cytotoxic T cell clone to another (56). This strategy was then tested against several antigens in haematological and solid malignancies (57) with a recent trial against NY-ESO-1 reporting 58% overall response rate (58). TCR gene therapy, as opposed to CAR-T cell therapy, can recognise intracellular targets such as Wilms tumour 1 and p53, as well as surface antigens presented by the MHC. Moreover, signalling through the TCR is particularly sensitive with 10-100 MHC-peptide complexes capable of triggering T cell activation (59).

Despite promising therapeutic results, TCR gene therapy faces challenges and risks. One challenge is the diversity of HLA alleles, as some patients may not be able to present the same neoantigens and elicit a T cell response (1). A major concern is the pairing of the correct TCR α and β chains to avoid mismatches (e.g. cross-pairing of endogenous and transgenic chains) that could generate altered T cell specificity which could lead to pathological auto-reactivity as reported in mouse experiments (60). Even with the correct targeted specificity, the choice of the right targeted antigen requires very careful planning to avoid treatment-related devastating consequences. The MAGE-A3 clinical trial offers a key example: MAGE-A3 TCR-engineered cells cross-reacted with a muscle-specific peptide, causing severe myocardial damage that ultimately led to death by cardiac shock within a few days of treatment (61). Other examples of on-target off tumour toxicities towards healthy tissues involved the tumour associated antigens (TAAs) MART1, gp100 and CEA (62). Moreover, the downregulation of MHC-I presentation is a common immune escape mechanism exploited by cancer cells (63). Strategies to maximise TCR expression, to silent endogenous TCR activity and to enhance signalling have been developed to improve the applicability of TCR engineered cells to mediate physiological anti-tumour ACT (57).

1.2.1.3 CAR-T cell Therapy

1.2.1.3.1 Definition and structure

The initial concept of a Chimeric Antigen Receptor (CAR) emerged when the TCR α and β chains were replaced with the variable heavy (VH) and variable light (VL) chain regions of antibodies thereby imparting MHC-independent antigen recognition (64, 65). This was followed by the cloning of a single-chain variable fragment (scFv) format in which the variable regions are linked by a flexible linker sequence to simplify molecular cloning and transduction (66).

CARs are synthetic fusion proteins consisting of an extracellular antigen-recognition domain linked to intracellular signalling domains which are capable of activating immune cells (67). The extracellular component is usually made of a scFv, which binds to a specific antigen and is anchored to

the cell with a spacer (or hinge) and a transmembrane domain to provide distance, flexibility and stable cell surface expression (68). The distance, which can be edited, is crucial for efficient CAR-T cell functioning by allowing correct cytotoxic synapse formation, granule release and exclusion of inhibitory phosphatases (69).

There are currently three generations of CAR-T cells based on different intracellular domains and summarized in Figure 1-4 (70). The 1st generation CAR contains a TCR-derived CD3ζ intracellular domain which mimics canonical signal 1 (left diagram); in patients, this resulted in specific but poor anti-tumour efficacy due to the limited expansion and persistence of the transferred T cells (71-74). 2nd generation CAR-T cells were designed to achieve full T cell activation through co-stimulation (canonical signal 2) via intracellular fusion proteins such as CD28-CD3ζ or CD137(4-1BB)-CD3ζ (two central diagrams) (75). The additional costimulatory domain showed strikingly improved expansion and persistence of T-cells (76, 77). 2nd generation constructs are still the most widely used in clinical trials (78, 79). *In vitro* and *in vivo* models suggest that T cells are less exhausted and last longer with the 41BB costimulatory domain, whilst CD28 containing CAR-T cells convey stronger cytotoxicity at early activation stages (78, 79). 3rd generation constructs include a further costimulatory domain (right diagram) resulting in enhanced activation and proliferation with eventual enhanced cytotoxicity in pre-clinical studies (80). However, clear superior activity compared to 2nd generation has yet to be demonstrated in a clinical setting (81, 82).

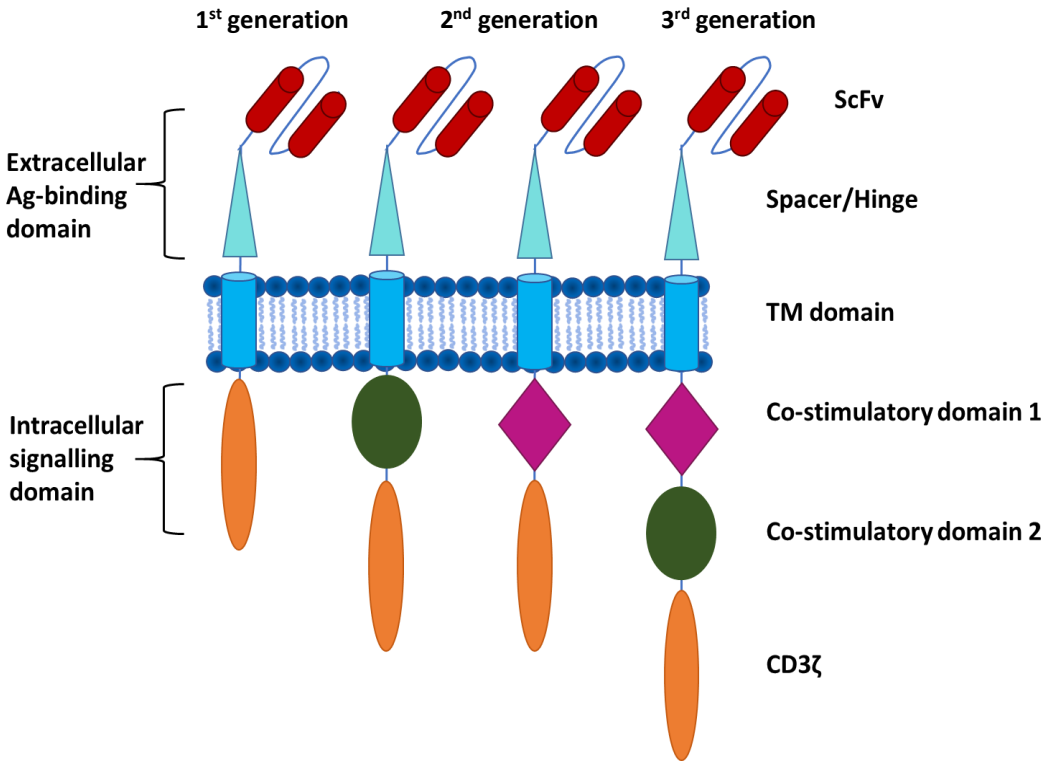

Figure 1-4 CAR structure. The chimeric receptor is made of an extracellular antigen-binding domain, usually made with an antibody-derived scFv. The scFv is followed by a spacer or hinge to allow flexibility. The transmembrane domain connects the extracellular portion to the intracellular signalling domain. Different CAR generations contain different elements: the first generation had only the CD3ζ domain which led to specific but transient response; the addition of one co-stimulatory domain (CD28 or 41BB being the most used) made the second generation of CAR-T cells, which were able to elicit more potent and long lasting responses in vivo. Third generation CARs were made with two co-stimulatory domains and showed superior activity which is still not fully demonstrated in a clinical setting.

Next-generation CAR-T cells, also known as 4th generation, are 2nd generation CAR-T cells engineered to release soluble pro-inflammatory mediators such as IL-12 (TRUCKs or T-cell Redirected for Universal Cytokine-mediated Killing) (83) or heparinase to disrupt the tissue micro-environment to promote tumour infiltration and immune responses against solid malignancies (84). These are just two examples of editing strategies to enhance CAR-T cell (and potentially other immune cells) efficacy. Further strategies will be discussed in the section 1.2.1.3.6.

1.2.1.3.2 CAR-T cell generation via viral transduction

The concept of immunotherapy using engineered CAR-T cells is based on the adoptive transfer of a patient's own T cells (autologous) that have been isolated, ex-vivo expanded and genetically modified to exert their immune response (85-87). Once produced, the engineered cells are cryopreserved until patients have received preconditioning chemotherapy (e.g. with fludarabine and cyclophosphamide) to support efficient engraftment (88).

Retroviral and lentiviral vectors represent the main engineering approach for T cells. Retroviruses are double stranded (ds) RNA viruses able to infect only dividing cells. Following infection, the viral reverse transcriptase (RT) generates a DNA template which is then inserted into the genome of the host cell. The viral genome is switched with a transgene of interest (the CAR sequence) to allow permanent cell modification and expression of the transgene. Lentiviruses are a subclass of retroviruses which can infect also non-dividing cells and contain additional genes regulating viral gene expression and assembly (89, 90).

To be safe, viral vectors need to deliver the transgene of interest into the host cells without making new replication competent virions. To make vectors replication incompetent the genes needed for viral production are placed into separate plasmids named helper plasmids. Helper plasmids for the packaging system encode for *gag* and *pol* genes, which are needed for structural proteins and reverse transcriptase respectively; a further helper plasmid encodes for the *env* gene for the viral envelope. 2nd generation lentiviral vectors require three plasmids: the transfer plasmid and two helper plasmids: one containing env and the other containing gag, pol, rev and tat. Rev and tat are additional genes necessary for lentiviral vector generation. To further improve safety and lower the risk of having replication-competent virus, the 3rd generation system was made placing rev on an additional plasmid (90, 91). Packaging, envelope and transfer plasmids are required to make functional virus and are transfected together into a packaging cell line, such as HEK-293T cells.

Regarding manufacturing, CAR-T cell therapy presents challenges such as great variation in numbers of genetically modified cells, their composition and fitness between patients. Moreover, the manufacturing process is still labour intensive and requires highly specialised staff, which drastically increases the costs making this therapy still unable to meet demand. (92, 93).

1.2.1.3.3 CAR-T cell therapy for haematological malignancies

The most successful CAR-T cell therapy to date targets the B cell antigen CD19 in haematological malignancies, with reports of up to 90% response rates in patients that failed conventional therapy (94-96). This success led to the recent FDA and EMA approval of two CD19 CAR-T cell therapies to treat children and young adults with relapsed/refractory Acute Lymphoblastic Leukaemia (ALL) and adults with diffuse Large B Cell Lymphoma (DLBCL) (97, 98). Remarkable and durable responses have also been observed with CAR-T cells targeting B-cell maturation antigen (BCMA) in multiple myeloma, the second most common haematological malignancy (99).

Despite the therapeutic effect, up to 60% ALL patients relapse because of the rising of CD19- tumour cells. To counteract this common mechanism of tumour escape, a promising strategy is to combine different CARs, either as combination therapy (NCT02465983 as example of a clinical trial) or by expressing two full CARs on the same T cell. Preclinical examples of the latter were described by Ruella et al, where they engineered T cells to co-express CD19 CAR with a CAR targeting the IL-3 receptor α chain CD123, expressed on haematopoietic progenitor cells as well as ALL cells; moreover, two independent studies by Zah and colleagues and by Abken's group used a single-chain, bispecific CAR against target cells expressing either CD19 or CD20, using the OR-gate recognition strategy (activation by either antigen). The common findings of the two studies suggest that using a CAR-T cell that is triggered by 2 different antigens simultaneously can result in increased efficacy and lower chances of relapse due to antigen escape (100-102).

Another promising target for CAR-T cell therapy in haematological malignancies is CD22. Results from a phase I clinical trial using CD22 CAR-

T cells in children and adults with B-cell ALL (naïve or CD19 CAR-T cell therapy refractory patients), showed a very promising anti-leukemic activity, with 73% of complete response that included all patients with $CD19^{low}$ or CD19- disease (103).

Although CD19 CAR-T cell therapies showed durable complete remissions and prolonged survival rates even in patients refractory to standard treatments, CAR-T cells targeting other antigens is still unable to achieve the same remarkable outcomes, especially in the context of solid malignancies (71, 104).

1.2.1.3.4 CAR-T cell therapy for solid malignancies

CAR-T cell therapy, like other forms of immunotherapy, is facing multiple challenges that make successful treatment of solid tumours difficult to achieve. These challenges include intrinsic features of solid tumours such as ineffective homing and persistence, immunosuppressive TME as well as the selection of the targeted antigen given the highly cytotoxic potential of CAR-T cells. Further details will be given in a following section.

Early clinical reports using 2^{nd} generation constructs reported limited but encouraging therapeutic effects such as delayed disease progression and increased survival (105, 106). Some studies suggest that a local administration of CAR-T cells may be better to achieve optimal anti-tumour efficacy (107).

1.2.1.3.5 Toxicity and methods to improve safety

There are two main side effects that can arise from CAR-T cell therapy. The first and most common one is cytokine release syndrome (CRS) which consist of a rapid and large release of pro-inflammatory cytokines such as IL-6 into the blood which can lead to a supraphysiological immune system activation. Importantly, CRS is also considered as a sign of an effective anti-tumoral response or on-target toxicity. CRS typically arises within the first few days following CAR-T cell infusion. Patients presenting a high disease burden

and/or elevated antigen load have increased risk and severity of CRS. The severity is usually mild but if not treated it can become severe and life-threatening (85, 108, 109). IL-6 receptor blocker antibody tocilizumab and corticosteroids are the preferred treatment for severe CRS (110).

The second most common side effect is neurotoxicity, also known as CAR-T-cell-related encephalopathy syndrome (CRES); it can have mild clinical manifestations such as confusion, swelling of the brain and mild movement disorders but can also become life threatening (109). Interestingly, CD19 CAR-T cell-mediated neurotoxicity seems more frequent in ALL and seems to occur independently from leukemic localization in the CNS. This, combined with the frequent detection of neurotoxicity with the use of the bispecific T cell engager CD3xCD19 blinatumomab, led to speculations about a link between CD19 and neurotoxicity (111, 112).

It is supposed that CRS and neurotoxicity may be unrelated as the latter can arise concurrently with or after CRS (110). Risk factors for both CRS and neurotoxicity include disease burden, CAR-T cell dose and manufacturing.

Another form of toxicity, known as 'on target-off tumour' toxicity, arises when the target antigen is also expressed on normal healthy tissues. For CD19 this is manifested by profound, but non-lethal B-cell aplasia due to CD19 expression on normal B cells and B-cell precursors. B-cell aplasia causes hypogammaglobulinemia, which can be managed via intravenous immunoglobulin (IVIG) administration (113). For other TAAs this can lead to severe toxicity and treatment-related deaths like the HER2-CAR-mediated death via recognition of low ERBB2 antigen expression on healthy lung cells (114).

Tumour lysis syndrome, another potential side effect, occurs when tumour cells release contents into the bloodstream either in response to therapy or spontaneously. In the setting of CAR T-cell therapy, evidence suggests an increased risk of tumour lysis syndrome in patients that are not pre-treated with suppressive chemotherapy. Calcium deficiency, elevated uric acid in blood, hyperphosphatemia, and hyperkalemia are the characteristic findings

of tumour lysis syndrome. Patients require vigorous fluid resuscitation with alkalinization to prevent acute kidney injury (113).

Overall, the magnitude and timing of the clinical manifestation of side effects range between mild (fever, flu-like syndromes) to life-threatening (multi-organ dysfunction), including some fatalities (67, 114-116). Due to the considerable diversity in CAR composition, manufacturing and administration protocols, as well as patient selection and disease type, there is no standardised guideline for monitoring, grading, and managing toxicities (117). Attempts to create consensus guidelines on CAR-T cell-related toxicities are being made, such as the work from Neelapu and colleagues based exclusively on clinical data using Yescarta, one of the two CD19 CAR-T cell therapies approved for clinical use (109).

It is important to highlight that the presence of a target antigen on one or more healthy tissues doesn't necessarily lead to on-target, off-tumour toxicity as shown by Künkele et al in their pre-clinical assessment of CAR-T cells targeting CD171 (118).

Ongoing extensive work is focusing on ways to improve safety of CAR-T cells. This can be achieved with several strategies, like a drug-mediated induction of apoptosis with small molecules or monoclonal antibodies (119, 120). Alternatively, engineered cells can be edited to express additional cell surface proteins, which can be targeted efficiently by therapeutic antibodies. Examples include the truncated form of the Epidermal Growth Factor Receptor (tEGFR) which is recognised by cetuximab (121) or RQR8, which contains the CD20 epitope targeted by Rituximab (122).

A further example is to arm CAR-T cells with an inducible suicide gene, such as Caspase9 (123), to guarantee the elimination of the infused engineered T cells via administration of the inducer molecule in the event of severe toxicity. The downside of this strategy is that the switching-on of the suicide gene leads to immediate induction of apoptosis in most of the gene-modified T cells, which may lead to disease progression (120, 124, 125).

Another strategy is to make the surface CAR expression inducible. This could be achieved via administration of an inducer molecule (126) or via the SynNotch + AND-gate system, where cells are engineered to express a synthetic notch receptor (SynNotch) that, upon activation, induces CAR surface expression. This approach shows that AND-gate T cells spare single antigen bystander/healthy cells but kill dual antigen tumours *in vivo* (127, 128).

A final example consists of the modular antibody-based platform technology named UniCAR, where the cross-linking of CAR-T cells and target cells is mediated through an additional molecule. This second component is composed of a binding moiety against a tumour antigen of choice fused to a UniCAR tag, the epitope recognised by the UniCAR-T cell. The two key advantages offered by this system are: UniCAR T cells can reversibly be armed with one or multiple target molecules sharing the same UniCAR tag and, in case of tumour eradication or severe side effects, stopping infusions of the additional molecule should be enough to inactivate the UniCAR T cells (129-131).

1.2.1.3.6 Strategies to improve efficacy

Figure 1-5 from (73) shows a summary of the main limitations of CAR-T cells, with the majority being related to the intrinsic features of T cells and therefore shared with the canonical immunological response.

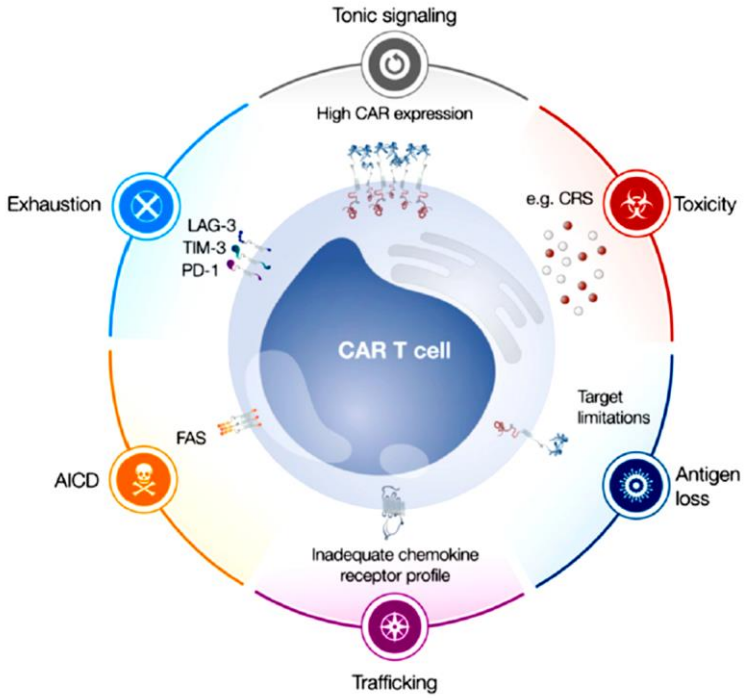

Figure 1-5 Limitations of chimeric antigen receptor (CAR) T cells (67). Tonic signalling, exhaustion and aactivation-induced cell death (AICD) limit T cell functionality, proliferation and persistence. Tracking of CAR T cells to the tumor site may be limited due to an inadequate chemokine receptor profile. Antigen loss can lead to tumor escape, while cytokine release syndrome (CRS) constitutes a frequently observed adverse event. Abbreviations: PD-1, programmed cell death protein 1; LAG-3, lymphocyte activation gene 3; TIM-3, T cell immunoglobulin mucin 3.

As most of these limitations will be discussed in a following paragraph, CAR-derived tonic signalling will be described here. It could be defined as a non-coordinated but sustained T cell activation and can be divided into two categories: constitutive, meaning in the absence of the targeted ligand, and ligand dependent. The former is characterized by *in vitro* extensive proliferation and a terminally differentiated phenotype, which can lead to poor antitumor efficacy, impaired survival, and reduced persistence *in vivo*. The latter can promote T cell anergy, exhaustion and activation-induced cell death (AICD). Strategies to overcome constitutive signalling are focusing on vector engineering, as factors like CAR structure (e.g. CD28 versus 41BB)

and the promoter used to drive CAR expression seem to influence the degree of tonic signalling (132).

There are several strategies being tested to overcome common limitations and improve migration, survival and effector functions of CAR-T cell therapy. Key approaches are summarised in Figure 1-6 (133) and will be described further:

'Armoured' CAR-T cells express additional immune-modulatory proteins such as pro-inflammatory cytokines (133, 134). TRUCKs are a promising example of armoured CAR-T cells: the targeted delivery of pro-inflammatory cytokines IL-12 or IL-18 has shown to boost the therapeutic response via activation of the innate immune response from bystander cells (85, 135-137).

A further example already described in the context of haematological malignancies consists of dual receptor, or bispecific CARs. Recognition of two different TAA's could result in increased specificity and reduced on-target, off-tumour side effects. Frequency of antigen escape by tumour cells could be elevated in case both antigens are required for full CAR-T cell activation (101, 138-141); conversely the frequency could be reduced when the two CARs are fully functional (142, 143).

Another promising strategy to overcome antigen escape was reported by Maus and colleagues, where they engineered EGFRvIII-targeted CAR-T cells to constitutively secrete Bispecific T cell engagers (BiTEs) targeting the endogenous form of EGFR. In this way, BiTEs would redirect an effective anti-tumour response against EGFR+ tumour cells that downregulated EGFRvIII antigen as mechanism of tumour escape. In their EGFRvIII+ glioblastoma model, they reported complete and durable responses in all treated mice following treatment with CART-EGFRvIII.BiTE-EGFR cells (144).

Efficient trafficking also depends on the appropriate expression and matching between the chemokine receptors (mainly CXCR3 and CCR5) on CAR-T cells and the chemokines secreted by the tumours. However, there is often a chemokine/receptor mismatch which leads to inefficient targeting of the

CXCR3^{high} CD8^{+} CAR-T cells to tumour sites (145). One possibility to overcome this issue is to make CAR-T cells co-express better-matched chemokine receptors: a successful example reported by two groups is CCR2b to treat tumours that make large amounts of CCL2, which led to enhanced homing of CAR-T cells and increased tumour eradication (146, 147).

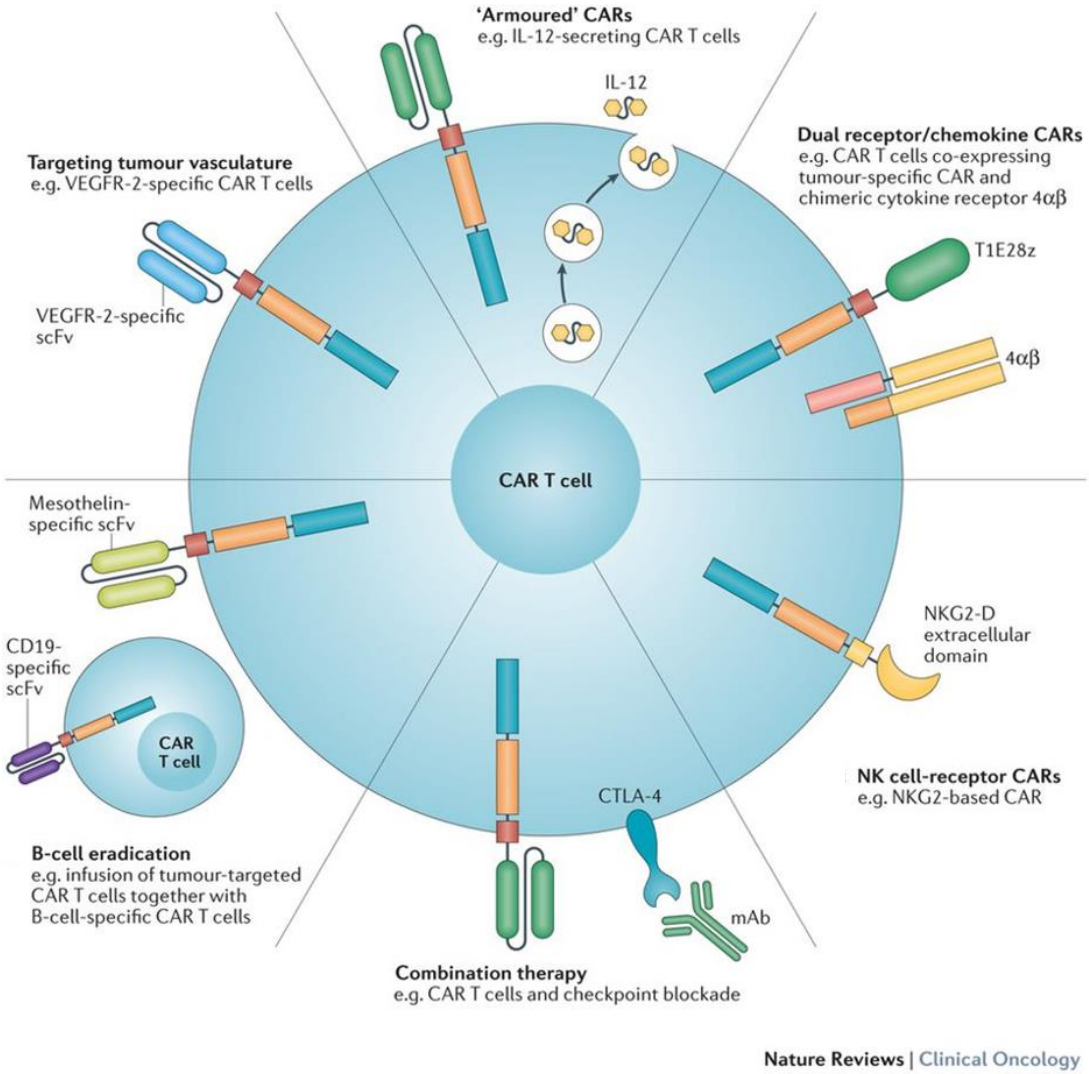

Figure 1-6 Key strategies to improve CAR-T cell efficacy. From Jackson et al. (43).

1.2.1.3.7 CAR-T cell and checkpoint blockade

CAR-T cells, like endogenous T cells, upregulate exhaustion markers which can be exploited by overexpression of their ligands by tumour cells to hamper the therapeutic response. While there are currently several approaches that focus on combining ACT therapy with immune checkpoint blockade (148, 149), we will focus on combination therapies in the context of CAR-T cells.

In the clinical setting, combination therapy with PD-1 blockade seems to improve CAR-T cell efficacy. Gargett and colleagues reported that PD-1 blockade was able to rescue from AICD and restore pro-inflammatory cytokine production from their 3rd generation GD2 CAR-T cells that were isolated from melanoma patients (150).

In another study, primary mouse T cells expressing anti-HER2 CARs were tested in a HER2 transgenic recipient mice, where they showed a significant improvement in tumour control and increased IFNγ production in the presence of PD-1 blockade compared to CAR-T cells alone (151). When they tested the same treatment conditions in established subcutaneous tumours in transgenic mice, they confirmed the PD-1 blockade-mediated enhanced regression of HER2+ sarcoma and breast cancer tumours. Moreover, more in-depth analysis confirmed increased IFNγ production and unaltered CAR-T cell frequency, but when they looked at immunosuppressive populations they reported same Treg numbers but decreased $Gr1^+$ $CD11b^+$ MDSCs within the TME, suggesting an indirect mechanism affecting MDSC numbers and, at the same time, enhancing CAR-T cell therapeutic effect (152).

The following studies used different mechanisms based on further engineering of the CAR-T cell to disrupt the PD-1/PD-L1 axis, showing various degrees of enhanced therapeutic effect:

Cherkassky and colleagues generated a dominant negative PD-1 receptor (DNR) lacking intracellular signalling domains that was shown to mitigate PD-1-mediated exhaustion of mesothelin (M)-targeted CAR-T cells via

saturation of PD-1 ligands. Compared to 2nd generation M-CAR, DNR-M-CAR-T cells had enhanced proliferation, cytotoxicity and pro-inflammatory cytokine secretion *in vitro* and were able to control tumour burden and increase the survival of mice with an established mesothelin+ pleural tumour (78). In a different study, the CRISPR/Cas9 system has been successfully used to disrupt PD-1 enhancing antitumor activity of CAR-T cells (153).

A further approach used by Liu et al was to turn the inhibitory PD-1 signalling into a pro-inflammatory signal using a so-called 'switch receptor' consisting of a PD-1 extracellular domain and CD28 intracellular domain on CAR-T cells: this resulted in improved *in vivo* anti-tumour activity and reduced exhaustion when compared to treatments with CAR T cells alone or PD-1 antibodies (154). Moreover, Rupp and colleagues reported that their PD-1 deficient CD19-targeted CAR-T cells were more efficient at eradicating PD-L1+ tumour cells *in vivo* compared to canonical CD19 CAR-T cells (155).

Suarez et al showed that secretion of anti-PD-L1 antibodies by armoured CAR-T cells improved CAR-T cell efficacy in a mouse xenograft model (156). Similarly, a recent study by Rafiq and colleagues showed the use of 'armoured' CAR-T cells constitutively secreting anti-PD1 scFv and efficiently targeting a range of PD-L1+ haematological and solid tumours in clinically relevant xenogeneic and syngeneic mouse models. Notably, they observed comparable or better efficacy than that achieved by combination therapy with CAR-T cells and a checkpoint inhibitor. Importantly, despite the constitutive scFv secretion, they reported no off-target checkpoint blockade-derived side effects in multiple *in vivo* models (157).

The next section will cover another main form of immunotherapy: monoclonal antibody (mAb) therapeutics, which offer great potential to modulate the immune response treat cancer.

1.2.2 Antibody-based therapies

Antibodies are highly specific, naturally evolved molecules that recognise and eliminate pathogenic antigens (158). The past 30 years of antibody research

and technology development have hinted at the promise of new versatile therapeutic agents to fight cancer, autoimmune diseases and infection: therapeutic antibodies (158) .

The idea of using antibodies to selectively target tumours was suggested by Paul Ehrlich more than 100 years ago (159). The advent of hybridoma technology allowed to produce monoclonal antibodies (mAbs). Early studies with mouse-derived mAbs showed high immunogenicity in humans and poor immune effector responses, but advances in antibody engineering provided platforms for the development of chimeric, humanised and fully human mAbs which were able to address many of these problems (160).

Therapeutic antibodies exert their effects through direct antibody-mediated cytotoxicity such as receptor blockade (161), or via the immune-mediated cell killing mechanisms named antibody-dependent cell-mediated cytotoxicity (ADCC) and the complement-dependent cytotoxicity (CDC), where the complement-derived membrane attack complexes generate pores in targeted cells (162). Additionally, there is increasing evidence suggesting a role for antibody therapy in inducing an adaptive immune response via ADCC-mediated cross-presentation to T cells by dendritic cells (Figure 1-7 adapted from (160).

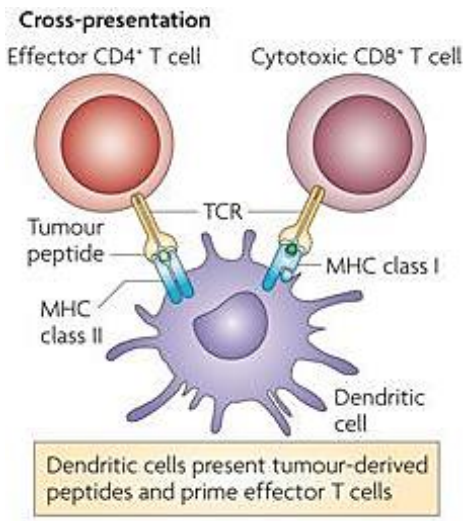

Figure 1-7 Cross-presentation to T cells. Peptides derived from lysosomal degradation of tumour cells can be loaded on to MHC class II molecules, leading to the activation of CD4+ helper T cells. In addition to CD4+ T cell activation, dendritic cells can cross-present tumour cell antigens and prime cytotoxic CD8+ T cells. TCR, T cell receptor (154).

Rituximab, the most widely used antibody in oncology, is a very successful example of antibody-based therapies. This chimeric IgG1 mAb binds to the B cell antigen CD20 (163) and showed promising results when given as a single agent in the treatment of relapsed or refractory diffuse large-B-cell lymphoma (DLBCL) and indolent lymphomas (164-166). Following clinical studies in which rituximab was combined with standard CHOP regimen (cyclophosphamide, doxorubicin, vincristine, and prednisone) reported a good safety profile and responses in more than 90% of lymphoma patients (167, 168). Particularly, the study by Coiffier et al reported that the longer survival in the CHOP + rituximab group was due to a lower rate of disease progression during therapy and fewer relapses for patients who had a complete response (163). Moreover, combination treatment was well tolerated, with no increased severe/serious adverse events compared to the CHOP group which is important considering that the majority of DLBCL patients are over 60years old (169).

Notably, great variation in therapeutic responses against different tumours has been reported. Antibody isotype (class) choice seems to be play a key role in this variation: for instance, the mAb IgG Fc domain is known to mediate ADCC via engagement of Fc receptors for IgG (FcγRs) on immune cells inducing adaptive immune responses (160, 170, 171).

Moreover, monoclonal antibodies (mAbs) showed synergistic anti-tumour effects when combined with other immunomodulatory approaches including radiotherapy, chemotherapy, vaccines, targeted therapy agents or other immunomodulatory molecules (160).

One successful strategy applies 'armed' antibodies with toxins or radioactive nucleotides (172). Brentuximab Vedotin (SGN-35) is an example of antibody-drug conjugate which upon binding to CD30, it results in internalisation and release of Monomethyl auristatin E, triggering cell death (172). Remarkable clinical activity has been reported in patients with relapsed or refractory CD30+ lymphomas: durable objective responses and tumour regression were observed for most patients, while treatment-related side effects ranged from mild to moderate (173, 174).

Functional limitations of therapeutic antibodies include ineffective pharmacokinetics and tissue homing as well as impaired interactions with immune cells (169). For examples, their large size and the Fc region can be beneficial in terms of pharmacokinetics, but can severely impair their ability to penetrate large tumours (175).

1.2.2.1 Bispecific T-cell engagers (BiTEs)

Conventional antibodies do not recruit or utilise T cells for their cytotoxic effector function. Bispecific T cell engagers or BiTEs are a class of bispecific antibodies (BsAb) that have been successfully used to specifically redirect and activate endogenous effector T cells against tumours with generally mild and transient toxicity (176).

Their structure is made of small flexible molecules composed of two antibody-derived scFv linked in tandem. These scFvs are designed to simultaneously bind to a tumour-associated antigen (e.g. CD19) and to signal molecules such as the CD3 subunit on T cells (Figure 1-8 adapted from (177).

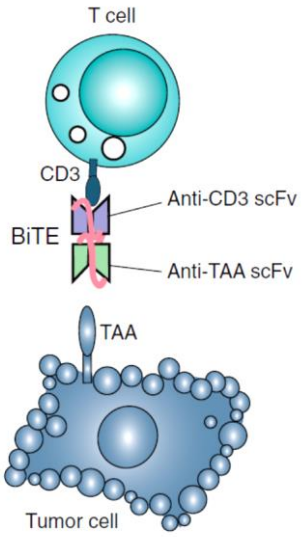

Figure 1-8 BiTE mechanism of action. The BiTE creates an immunologic synapse (IS) by binding simultaneously to a TAA on a tumour cell, and to CD3 on a T cell. Adapted from (171).

Once both cells have been linked via BiTE, a cytolytic synapse between the T cell and the target cell occurs. This is followed by the release of granzymes and perforins by the cytotoxic T cell leading to apoptosis of the target cell. These activated T cells are also able to release pro-inflammatory cytokines which can in turn activate other immune cells (178, 179). The key advantage of the BiTE approach is that antigen recognition and T cell activation occur independently of MHC, antigen presentation and costimulatory molecules (179, 180).

A further benefit of BiTE versus T-cell based therapies is the lack of ex-vivo manipulation and/or engineering of the patient's own T cells. Moreover, BiTE-related adverse events are normally reversible after application of steroids and/or withdrawal of BiTE infusions, given the short half-life of the molecule in circulation (181). Against solid malignancies, the use of BiTE therapy is limited, which may be linked to the poor efficacy reported so far (182-184).

The CD19xCD3 blinatumomab is the most successful BiTE to date. It showed major clinical benefits, including partial and complete remissions, against a range of haematological malignancies (185) even as single agent (186), and achieved a breakthrough therapy designation by the US Food and Drug Administration (FDA) (187-189).

Because blinatumomab is the most widely used BsAb, its toxicity profile is well established and presumably like the ones from other CD3-activating BsAbs (190). Blinatumomab-derived adverse events are usually manageable and dose-limiting; frequent toxicities include neurologic events, cytokine-release syndrome, neutropenia (111, 191), anaemia and thrombocytopenia (189).

Although successful in inducing remissions, these antibodies face the same limitations as monoclonal antibodies (192) such as rapid renal clearance due to their relatively small size (~55 KDa), requiring continuous infusions over 4–8 weeks to achieve clinical effect. Additionally, the modest size of these

bivalent constructs may also facilitate their leakage into the central nervous system (185, 190).

1.2.2.2 Checkpoint Blockade

T cell dysfunction or exhaustion is a major mechanism contributing to impaired effector T cell responses against tumours or pathogens. One key signature of T cell dysfunction and exhaustion, is enhanced expression of immunoregulatory receptors such as Programmed cell death protein 1 (PD-1), T cell co-receptor cytotoxic T cell antigen-4 (CTLA-4) (7, 193), lymphocyte activation gene 3 (LAG3) and T-cell immunoglobulin mucin receptor 3 (TIM3) (194), VISTA (195), and BTLA (196).

Under physiological conditions, immune checkpoints play a crucial role to prevent autoimmunity (or maintenance of immunological tolerance) and protect healthy tissues from damage when the immune system is responding to pathogens (15).

The term checkpoint blockade refers to immune checkpoint inhibitors (usually monoclonal antibodies) that bind to immunomodulatory receptors on immune cells to block the interaction with the respective checkpoint ligands; this would reduce suppression of effector T cells and augment tumour-specific immune responses (7, 71). The goal of checkpoint blockade therapy is therefore to remove inhibitory pathways that hamper effective anti-tumour T cell responses (197); it has been showing remarkable efficacy and is likely to be a major treatment modality for a variety of malignancies.

Anti-CTLA-4 antibody therapy has shown therapeutic effects in several types of cancer (198) and is the first checkpoint inhibitor approved by US FDA for the treatment of metastatic melanoma for being the first therapy that induced survival benefit in these patients (15, 199).

In the context of other malignancies, ipilimumab combined with paclitaxel and carboplatin improved progression-free survival compared to either agent

alone for patients with non–small-cell lung cancer (NSCLC) in a Phase II study (200). Another CTLA-4–blocking antibody named tremelimumab has shown responses in patients with mesothelioma in a Phase II trial, with other trials under way (201, 202). Interestingly, many patients treated in early studies with CTLA-4 blockade showed early evidence of disease progression that ultimately became disease response; moreover, a report combining some of the first patients treated with CTLA-4 blockade stated that the median time it took to achieve an ultimate complete response was 30 months (203).

The preclinical successes of anti-CTLA-4 in achieving tumour eradication in animal models and the ultimate clinical success opened a new field of immune checkpoint therapy (197). Table 1 summarises the checkpoint inhibitors currently being evaluated in clinical trials. For the purpose of this project, the following paragraphs will focus on the PD-1/PD-L1 interaction.

Table 1 Clinical trials evaluating checkpoint blockade therapy. 11 out of 67 clinical trials registered on clinicaltrials.gov; trials list filtered for: either recruiting, active or completed as of September 2019.

Name compound	Targeted antigen	Condition	NCT number
Durvalumab + Tremelimumab	PD-L1 and CTLA-4	Locally Advanced Head and Neck Squamous Cell Carcinoma	NCT03426657
Pembrolizumab	PD-1	Non-Small Cell Lung Cancer, Metastatic Melanoma, Metastatic Renal Cell Carcinoma, Head and Neck Squamous Cell Carcinoma	NCT03474497
PD-1 inhibitor non specified	PD-1	Renal Cell Carcinoma, Urothelial Carcinoma, Bladder Cancer	NCT03291028
Nivolumab	PD-1	Mesothelioma	NCT03063450
Ipilimumab versus Nivolumab	CTLA-4 and PD-1	Non-Small Cell Lung Cancer Metastatic	NCT03168464
Nivolumab	PD-1	B cell lymphomas	NCT03920631
Durvalumab + Tremelimumab	PD-L1 and CTLA-4	Colorectal Cancer Metastatic	NCT03007407
M7824	Anti-PD-L1/TGFbetaRII Fusion Protein	Anatomic Stage IV Breast Cancer AJCC v8, Estrogen Receptor Positive, HER2/Neu Negative	NCT03524170
Avelumab	PD-L1	Thymoma, Thymic Carcinoma	NCT03076554
Niraparib + Nivolumab or Ipilimumab	LAG3, PD-1 and CTLA-4	Pancreatic Adenocarcinoma,	NCT03404960
PDR001 + LAG525	PD-1 and LAG-3	Small Cell Lung Cancer, Gastric Adenocarcinoma, Esophageal Adenocarcinoma	NCT03365791

1.2.2.2.1 Expression of PD-1 receptor and its ligands

PD-1 is a type I transmembrane domain that is upregulated on activated T cells at late-stage immune responses and when terminally differentiated in peripheral tissues and in the TME. PD-1 is also expressed on Tregs, B cells, Natural Killer and some myeloid cells. High and sustained expression has been observed on exhausted CD8+ T cells in the course of chronic viral infections (204, 205) as well as on post-infused engineered T cells compared to the pre-infused population (206). Recently, PD-1 expression was also

observed in a compartment of melanoma cells promoting tumorigenesis in a mouse model (207).

PD-L1 and PD-L2 are expressed by many cell types, from tumour cells to haematopoietic cells like T and B cells, dendritic cells and macrophages (208). In cancer, tumour cells and myeloid cells are thought to be the main cell types mediating T cell suppression through PD-1 activation (7). Moreover, PD-L1 expression on the cell surface can be upregulated on both tumour cells and other cell types in the presence of type I or type II interferons (IFNs), radiation or chemotherapy (209, 210).

1.2.2.2.2 PD-1 mechanism of action

PD-1 binds to PD-L1 (B7-H1 or CD274) and PD-L2 (B7-DC or CD273), which belong to the B7 family (211). Engaged PD-1 must be recruited to the immunological synapse to exert its inhibitory functions, which are delivered though its cytoplasmic domain made of an immunoreceptor tyrosine-based inhibitory motif (known as ITIM) and a tyrosine-based switch motif (or ITSM) (Figure 1-9). Activated PD-1 strongly counteracts both TCR signalling and CD28 co-stimulation even when expressed at low levels. As a result, PD-1 contributes to prolonged TCR down-modulation and abrogates cytokine production and cell survival (212-214). PD-1 and other inhibitory pathways are often called immunological checkpoints (5-7, 211). In addition to PD-1, many reports showed that PD-L1 can bind to CD80 (or B7.1), expressed on APCs and activated T cells (215, 216) with three times more affinity than CD28 leading to T cell anergy in two ways: the first one is by blocking the essential co-stimulatory signalling via CD80/CD28, the second is upon PD-L1 binding where CD80 expressed on T cells can deliver “reverse signalling” into the T cell that is anti-inflammatory and tolerogenic (217, 218).

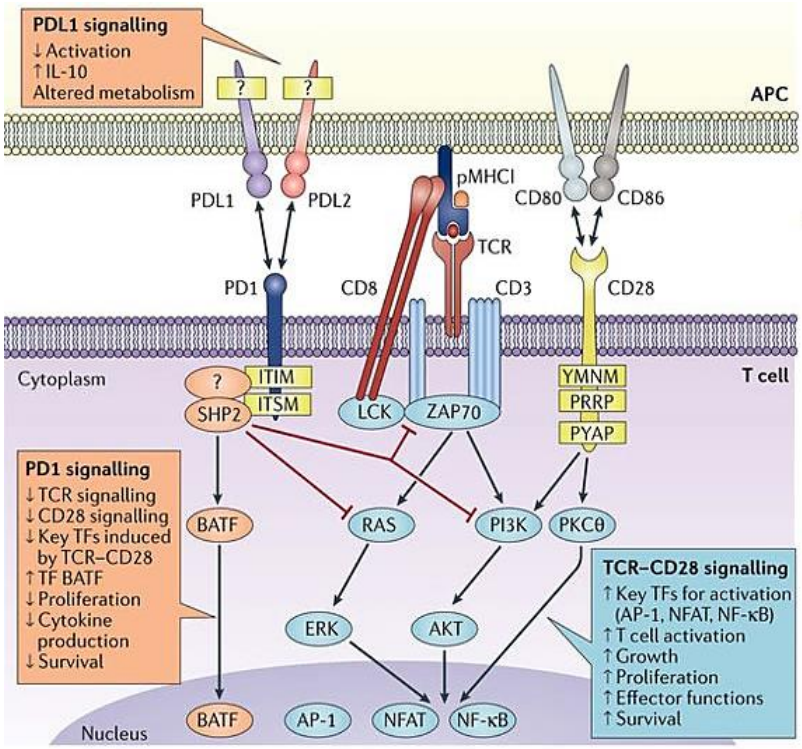

Figure 1-9 Key activated PD-1-mediated effect on T cells. Activated PD-1 can simultaneously counteract signalling from ZAP70, PI3K and RAS which leads to decreased activation of key TFs essential for T cell survival, proliferation and release of pro-inflammatory cytokine production. Adapted from Nature Reviews Immunology volume 18, pages 153–167 (2018)

Preclinical studies showed that blocking the PD-1/PD-L1 interaction increases the numbers of effector T cells and their cytolytic activity, it enhances the production of pro-inflammatory cytokines and reduces the numbers of Tregs at the tumour sites (5, 210).

1.2.2.2.3 PD-1/PD-L1 inhibitors

Therapeutics blocking the PD-1/PD-L1 interaction have shown promising results in clinical trials revolutionising immunotherapy (210). Reported effects include: increased numbers of cytotoxic T cells and their effector functions, enhanced production of pro-inflammatory cytokines and reduced numbers of Tregs at the tumour sites (5, 210). Moreover, PD-1 blockade can provide a response over a longer period through activation of anti-tumour immune responses that target tumour cells with mutated proteins (219).

Following anti-PD1 therapy, durable objective (either partial or complete) responses were observed in patients with advanced melanoma (31–44% of patients), non-small-cell lung cancer (NSCLC, 19–20%) and renal cell carcinoma (RCC, 22–25% patients). These results, combined with the observed extended overall survival when compared with other conventional therapies, supported FDA approvals of the PD-1 blocking mAb nivolumab (BMS) (6) and Pembrolizumab (Merck) as standard treatment in these settings (194).

Several other antibodies targeting this pathway have also entered clinical testing. Checkpoint blockade has generated encouraging results for the treatment of a wide range of cancers, although the precise molecular and cellular mechanisms are still poorly understood.

While a sustained and long-lasting expression of PD-1 alone has been used to define T cell exhaustion or dysfunction (220), it has become clear that these T cell subsets overexpress multiple IRs, including CTLA-4, TIM-3 and LAG-3 (24, 221). Moreover, this upregulation seems to increase with progressive decrease in effector functions (26).

IRs may also play an indirect role in inducing cytotoxic T cell exhaustion. An example is given by Sakuishi and colleagues, where they highlighted expression of TIM-3 on highly suppressive tissue-resident regulatory T cells. They showed that depletion of these cells prior appearance of exhausted CD8+ T cells, interferes with the development of such phenotype (222).

PD-1 blockade has shown to only partially reinvigorate exhausted T cells (24), while the use of combined checkpoint blockade therapies (for example LAG-3 and PD-1 blockade) can have a synergistic effect on TILs and successfully reinvigorate their effector functions (26, 223). When looking at exhausted cells, PD-1 expressing cells could also be divided into two main subsets: stem-like or progenitor cells (PD-1^{hi}TIM-3^{low}TCF1+), and terminally differentiated cells (PD-1^{hi}TIM-3^{hi}TCF1^{-}). The former can undergo proliferation, self-renewal, and elicit quick effector responses following PD-1

blockade. It also gives rise to the terminally differentiated group, which has overall limited effector functions (22).

1.2.2.2.4 Immunological checkpoints as prognostic markers

Several clinical studies suggest that PD-1 overexpression seems to correlate with a reduced anti-tumour T cell response. An example comes from a meta-analysis of twelve different epithelial cancers that showed significantly shorter overall survival (OS) for patients having PD-1+ tumour infiltrating lymphocytes (TILs) (7, 210, 224). Additionally, tumour infiltration of PD-1+ memory CD8+ T cells may be used as predictor of patient response to anti-PD-1 therapy in the context of melanoma (225) as it has been reported that reactivation of these experienced memory T cells might boost checkpoint blockade-mediated efficacy in patients with PD-L1+ tumours (226).

Regarding PD-L1, analysis of a correlation between the ligand overexpression on tumour cells and disease outcome revealed mixed results. For example, a study of primary and metastatic melanoma samples, many of which were also taken from the same patient, showed that PD-L1 expression patterns differed between primary tumours and metastatic lesions and also between intra-patient metastases (197). Further research to identify predictive biomarkers is needed to select patients who are most likely to respond to anti-PD-1 therapy while minimizing systemic adverse events (5, 7, 227).

Moreover, it has been shown that PD-1/PD-L1 interactions may also take place between melanoma cells to disseminate survival signals to cancer cells and boost in vivo tumour growth in the absence of T cells. To support this hypothesis, the authors of the study show that elimination of PD-1 expression or the use of blocking antibodies directly delayed tumour growth without the need of enhanced T cell anti-tumour activities (207).

Collectively, these regulatory receptors control the quality, duration and intensity of the immune response (228).

1.2.2.2.5 Adverse effects

Because checkpoint blockade is not targeted to enhance exclusively tumour-specific immune responses, adverse effects can arise through nonspecific immunologic activation. Adverse effects from these agents are termed immune-related adverse events (irAEs). Generally, the rate of grade 3 or 4 toxicity with immune checkpoint blockade (approximately 10% to 20%) is no greater than that seen with many standard chemotherapy or targeted therapy regimens (202, 229).

IrAEs include dermatologic (the most common for PD-1 blockade), gastro-intestinal, hepatic, endocrine, and other less common inflammatory events (196). Standard treatments for moderate symptoms include temporary immunosuppression with oral corticosteroids and tumour necrosis factor (TNF)α antagonists (230, 231). PD-1 blockade therapy seems to induce less high-grade toxicities compared to other therapies. An example is the study from Brahmer and colleagues on patients with advanced lung cancer where they reported 7% (nivolumab-treated) versus 55% (chemotherapy-treated) frequency of grade 3 or 4 side effects (232).

Despite the great promise of checkpoint blockade therapy, such as the induced durable clinical responses that can last a decade and more, more than 50% of cancer patients fail to respond to checkpoint blockade therapy (197).

1.3 Mechanisms of tumour escape

Despite improvements made in conventional tumour treatments, in many cases patients relapse because therapies often fail to fully arrest disease progression into a more aggressive form characterized by bone and organ metastases (86, 233).

Factors that have an impact on treatment efficacy include: mutations that affect antigen presentation (MHC and antigen processing), inhibitory

checkpoint expression on tumour and/or TILs (e.g., PD-L1, PD-L2, CTLA-4), patient's age, history of infection and vaccination (6, 234).

The selection of the target antigen is extremely important when designing adoptive transfer strategies (235, 236). When therapies are targeted to a single specific tumour antigen, missing tumour recognition may happen through mechanisms such as acquired mutations (formation of neo-antigens) and targeted antigen loss (via mutations, downregulation or deletion) which can lead to survival of tumour subpopulations expressing low/no targeted antigen (237). The recruitment of immunosuppressive cells such as tumour associated macrophages (TAMs), tumour associated neutrophils (TANs), Tregs and myeloid-derived suppressor cells (MDSCs) is another key mechanism that hampers therapeutic responses (7, 149, 210, 238-240).

Regarding solid tumours, three major contributors make effective treatments so challenging: the first one is failure of T cells to enter, accumulate and expand within the hostile TME characterized by oxidative stress, nutritional depletion, hypoxia and acidic pH; secondly, antigen selection is difficult due to antigen heterogeneity and/or loss across the same malignancy, which is generally higher in solid tumours than liquid malignancies. Lastly, the issue of 'on-target, off-tumour' toxicity is more prominent because potential target antigens are more likely to be expressed in healthy organs or tissues (TAAs) (85, 86, 134, 234, 241, 242).

1.3.1 Tumours difficult to treat: triple negative breast cancer (TNBC)

Breast cancer is the most common tumour type in American women and the second leading cause of cancer-related deaths in the United States (243, 244). Hormone receptors can be indicative of patient prognosis and response to targeted therapy. Two key receptors are the oestrogen (ER) and progesterone receptors (PR); if present, patients that respond well to targeted hormone therapy tend to have improved prognosis. Another key receptor in breast cancer subtyping is HER2. Unlike the hormonal receptors, high HER2 expression correlates with disease recurrence and poor prognosis (245).

Triple negative breast cancer (TNBC) is a subtype of breast cancer characterized by negative ER and PR expression, as well as a lack of HER2 overexpression (16). This group constitutes about 10–20% of all breast cancers and it has higher incidence in younger patients and African American women. As TNBC patients cannot benefit from endocrine therapy or HER-2 targeted therapies (such as therapeutic antibody trastuzumab) there is still lack of available targets for prognosis and therapeutic purposes. Pre-surgical (neoadjuvant) chemotherapy is the standard treatment, but despite having higher rates of clinical response compared to other breast cancer types, TNBC is very heterogeneous, highly metastatic (especially to the viscera like lung and brain) and is associated with poorer outcome, with a 5-year survival rate below 30% (246-250).

Different strategies have been implemented to classify these tumours, including classical pathology, protein and mRNA expression profiling, and genomic alterations. The heterogeneity of the immune microenvironment plays a considerable role in influencing the risk of relapse and response to chemotherapy and has provided the rationale for the application of immunotherapies. Breast cancer patients with increased cytotoxic TIL levels in the tumour (also defined as 'hot' tumour) are more likely to respond to immunotherapy versus patients with 'cold' tumours (i.e. very little immune infiltrate) and this seems true for TNBC patients as well. However, clinical success of adoptive T-cell therapy (ACT) with autologous T lymphocytes has been limited in TNBC, likely due to the multiple suppressive mechanisms that operate in the breast cancer microenvironment (251-254). PD-L1 expression seems significantly associated with the presence of TILs, suggesting that TNBC is using a regulatory feedback (acquired resistance) to upregulate PD-L1 in repose to immune engagement (39). Checkpoint blockade therapy, either alone or in combination, is being actively tested in several ongoing clinical trials. For instance, in the phase Ib KEYNOTE-012 clinical trial (NCT01848834), therapeutic αPD-1 antibody pembrolizumab was given as single-agent to patients with advanced PD-L1-positive TNBC showed an overall activity of 18.5% with an acceptable safety profile (255).

A more targeted approach with personalised treatment strategies seem the best solution for those patients that do not respond to chemotherapy. Apart from immune checkpoint blockade, other strategies currently evaluated in the clinic include PARP inhibitors, PI3K inhibitors, EGFR and MEK inhibitors, either alone or in combination. Clinical data is still limited with contrasting findings which make difficult to confirm clear clinical benefit (39).

Overall, there is urgent need to better characterise the molecular basis of TNBC and the adaptive immune response to improve current immunotherapy approaches. For instance, Lehmann and colleagues were able to identify 6 TNBC molecular subtypes based on gene expression and showed that cell lines derived from these subtypes had different susceptibility to targeted therapeutics (250). Similar studies were published by Burstein et al., where they used RNA profiling to highlight distinct TNBC subtype-specific markers that could be used for TNBC subtype-specific prognosis and treatment (256). Going forward, it will be important to understand the mechanisms behind the subtype-specific differences in immune infiltration and prognostic association (16), as well as to find markers to predict therapeutic responses. Current clinical trials (examples found in Table 2) will hopefully help to answer these questions (257).

Finally, few studies reported association between ROR1 expression and triple negative hormonal receptor expression, higher metastatic potential and survival, and enhanced epithelial-mesenchymal transition (258-260).

Table 2 Clinical trials in TNBC. 9 examples of clinical trials either active, recruiting or completed as of September 2019 from clinicaltrials.gov

Name Study	Intervention	NCT number
Study of Safety and Efficacy of Novel Immunotherapy Combinations in Patients With Triple Negative Breast Cancer (TNBC).	Biological: spartalizumab; Biological: LAG525; Drug: NIR178; (and 3 more...)	NCT03742349
A Study Evaluating the Efficacy and Safety of Multiple Immunotherapy-Based Treatment Combinations in Patients With Metastatic or Inoperable Locally Advanced Triple-Negative Breast Cancer (Morpheus-TNBC)	Drug: Capecitabine Drug: Atezolizumab Drug: Ipatasertib (and 6 more...)	NCT03424005
Avelumab With Binimetinib, Utomilumab, or Anti-OX40 Antibody PF-04518600 in Treating Triple Negative Breast Cancer	Biological: Anti-OX40 Antibody PF-04518600 Drug: Avelumab Drug: Binimetinib Biological: Utomilumab	NCT03971409
Adjuvant PVX-410 Vaccine and Durvalumab in Stage II/III Triple Negative Breast Cancer	Biological: PVX-410 Biological: Durvalumab Drug: Hiltonol	NCT02826434
Olaparib and Durvalumab in Treating Participants With Metastatic Triple Negative Breast Cancer	Biological: Durvalumab Drug: Olaparib	NCT03544125
Genetically Modified T-Cell Therapy in Treating Patients With Advanced ROR1+ Malignancies	Other: Laboratory Biomarker Analysis Biological: ROR1 CAR-specific Autologous T-Lymphocytes	NCT02706392
A Study Of Avelumab In Combination With Other Cancer Immunotherapies In Advanced Malignancies (JAVELIN Medley)	Drug: Avelumab Drug: Utomilumab Drug: PF-04518600 (and 2 more...)	NCT02554812
T-Cell Therapy for Advanced Breast Cancer	Drug: Cyclophosphamide Biological: Mesothelin-targeted T cells Drug: AP1903	NCT02792114
Targeted T Cells After Neoadjuvant Chemotherapy in Treating Women With Stage II or III Breast Cancer Undergoing Surgery	Biological: HER2Bi-armed activated T cells Drug: cyclophosphamide Drug: doxorubicin hydrochloride (and 4 more...)	NCT01147016

1.3.2 Tumours difficult to treat: non-small cell lung cancer (NSCLC)

Lung cancer is the most commonly diagnosed (11.6% of the total cases worldwide) and leading cause of cancer-related death (18.4% of the total cancer deaths) (261). Non-small-cell lung cancers (NSCLC) account for about 85–90% of lung cancers, while the frequency of small-cell lung cancer (SCLC) has been decreasing over the last two decades (262).

Smoking is the main cause of lung cancer, responsible for more than 80% of cases therefore prevention and smoking cessation are still the main approaches to decrease death incidences (263). Despite the observed increase in both incidence and mortality worldwide, countries with effective tobacco control measures have registered a decline in the incidence of new lung cancer in men and a plateau for women (264). Additional risk factors include exposure to asbestos, arsenic, and radon (265); moreover, an increase in the incidence of non-smoking associated NSCLC has been observed and is considered a distinct disease entity, where specific molecular and genetic tumour features are being recognised (266).

Better understanding of the molecular changes that play a key role in driving tumour progression has revolutionized the clinical management of NSCLC. Most NSCLC patients harbour an oncogenic driver mutation; in the presence of a therapeutically targetable lesion, more treatment options may be available which can lead to improved survival and safety compared with conventional chemotherapy (267). One example is the anaplastic lymphoma kinase (ALK) fusion genes; ALK activity has been effectively targeted by ALK-tyrosine kinase inhibitors (TKIs), making routine testing for ALK rearrangements a standard of care (268). Moreover, the testing of several targeted approaches for other driver alterations such as serine/threonine-protein kinase b-raf (BRAF), ROS1 proto-oncogene receptor tyrosine kinase (ROS1) and other less established onco-proteins is under evaluation (269, 270). Figure 1-10 adapted from (270) summarises the milestones in targeted therapy for NSCLC.

A further example is the activating genetic alterations (or fusions) in the epidermal growth factor receptor (EGFR or ERBB1). Therapy with EGFR-TKIs named gefitinib and erlotinib have shown clinical efficacy with significant delay in disease progression for patients with advanced NSCLC bearing EGFR-activating mutations (271-274), with the recent Phase III clinical trial reporting superior outcome for patients treated with gefitinib, compared with standard first-line cytotoxic chemotherapy (275).

However, the prognosis remains poor. For example, despite the dramatic benefits from EGFR and ALK TKIs, all patients will ultimately develop disease progression through primary or acquired resistance (265). Two mechanisms of acquired resistance involve mutations in EGFR itself, with the EGFR T790M mutation reported in 50% of resistance cases, and amplification of the MET oncogene in 20% of resistance cases (276). Strategies for overcoming acquired resistance to both agents are undergoing clinical evaluation, such as the use of EGFR inhibitors to overcome the *EGFR* T790M mutation (277). However, there are currently no methods to predict the specific resistance mechanism that a cancer will develop (276).

Additionally, overall outcomes have been poor for patients receiving chemoradiotherapy, with only 15-30% of patients alive at 5 years, corresponding to a median survival of 28 months (278, 279). Several studies have reported the use of systemic therapy that, to date, have proved ineffective, with a median survival ranging from 18 to 23 months (280).

The anti–PD-L1 antibody atezolizumab induced an overall survival benefit in patients with metastatic NSCLC regardless of PD-L1 expression (281) and showed promising therapeutic effects with a good safety profile when combined with platinum-doublet chemotherapy in patients who have not previously received chemotherapy (282). Moreover, a recent open-label, phase III study evaluated atezolizumab plus anti-EGFR mAb bevacizumab plus chemotherapy in patients with metastatic non-squamous NSCLC who had not previously received chemotherapy. Results showed that the addition of atezolizumab to bevacizumab plus chemotherapy (BCP) significantly improved overall survival for patients with metastatic non-squamous NSCLC, regardless of PD-L1 expression and EGFR or ALK genetic alteration status, compared to BCP treatment (283).

Identification of the complexity of the molecular changes underlying the development of treatment resistance is needed to better understand the key mechanisms of tumour cell survival and clinical progression following treatment. The successful implementation of personalized medicine in the treatment of non-small cell lung cancer will require better evaluation of

pathways that drive tumour growth at baseline and during the course of therapy, to design tailored treatments to prevent tumour evolution and treatment resistance (270).

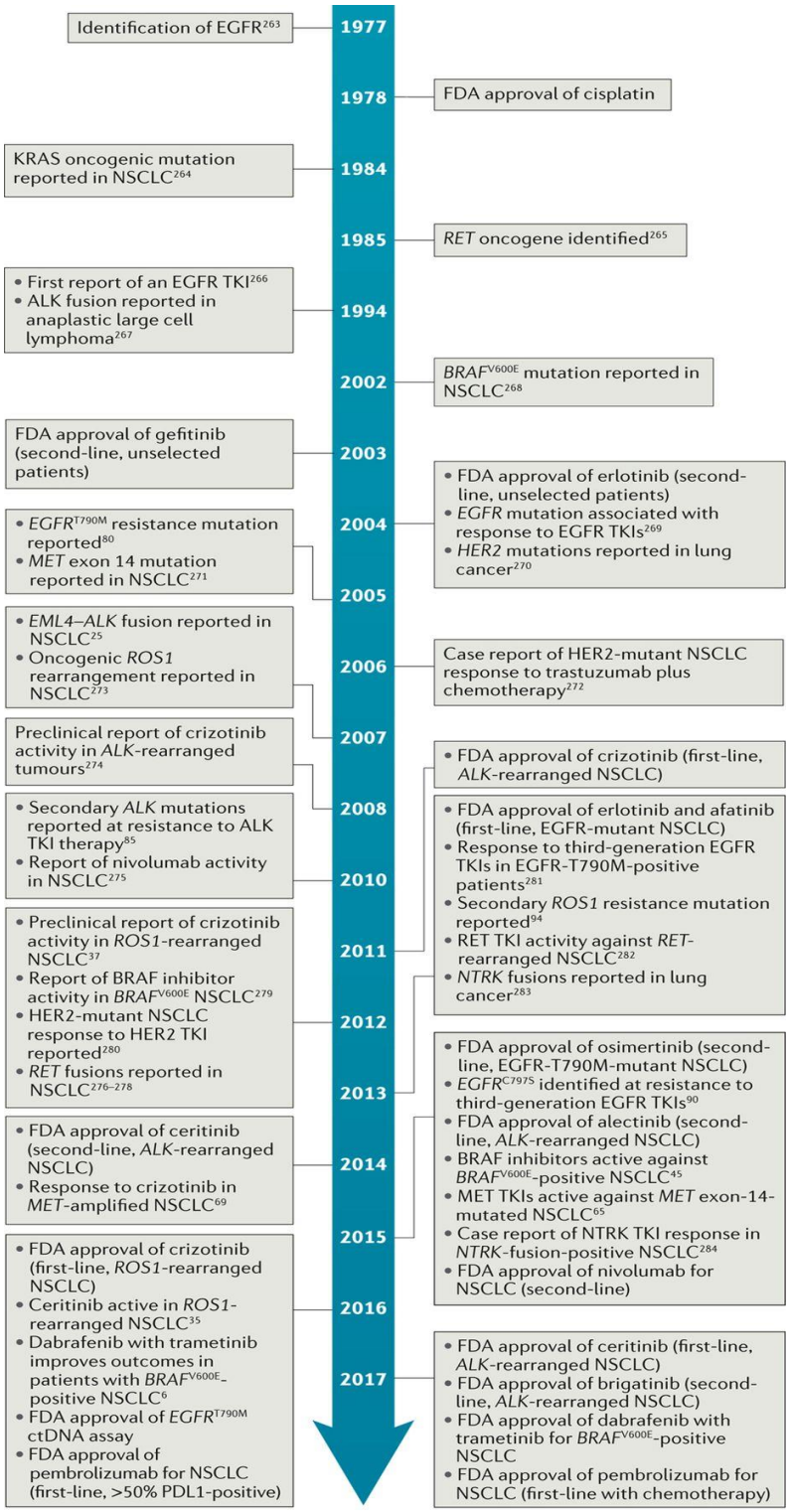

Figure 1-10 Timeline of NSCLC therapy evolution. ALK, anaplastic lymphoma kinase; BRAF, serine/threonine-protein kinase b-raf; ctDNA, circulating tumour DNA; EGFR, epidermal growth factor receptor; EML4, echinoderm microtubule-associated protein-like 4; HER2, human epidermal growth factor receptor 2; MET, hepatocyte growth factor receptor; NSCLC, non-small-cell lung cancer; NTRK, neurotrophic tyrosine kinase; PDL1, programmed cell death ligand 1; RET, proto-oncogene tyrosine-protein kinase receptor Ret; ROS1, ROS1 proto-oncogene receptor tyrosine kinase; TKI, tyrosine kinase inhibitor (260).

1.4 Tumour-associated antigens as therapeutic targets

To better understand and create efficient anti-tumour immunity for cancer therapy, great efforts have been made for the identification of cancer antigens recognised by immune cells or antibodies (284).

There are two main categories of tumour antigens: tumour-specific (TSA) and tumour-associated (TAA) antigens. TSAs are expressed only by tumour cells (285), whereas TAAs are proteins that can also be found on healthy cells and tissues (87). Examples of TAA include: antigens expressed at lower levels on normal tissues (like Wilms tumour 1) or on immune privileged sites (like cancer testis antigens) and TAA derived from oncogenic viral infections (human papillomavirus). A further group is made of neo-antigens, which arise upon extensive somatic mutation in cancer cells. It is particularly challenging to develop targeted therapeutics against neo-antigens as they tend to be highly tumour and patient specific (286).

In targeting TAAs, CAR-T cell-mediated on-target off-tumour reactions are very common, and their tolerability will depend greatly on the types of healthy cells that are targeted (287). For instance, the TAA CD19 is considered an ideal target for many reasons. These include its overexpression on malignant B-cells and lack of expression outside the B cell lineage. Moreover, patients successfully treated with CD19-secific CAR-T cells likely develop profound B-cell aplasia which is largely managed via intravenous immunoglobulin (Ig) as replacement therapy (288).

Results from several clinical trials of CAR-T cells targeting other TAAs in solid tumours such as mesothelin (MSLN), carcinoembryonic antigen (CEA) and the GD2 ganglioside highlight that the lack of toxicity is often linked to minimal anti-tumour activity. In fact, one study reported fatal neurotoxicity in preclinical models when more potent GD2-specific CAR T cells were used (289).

Moreover, T cells may target healthy tissues more efficiently than solid tumours independently of the surface antigen density, given the intrinsic features of tumour cells including defects in antigen processing and

presentation, and overexpression of inhibitory molecules. This is supported by the clinical results of T cell therapies s targeting the TAAs CAIX and CEA; healthy tissue injury was reported in half of treated patients in the CAIX trial and in all patients in the CEA trial, but only a single partial response was reported in the CEA setting (115, 290, 291).

One example of TSA that demonstrated safe targeting is the alternately spliced variant of epidermal growth factor receptor (EGFRvIII), despite causing relapse via antigen loss (292).

Table 3 adapted from (133)summarises targets currently tested in clinical trials using CAR-T cell therapy, excluding CD19.

Overall, target antigens selected for adoptive T-cell therapy should not be expressed by critical healthy tissues. Unfortunately, with the existing technology and tissue specimens, it is currently impossible to confirm the absolute absence of a targeted antigen from crucial healthy tissues. As such, targeting TAAs generally leads to uncertainty about which healthy tissues may be at risk of T cell–mediated attack (293). The risk of adverse events may be further reduced by avoiding cross-reactivity against epitopes in healthy tissues. In general, a scrupulous approach for target selection and considerate preclinical and clinical studies are pivotal to move these promising treatments forward (293).

Table 3: Tumour targets being evaluated in CAR-T cell based clinical trials. Currently active trials from clintrials.gov as of September 2019. MM=multiple myeloma, AML=acute myeloid leukaemia, HL=Hodgkin lymphoma, NHL=non-Hodgkin lymphoma, FL=follicular lymphoma, CLL=chronic lymphoblastic leukaemia, DLBCL=diffuse large B cell lymphoma.

Name compound	Condition	NCT number
PSMA	Prostate cancer	NCT01140373 and NCT00664196
Mesothelin	Malignant pleural mesothelioma, Pancreatic Cancer, Ovarian Cancer	NCT01355965, NCT02465983, NCT01583686
Mesothelin	Metastatic pancreatic (ductal) adenocarcinoma, epithelial ovarian cancer and malignant epithelial pleural mesothelioma	NCT02159716 and NCT02414269
FAP	Mesothelioma	NCT01722149
EGFRvIII	Glioma	NCT02209376 and NCT01454596
EGFR	Malignant glioma	NCT02331693
CEA	Liver metastases	NCT02146466
CEA	Lung, colorectal, gastric, breast and pancreatic cancer	NCT02349724
CD171	Neuroblastoma	NCT02311621
GD2	Neuroblastoma, osteosarcoma and melanoma	NCT02107963
GD2	Neuroblastoma and Sarcoma	NCT01822652 and NCT01953900
Glypican-3	Advanced-stage hepatocellular carcinoma	NCT02395250
HER2	Glioblastoma	NCT02442297
HER2	Glioblastoma multiforme	NCT01109095
IL-13	Glioma	NCT02208362
CD22	FL, NHL, DLBCL, B-ALL	NCT02315612
CD20	CD20 positive malignancies	NCT01735604
ROR1	CLL, SLL	NCT02194374
Igk	CLL, low-grade B-cell malignancies	NCT00881920
CD30	HL, NHL	NCT01316146
CD123	AML	NCT02159495
CD33	AML	NCT01864902
LeY	AML	NCT01716364
BCMA	MM	NCT02215967
CD138	MM	NCT01886976

1.4.1 Receptor Tyrosine Kinase-Like Orphan Receptor 1

The focus of our immunotherapeutic strategies has been the TAA Receptor Tyrosine Kinase-Like Orphan receptor 1 (ROR1).

1.4.2 ROR1: Definition, structure and function

ROR is a member of the receptor tyrosine kinase (TK) family. There are two forms (ROR1 and ROR2), discovered more than 20 years ago by Masiakowaski and Carroll in a neuroblastoma cell line while screening for putative TK receptors (294).

The ROR1 and ROR2 are type I transmembrane proteins consisting of extracellular (Ig-like, frizzled-like and kringle domains), transmembrane, and intracellular domains (one TK-like domain and two serine/threonine-rich domains flanking a proline-rich domain, Figure 1-11) (295). The inter-species sequence conservation for ROR1 is high, with frizzled and kringle domains having 99% amino acid similarity between human and mouse ROR1 (296).

ROR proteins play an active role in many cell stages and functions: proliferation, differentiation, angiogenesis and migration, cell metabolism, cell–cell interaction, and early stages of embryonic development of various organs and tissues (297). It is therefore not surprising that interfering with these proteins leads to severe developmental defects and diseases (298). In the context of cancer, ROR1 expression is associated with poor prognosis in many malignancies (259, 299) including TNBC and lung adenocarcinoma (259, 299). When activated, it supports tumour cell growth and metastasis by mediating key signalling pathways involved in cancer including EGFR signalling, PI3K/Akt/mTOR and p38 signalling pathways (300, 301). Moreover, ROR1 silencing has been shown to downregulate the epithelial-to-mesenchymal (EMT) transition, thus impairing the tumour cell migration and invasion ability (260).

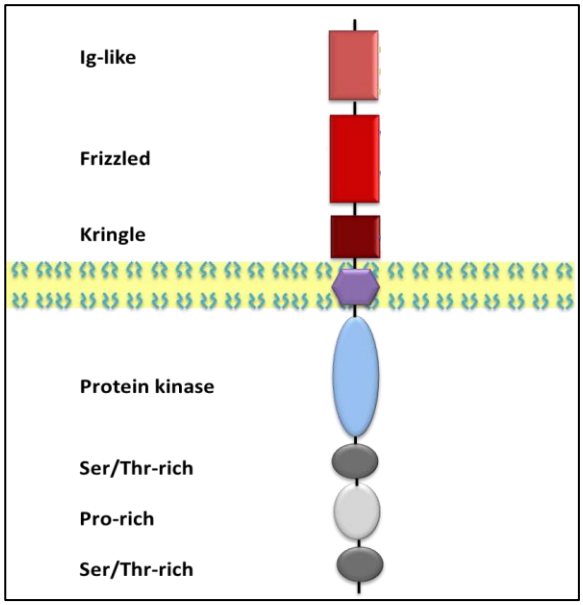

Figure 1-11 Topographical Human ROR1 structure Adapted from the website http: //www.acrobiosystems.com/A1033-Recombinant-ROR1--ROR2-Proteins.html

1.4.3 ROR1 cell and tissue expression

ROR1 is overexpressed in several solid and haematological malignancies. Different surface expression levels of ROR1 have been detected in almost all peripheral blood mononuclear cells (PBMCs) of CLL patients (302, 303). ROR1 is also expressed in leukemic cells of ~40% patients, more frequently in B-acute lymphoblastic leukaemia (ALL) compared to T-ALL (304).

In the context of solid malignancies, ROR1 expression has been detected in a wide range of cancers including breast (258, 259), ovarian, colon, skin, lung, pancreas, testis, uterus, bladder and prostate (299, 305, 306).

To further highlight the potential of targeting ROR1, Kipps' group published studies where they demonstrated ROR1 expression on human ovarian and breast cancer stem cells (CSCs), on which it might have a functional role in promoting *in vitro* migration, invasion, spheroid formation and tumour engraftment in immune-deficient mice. CSCs are more resistant to therapy

and are likely responsible for relapse or metastasis (307, 308). Additionally, another group reported ROR1 expression on glioblastoma stem cells (309).

Regarding ROR1 expression on healthy tissues, initial mRNA data showed low expression on adipocytes, which was also confirmed by flow cytometry (310). Subsequent tissue cross reactivity IHC studies using cirmtuzumab, a high affinity ROR1 antibody, confirmed no staining on healthy tissues (311). These findings were then challenged by a study from Balakrishnan et al, whereby using their own ROR1 antibody they reported expression on several normal tissues including parathyroid, pancreatic islets and regions of the oesophagus, stomach, and duodenum. Positive expression on multiple healthy tissues was also confirmed by the human protein Atlas datasets (312), raising concerns for on-target off-tumour toxicities, therefore accurate monitoring during clinical testing of ROR1-targeted therapies in patients will be necessary (306).

1.4.4 ROR1 therapeutics: therapeutic antibodies

Cirmtuzumab, the most clinically advanced mAb against ROR1, functions by inhibiting the receptor mediated signalling. Through humanisation and affinity maturation editing it was able to inhibit epithelial-to-mesenchymal transition and survival of cancer cells (307). Early phase I clinical trials showed safety but lack of clinical response (311), although further clinical trials have been planned (Table 4 for currently active ROR1-targeted clinical trials).

An armed version of cirmtuzumab (conjugated with a toxin) has been tested, but despite early impressive in vitro data, no further assessment has been reported (313). Encouraging results were reported from *in vitro* testing of the 2A2 ROR1 antibody labelled with a Pseudomonal exotoxin, however no clinical valuation has been planned (314, 315).

Other groups have developed their own antibodies against ROR1. Daneshmanesh et al developed a panel of anti-ROR1 antibodies and, when they tested their effector functions, they noted that the ones binding to more

membrane proximal epitopes had enhanced function (316, 317). Additionally, Riddell's group developed the R12 binder that demonstrated some ADCC but only at supra-physiologically high concentrations of effector cells. The same binder has also been utilised in a CAR format (318).

1.4.5 ROR1 therapeutics: CAR-T cells

ROR1 has been targeted primarily in the context of haematological malignancies due to its expression on B-CLL and mantle cell lymphoma and absence on healthy B cells, a clear advantage compared to CD19/CD20.

Hudecek et al were the first to report the use of ROR1 targeted CAR-T cells using the clone 2A2: they showed targeted cytotoxicity against primary B-CLL and mantle cell lymphoma cells (310). The same group subsequently compared the 2A2 with clone R12 and reported enhanced cytotoxicity by R12 due to its higher affinity, but as the two binders recognise different epitopes, this is not a true comparison. However, they did demonstrate the key role of the spacer as their hinge-only spacer derived from the IgG stalk showed optimal cytotoxicity (69). R12 CAR was then evaluated for toxicity in non-human primates for their comparable ROR1 tissue expression with humans, as well as cross-reactivity between human and macaque ROR1. They did not report any toxicity even at high CAR T cell doses (319). After reporting efficacy in targeting sarcoma, breast cancer and neuroblastoma cell lines (320, 321), the R12 CAR was licensed to Juno therapeutics and is being investigated in a Phase 1 clinical trial for breast cancer, ALL, MCL, CLL and NSCLC (NCT02706392), with a recent report highlighting safety of the CAR infusions even at high dose (322).

Recently, Riddell's group reported that their ROR1 CAR, edited to recognise murine kringle domain, elicited lethal bone marrow failure via recognition of ROR1+ healthy stromal cells in pre-irradiated C57BL/6 mice. Interestingly, when they repeated the experiment in immunocompromised mice ($Rag2^{-/-}$), they reported no morbidity nor deaths. The authors highlight that the safety of CAR-T cells specific for a TAA can be highly context dependent, claiming

that both the CAR T cell dose and the intensity of lymphodepletion are critical variables for potential toxicity (323).

Deniger et al. used the ROR1 CAR containing the 4A5 scFv clone derived from the Kipps group and showed *in vitro* cytotoxic potential; however, the *in vivo* model required repeated IL-2 infusions, which should not be usually required with a canonical 2nd generation CAR structure. Moreover, the toxicity may have been linked to the to the sleeping beauty manufacturing process to engineer the T cells, which requires considerable ex vivo manipulation (190).

Table 4 Active ROR1-targeted clinical trials. As of September 2019 from clinicaltrials.gov

Name study	Conditions	Phase	NCT Number
Genetically Modified T-Cell Therapy in Treating Patients with Advanced ROR1+ Malignancies	Estrogen Receptor Negative; HER2/Neu Negative; PR negative; (and 6 more...)	Phase 1	NCT02706392
A Study of Cirmtuzumab and Ibrutinib in Patients With B-Cell Lymphoid Malignancies	B-cell Chronic Lymphocytic Leukemia; Small Lymphocytic Lymphoma; Mantle Cell Lymphoma	Phase 1 Phase 2	NCT03088878
Study of Cirmtuzumab and Paclitaxel for Metastatic or Locally Advanced, Unresectable Breast Cancer	Breast Neoplasms	Phase 1	NCT02776917
UC-961 (Cirmtuzumab) in Relapsed or Refractory Chronic Lymphocytic Leukemia	Chronic Lymphocytic Leukemia	Phase 1	NCT02222688

Chapter 2 Project Aims

This research project is focused on the development and characterisation of ROR1-targeted CAR-T cell therapeutics. We hypothesise that effective ROR1-targeted CAR-T cells may be used to treat a broad range of malignancies including those with unmet therapeutic need such as TNBC and NSCLC.

We have successfully developed a fully humanized anti-human ROR1 binder and previously reported its efficacy against a broad range of malignancies in a Bispecific T-cell engager (BiTE) (324) and in a second-generation CAR format (325).

My aim was to optimise CAR-T cell-mediated killing of solid tumours, a highly desirable feat but one that has so far been unachievable. A major feature of the tumour microenvironment is the overexpression of inhibitory receptor ligands such as PD-L1 which suppresses T cell responses, including those from CAR-T cells. We therefore hypothesised that an effective way to improve the killing of ROR1+ target tumour cells was to combine CAR-T cell therapy with immune checkpoint blockade therapy. The combination of ROR1 and PD-1 blockade therapy provides a novel approach to treat solid tumours.

2.1 Generation and characterisation of PD-1 binder and the NFAT-based inducible promoter

We started with cloning to generate a PD-1 binder in a scFv format. The aim was therefore to confirm effective binding to PD-1 protein via multiple functional assays.

In parallel, cloning was performed to generate the NFAT-IL2p cassette consisting of 6 repetitions of NFAT binding sites and a minimal IL-2 promoter, which allow for expression of the transgene (the αPD-1 scFv in this context) via CD3ζ signalling cascade upon CAR activation. Once we generated the expression cassette, the aims were to confirm that the induction was specific and effective by using the reporter gene GFP and *in vitro* co-culture assays.

2.2 Generation of a functional ROR1 CAR with the inducible system (i-CAR)

This was followed by vector engineering to generate the expression vector combining constitutive CAR expression and the αPD-1 scFv secretion. The aim was to obtain a functional CAR, and to test secretion of scFv to confirm targeted and efficient production.

2.3 *In vitro* functional characterisation of i-CAR-T cells versus parental CAR-T cells

Next, we aimed to compare ROR1 i-CAR-T cells with the parental ROR1 CAR-T cells lacking inducible system. In parallel, we also tested combination therapy with a purified commercial anti-PD-1 antibody as control to confirm a PD-1 blockade effect on effector functions. Using a panel of ROR1+ and PD-L1+ cell lines, we specifically assessed: *in vitro* cytotoxicity, pro-inflammatory cytokine secretion, T cell phenotype (exhaustion markers, proliferation, cell type, immunological synapse strength).

2.4 *In vivo* functional characterisation of CAR-T cell therapy in a TNBC xenograft mouse model

We generated a reliable TNBC orthotopic xenograft mouse model to which we tested CAR-T cell therapy for the following: toxicity for the animals (on-target or off-target), anti-tumour effect and survival of the animals. We specifically aimed at comparing ROR1 CAR-T cells versus combination versus i-CAR-T cells.

In parallel, we used Nanostring technology to obtain more comprehensive information about the two CAR-T cell constructs. Specifically, we looked at differences in specific features such as cell type and phenotype between ROR1 CAR and i-CAR, and between *in vitro* and *in vivo* (TILs) CAR-T cells.

Chapter 3 Materials and Methods

3.1 Cloning

3.1.1 DNA construction using Phusion Polymerase

We perform this technique to isolate a DNA fragment from a plasmid, to amplify a DNA sequence (e.g. G-Block) or to assemble DNA fragments together (overlap PCR). The following table contains the reagents used for a reaction:

Reagent	Amount
5x HiFid Buffer	10 µL
dNTPs [10µM]	1 µL
Foward Primer [25µM]	1 µL
Reverse Primer [25µM]	1 µL
DNA template	200ng-1µg
Phusion Polymerase	0.5 µL
DDI H_2O	up to 50µL

After mixing, the reagents are added to 100µl PCR tube(s) that are the transferred into PCR blocks. A standard thermocycling programme for Phusion PCRs with fragments that are up to 1.5 kbp length is normally used:

Cycle name	Temperature	Time
1-Denaturation	98°C	2 minutes
2-Amplicon denaturation	98°C	40s
3-Oligos annealing	65°C	40s
4-Extension	72°C	1 minute
5-Cycle to 2 for 35 times		
6-Clean up unfinished PCRs	72°C	10 minutes

Next, the PCR product is run on 1% Agarose gel (1g of Agarose powder dissolved into 100ml of TBE buffer) containing Sybrsafe (sensitive stain to visualize DNA bands in agarose gel under UV or blue light) along with 1kB DNA Ladder (Hyperladder I, NEB). Bands of interests are cut, transferred to 2ml Eppendorf tubes and the DNA is extracted using the Wizard® SV Gel and PCR Clean-Up System kit (Promega) following manufacturer's instructions.

The DNA is eluted with Nuclease-Free Water (NFW) into fresh labelled Eppendorf tubes.

Once the DNA of interest has been made and produced in larger quantities via transformation of competent bacteria cells (DH5-alpha E. Coli, NEB), the sequence is checked via sequencing of the region of interest (generally the insert) using our in-house primers and the sequencing service provided by Source BioScience (website: https://www.sourcebioscience.com/). The sequences received are compared to our SnapGene map(s).

3.1.2 Cloning of the inducible cassette

For the inducible system, I cloned the same inducible cassette used by Chmielewski M et al for their TRUCKs with inducible secretion of the pro-inflammatory cytokine IL-12. The name of their inducible vector is pSIN-$(NFAT)_6$-IL-12. For more information about the generation of the inducible system, refer to the paper (326). Briefly, two primers have been manufactured (IDT) with the following sequences: NFAT I (AATTAGGAGGAAAAACTGTTTCATACAGAAGGCGTCAATTGTC) and NFAT II (CCGGGACCAATTGACGCCTTCTGTATGAAACAGTTTTTCCTCCT).
The primers were mixed in equimolar amounts, melted in boiling water, reannealed and subsequently ligated into pBluescript KS1 (purchased from Addgene) digested with EcoRI and XmaI to yield pBS-NFAT#1 (all restriction enzymes were obtained from NEB). The same plasmid was further digested with MfeI and XmaI to ligate the next NFAT-binding site generating pBS-NFAT#2. This step was repeated once more to obtain pBS-NFAT#3. To get 6 NFAT-binding sites, pBS-NFAT#3 was cut with XhoI and EcoRV and in here the XhoI-SmaI fragment from pBS-NFAT#3 was ligated, resulting in pBS-NFAT#6. The minimal IL-2 promoter (pos.260 to 26) was amplified by PCR from one in-house plasmid containing the full IL-2 promoter. This amplicon was digested with XmaI and BamHI and ligated into pBS-NFAT#6 backbone to obtain pBS-NFAT#6-IL2Pmin. Between the NcoI and BamHI sites of the vector, the GFP was ligated generating pBSNFAT#6-IL2Pmin-GFP.

3.2 Cell characterization

3.2.1 Cell culture: cell lines and primary cells

Adherent cell lines are cultured in T25 or T75 cell culture flasks (ThermoFisher Scientific) containing cell growth medium (Gibco® ThermoFisher Scientific) supplemented with 10% or 15% of heath-inactivated Foetal Bovine Serum (FBS from Gibco®, ThermoFisher Scientific). Abbreviations for cell culture media:

RPMI 1640 Medium: Roswell Park Memorial Institute 1640 Medium
IMDM: Iscove's Modified Dulbecco's Medium
DMEM: Dulbecco's Modified Eagle Medium

The following table summarises cell lines used, source and culture media used:

Cell line	tissue/disease	cell type and source	culture media
MCF-7	Breast (metastatic)	Epithelial (ATCC)	RPMI+10% FBS
MDA-MB-231	Human breast adenocarcinoma	Epithelial (ATCC)	RPMI+10% FBS
H1975	Lung adenocarcinoma (NSCLC)	Epithelial (ATCC)	RPMI+10% FBS
A549	Lung carcinoma	Epithelial (ATCC)	RPMI+10% FBS
HEK 293-T	Human embryonic Kidney	Epithelial (ATCC)	IMDM+10% FBS
Kasumi2	Acute myeloblastic leukemia	Myeloblast (ATCC)	RPMI+10% FBS
Jeko-1	Mantle Cell Lymphoma	Lymphoblast (ATCC)	RPMI+10% FBS
SKW 6.4	B lymphocyte EBV transformed	Lymphoblast (ATCC)	RPMI+10% FBS
SupT1	T-cell lymphoblastic lymphoma	T lymphoblast (ATCC)	RPMI+10% FBS
Jurkat	acute T cell leukemia	T lymphocyte (ATCC)	RPMI+10% FBS

The cells are kept in a 5% CO_2 humidified atmosphere at 37°C (incubator). When needed or once reached 85%-95% confluency, the cells are sub-cultured: for adherent cell lines, 1-2ml of either Trypsin/EDTA (Sigma) or cell-dissociation reagent (Sigma) is added to detach cells that are subsequently added to fresh culture medium. Diluted cells equivalent to a 1:10 split ratio, are transferred to a new flask with fresh culture media (note: 10ml total volume was used for T25 flasks, 15ml for T75 and 20ml for T175 culture flasks). Suspension cell lines are cultured in either T75 or T25 cell culture flasks and sub-cultured every 3-4 days.

Cell lines are eventually re-suspended in 1ml of sterile freezing media (FBS + 10% Dimethyl Sulfoxide, Sigma), transferred into labelled cryovials (Greiner) and frozen down using Mr. Frosty™ Freezing Containers (ThermoFisher Scientific) at -80°C.

When fresh peripheral blood mononuclear cells (PBMCs) are needed, blood is collected from healthy volunteers using syringes containing EDTA (Sigma). In sterile conditions, the blood is diluted 1 to 1 with plain RPMI Media, then carefully added to 50ml falcon tube(s) containing Ficoll-Paque Plus (GE Healthcare Life Sciences). After centrifugation at 750rpm (no brake nor accelerator to not disrupt the layers), the PBMC layer is collected using sterile 2ml Pasteur pipettes (VWR). The PBMCs are washed twice with RPMI-10, counted using trypan blue and a counting chamber and re-suspended at $2x10^6$cells/ml. When frozen PBMCs are used, the cryovial(s) is thawed at 37°C then cells are transferred to a 15ml falcon tube containing RPMI-10 (RPMI plus 10% FBS). After washing them (centrifugation at 400rpm for 5 minutes), cells are re-suspended at $2x10^6$cells/ml.

3.2.2 Phenotype analysis by Flow Cytometry

ROR1 (or other antigen) surface expression: cells are collected and counted. 100,000 cells are added to FACS tubes (Corning™ Falcon™) along with 1ml of PBS, followed by a washing step. After removing supernatant, to each pair of FACS tubes is added a mastermix containing 0.1µl of viability dye (e.g. Fixable Viability Dye eFluor® 450, Biolegend) and either 5 µl of APC anti-

human ROR1 antibody (Clone 2A2, Biolegend) or the Isotype Control at same final concentration (APC mouse IgG1, κ Biolegend). FACS tubes are then vortexed and incubated at 4°C for 1h. After washing the FACS tubes as before, cells are re-suspended in 200 µl of PBS before Flow cytometry analysis using BD LSR Fortessa™ (Bioscience).

3.2.3 Confocal microscopy

Co-cultures of pre-labelled CAR-T cells (cell tracker blue) and target cell line MDA-MB-231 (cell tracker red) were plated onto 24well-plates for 24 h prior to fixation. Cells were stained with CD3-AF647 and phalloidin-AF488 for actin accumulation before mounting and imaging by confocal microscopy (Zeiss LSM880, 960 oil objective; Zeiss, Oberkochen, Germany). Example T cells are depicted with white arrows. Scale bar = 10 mm.

ImageJ was used to calculate the relative recruitment index (RRI) of phalloidin: briefly, cell conjugates with immunological synapses (IS) were identified manually and phalloidin recruitment quantified using mean fluorescence intensity in an area of cell contact (actin accumulation) and normalized against phalloidin signal in a non-contact area of the T cell plasma membrane. We then select an area of background to subtract using the following equation: (contact value-background)/(non-contact value-background), which gives us the % RRI. 3 donor-derived CAR-T cells were used with n=28 IS selected for RRI index quantification.

3.2.4 Protein analysis via Western Blot

Samples are prepared as follows for the SDS-PAGE using 10-well NuPAGE™ polyacrylamide precast gels (4-12% Bis-Tris protein gels, from Invitrogen™):

Gels are assembled into the gel tank (XCell sure lock Electrophoresis cell) and 800ml/gel tank of NuPAGE® MOPS SDS Running Buffer (20X, Invitrogen™) is added.

Each tube is prepared to contain NuPAGE® Sample Reducing Agent (10X), NuPAGE® LDS Sample Buffer (4X, both from Thermo Fisher Scientific) and protein (diluted with PBS). Each sample is heated at 100°C for 10 minutes to ensure protein denaturation. Once cooled down, 15-20µl of each sample is loaded into the gel(s) along with Novex® Sharp Pre-Stained Protein Standard (0.5µl to 5µl, Life technologies). The gel tank is then connected to the power pack and left running at 200V for 50 minutes (roughly 500mA).

After 50 minutes, proteins are transferred from the gel to a nitrocellulose membrane. The Transfer XCell Blot module is assembled in this order: bottom chamber (-), sponge pads (2-3), gel, Nitrocellulose Membrane (Amersham Protran 0.45µm), filter pads, sponge pads, and lid (+). All the components are soaked into transfer buffer (NuPAGE® Transfer Buffer 20X). After 90 minutes at 35V, the membrane is removed and transfer is checked by soaking the membrane into Ponceau solution (sigma) which stains the proteins.

Afterwards, the membrane is washed in PBS with 0.05% Tween20 and stored overnight at 4°C for the blocking step (in washing buffer + 5% milk). The day after, the membrane is washed 5 times (5minutes on slow agitation, then wash buffer is replaced and so on) followed by incubation with a recommended dilution of antibody (e.g. 1:2,500 for HRP-anti His Tag antibody) for 1h at room temperature. After 5 additional washing steps (and eventual addition of a secondary antibody with same protocol as for primary antibody), the HRP chemiluminescent substrate (Thermofisher) is added prior detection with X-ray films.

3.2.5 Surface Plasmon Resonance

To assess scFv binding affinity to PD1, we set up binding affinity experiments to recombinant PD1 protein (Acro biosystem, # PD1-H5221-100ug) using the Biacore Surface Plasmon Resonance System (GE Healthcare). Briefly, HEK-293T cells were transiently transfected to secrete the anti-PD1 scFv linked to a murine Fc stalk. The produced Fc-tagged protein was quantified via western blot using a purified mouse-IgG antibody (clone MG1-45, # 401401,

Biolegend) serially diluted and detected via HRP-anti-mouse IgG antibody (Abcam). For the Biacore experiment, we used a sensor chip CM5 with an immobilized anti-murine Fc antibody (mouse antibody capture kit, GE Healthcare) to which we loaded the supernatant from two independent transfections. To the system we then added increasing concentrations of recombinant PD1 in a single step multicycle protocol. To generate a baseline/control, we used a Chip containing an immobilized anti-human Fc to which the same reagents and protocols were used. Three independent runs with two fresh supernatants were performed. Data was analysed with X100 software to generate kinetics data.

3.2.6 Nanostring using the nCounter® CAR-T Characterization Panel

Nanostring technology uses optical molecular barcodes to label individual mRNA transcripts. The relative gene expression is quantified by counting each barcode bound to the slide surface. Briefly, the capture and reported probes bind to the same gene, one next to each other. The reported probes contain the barcodes specific for each gene. After removing the excess/unbound material, biotin binds on the streptavidin-coated surface of the cartridge and imaging is performed to count the number of individual barcodes corresponding to individual molecules.

To prepare the samples, the following hybridization protocol was used:

Into PCR tubes, add the following:

-8µl of mastermix containing hybridization buffer and reporter codeset

-up to 5µl of template RNA (we used cell lysates in RLT buffer)

-5µl of capture probes

Mix gently and incubate at 65°C for at least 16h (usually overnight). The following day, create the experiment template with the specific CAR-T panel

RLF datafile (kit codeset), load the samples on the cartridge, upload the cartridge and start the run on the nCounter SPRINT.

After completing the run (roughly 6h), we downloaded the raw data and uploaded them on the nSolver 4.0 software. The data that appears is represented as units of single raw counts of barcoded molecules. We performed the advanced analysis with generation of an nCounter Advanced Analysis Report. The software will automatically perform QC and normalization using internal controls.

3.3 CAR design and manufacturing

3.3.1 ROR1 CAR with inducible system design (scFvs: anti-PD-1 derived from nivolumab and pembrolizumab)

The first sets of experiments to test the inducible cassette system were made by co-transduction of fresh T cells using two vectors: the first one encoding for the anti-h ROR1 CAR_{BFP}, the second one containing the inducible cassette cloned from the plasmid pBSNFAT#6-IL2Pmin-GFP.

As co-transductions translate into low transduction efficiency, the aim is to have all the elements in one multicistronic expression vector to avoid co-transductions that usually result in a lower transduction efficiency.

The final expression vectors were therefore cloned to contain the following elements in this order after the PGK promoter:

- mCherry (reported gene) + T2A peptide
- F CAR (anti-hROR1 CAR) with final STOP codon
- IRES
- Either inducible promoter ($NFAT_6$+minIL2 promoter) or EF1α promoter
- Albumin/IL2 signal peptide (SP) and anti-PD-1 scFv(s)

The whole vector with the first two elements of the transgene (reporter gene + ROR1 CAR) comes from the in-house 2nd generation ROR1 CAR vector. The 2A peptide between reporter gene and CAR was placed to allow multiple protein production from one transcript. Modifications were made as follow: additional Kozak sequence (ACCATG, at the beginning of the signal peptide before the secreted protein) to allow improved protein translation: the internal ribosomal entry site (IRES) element in the intercistronic spacer between the two regions (reporter gene plus F CAR and new insert with either inducible or constitutive promoter followed by the secreted scFv) to get translation of the protein coding region downstream of the CAR independently of the 5'-cap structure bound to the 5' end of the mRNA molecule. Following the IRES, cloning was performed to transfer the 6xNFAT cassette and the minimal IL-2 promoter whereas for the constitutive system, a g-Block containing the EF1α promoter has been designed. As secreted protein, anti-PD-1 scFvs was selected.

3.3.2 Transfection of HEK 293Ts to make lentivirus

Functional lentiviral particles are generated by transfecting HEK-293 T cells with a 2nd or 3rd generation lentiviral packaging system (Addgene). Expression vectors for CARs contain a reporter gene that will be expressed by cells with plasmid DNA integrated in their genome. This gene encodes for the fluorescent protein mCherry (visible in the YG channel on the flow cytometry machine), BFP or GFP.

Other reagents required for the reaction are plain media (IMDM) and GeneJuice® Transfection Reagent (Millipore), a reagent optimized for maximum transfection efficiency and very low toxicity. The amounts of each reagent for a 10cm dish containing 293Ts at 75-90% confluency are summarized below:

Reagent	Amount (µl or µg)
IMDM	470 µl
GeneJuice	22.5 µl
Transfer vector	3.13 µg
pMDLgRRe (packaging)	* 4.06 µg
pMD.G2 (envelope)	2.19 µg
PRSV Rev (packaging)	* 3.3 µg

* For 2nd generation, these plasmids are replaced with pCMV delta R8.2 packaging vector (4.06µg).

3.3.3 PBMC activation

The day after the transfection, freshly isolated or thawed PBMCs are washed, counted and re-suspended at 2x10^{6}cells/ml of RPMI-10. Dynabeads® Human T-Activator CD3/CD28 (Thermo Fisher) are added following manufacturer's protocol to allow T cell expansion and activation. Cells are then seeded in a TC-treated 24well/plate at 1ml/well prior overnight incubation at 37°C.

The same day, a 24well-plate (non-tissue culture treated) is coated with 500µl/well with Retronectin (recombinant human fibronectin fragment, which enhances transduction efficiency) and stored at 4°C.

3.3.4 Transduction of activated PBMCs

The next day, early in the morning, 1ml/well of IL-2 at 1 IU/ml of RPMI-10 is added to the activated T cells to further expand them. At least 6 hours later, PBMCs are harvested, washed and re-suspended at 0.6x10^{6}cells/ml. The virus that will be used for transduction is harvested from the plates containing 293Ts and filtered using 0.45µm filters. Importantly, the virus from now on needs to be kept on ice. After removing Retronectin from a pre-coated plate (Retronectin can be transferred to a fresh plate and stored in the fridge until next use no more than twice), 0.5ml/well of cells (with 4IU/ml of IL-2) are added, followed by 1.5ml of fresh filtered virus. Importantly, we add 1.5ml I-10 media in well(s) to get 'non-transduced' (NT) T cells. It is possible to use frozen virus. The plate is then centrifuged at 1000xg for 40 minutes, followed by incubation at 37°C for 4 days.

After four days, cells are harvested and checked via flow cytometry for transduction efficiency based on percentage of T cells expressing the reporter gene against the negative sample (NT T cells). Cells are left in culture to expand with 0.5 IU/ml of IL-2 for several days depending on the amount needed for experiments but generally no longer than 2 weeks.

3.4 Anti-PD-1 ScFv design and manufacturing

The FASTA sequences for the anti-PD-1 antibodies pembrolizumab and nivolumab were obtained from ImGT website (ImMunoGeneTics, http://www.imgt.org). The final scFv is made of the variable heavy chain (up to CH1 sequence) and the variable light chain (up to VC sequence) from the full antibody sequence. The linker and the N-terminal His-tag used are the same used for the in-house ROR1 BiTE. The final sequences were synthesised as g-Block fragments (IDT) that were then cloned into PGK expression vectors. Those vectors, which allow for constant production of secreted scFvs, were transiently transfected into 293Ts and supernatant was collected for binding assays. Once confirmed the scFvs are secreted and bind to PD-1, cloning was done to insert the pembrolizumab scFv into the NFTA-inducible system.

For protein detection and quantification, the molecular weight of the scFv from pembrolizumab has been calculated using the ExPASy ProtParam website based on the one-code amino acid sequence.

3.4.1 Transient Transfection of 293Ts to make scFVs

The reagents required are plain media, polyethylenimine (PEI) transfection reagent and transfer vector. 10cm dishes are generally used to get the best transfection efficiency (per dish: 470µl plain media, 30 µl PEI and 12.5 µg DNA). All expression vectors contain a reporter gene for the green fluorescent protein (GFP) or mCherry. After 72h, supernatant containing the His-tagged protein(s) is harvested, filtered (0.22µm filters) and 293Ts are checked via flow cytometry for GFP/mCherry expression to get a quick indication of transfection efficiency. Our ScFvs in supernatant that are stored at 4°C are very stable and can last for months.

3.5 *In vitro* Functional assays

3.5.1 Binding characterization assays

To make sure that BiTEs or aPD-1 scFvs bind to their specific targets (e.g. ROR1 and CD3 for ROR1 F BiTE and PD-1 for the scFvs nivolumab and pembrolizumab), supernatants containing the His-tagged proteins are tested via Flow cytometry as follow: 72h after transfection of HEK 293Ts, at the bottom of FACS tubes target cells are pelleted (e.g. PBMCs and SKW which are CD3+ and ROR1+, respectively) and 1ml of supernatant containing the protein(s) is added on top of target cells prior to incubation at 4°C for at least 1h. After washing the tubes with PBS, the supernatant is carefully removed up to roughly 100µl/tube. APC-anti-His Tag antibody is added to each tube (R&D, 5µl/reaction) which is vortexed well before another incubation at 4°C for 1h. The negative control commonly used is made of target cells incubated with plain media followed by antibody staining which gives the background for the signal. The antibody should bind to all our His-tagged ScFv proteins (BiTEs, anti-PD-1, etc.). After the second incubation, FACS tubes are washed again and pellet cells are re-suspended in 200-300µl of PBS prior to flow cytometry analysis.

To test the induced secretion of scFvs, effector cells are incubated for 24h with targets positive and negative for ROR1 (e.g. Kasumi2 and SupT1) at an effector to target ration of 1:10. Supernatant is collected 24h later and binding checked via flow cytometry with target cells positive for PD-1.

3.5.2 Production quantification via ELISA

To quantify the secreted scFv, an in-house PD1 ELISA was developed. The standard curve was generated using serial dilutions of the FPLC purified scFv. Briefly, PD1 protein (#1086-PD-050, R&D Biosystem) was coated at 1µg/mL of carbonate buffer overnight at 4°C. All subsequent incubation steps were incubated at 37°C. We used TBS+0.1% Tween for the washing steps. Blocking was performed using TBS-Tween+3% filtered BSA (Sigma) for 1h. Samples were incubated for 4h, followed by incubation with anti-His HRP-conjugated antibody (1:10,000 dilution). Revelation was performed by adding

freshly made OPD for 5-10 minutes prior stopping the reaction with sulphuric acid. Absorbance was read at 492nm using a plate reader (SpectraMax® i3).

3.5.3 Killing assays with adherent cell lines

For adherent target cell lines, flat bottomed plates are used. On day one, targets are seeded at 10,000 cells/well in 50µl of media in a 96well-plate (short-term co-culture) or at 40,000 cells/well in 500µl media in a 24well-plate (long-term co-culture).

The following day, 100µl (96well) or 500µL (24well) of CAR-T cells/well are added at the wanted effector to target (E:T) ratio after eventual normalisation of transduction efficiency. Plates are then incubated at 37°C for up to 96h.

Cytotoxicity is assessed via flow cytometry: plates are washed with PBS, then Trypsin is added to each well. Plates are placed in the incubator until the cells are detached (via microscope). Cells are then harvested using a mastermix of PBS, 1%FBS and viability dye; when specified, labelled antibodies for CD3 (T cells) and/or target cells (such as CD19) are added to the mastermix as well. The whole well content is transferred to mini FACS tubes, which are incubated at 4°C for 30 minutes prior flow cytometry analysis.

Counting beads (Flow-Check™ Fluorospheres, Beckman Coulter) are used for the flow cytometry-based killing assay where the number of beads (events on the machine) is recorded, ranging between 1,500 and 5,000/sample. When analysing data, the numbers of targets and effectors in each well is normalised to the number of beads recorded in order to eliminate any human/machine errors or alterations.

3.5.4 Killing assays with non-adherent cell lines

V bottom 96-well plates are used for co-culture using non-adherent target cell lines. Both targets and effectors are seeded on the same day. 25,000 cells/well (in 50µl) is the standard minimum amount of targets seeded. To

add the effector cells, we use the same protocol used for adherent cell lines to add effectors. After seeding all the components, plates are centrifuged at 400g for 5 minutes and then stored in the incubator. After 24h (or when needed), cells are washed and harvested with the same mastermix used for adherent targets prior flow cytometry analysis.

3.5.5 Cytokine ELISA

Supernatants from co-cultures is collected 24h post set-up to be tested for cytokine production by CAR-T cells. The cytokines quantitatively tested are IL-2, IFNγ and TNFα. Supernatants are diluted 1/50 and tested using the ELISA MAX™ Deluxe kits and protocols (Biolegend). After reading the absorbance (last step on the protocol), data are converted to concentrations compared to the standard curve, and subsequently plotted on tables using GraphPad Prism software. Graphs always include error bars from the triplicates of each sample. 1way Anova is usually calculated with multiple comparisons; refer to figure legends for specific statistical analysis.

3.6 *In vivo* Functional assays

Animal work is performed under the authority of the United Kingdom Home Office Project and Personal License regulations and animals are bred, treated, and maintained under pathogen-free conditions in-house under University College London guidelines.

NOD Scid Gamma (NSG) mice are purchased from Charles River and at 6-8week old are injected subcutaneously with $2x10^6$ MDA-MB-231-fLuc+ cells in 100µl of PBS in the left mammary fat pad (orthotropic model). 6 days later tumour engraftment is confirmed via bioluminescence imaging (BLI); the following day (day 0) mice received 1 tail vein injection of $4x10^6$ CAR-T cells in 100µl of PBS. When combination therapy was used, mice received a total of 3x intraperitoneal (IP) injections of 250µg/mouse of anti-PD-1 monoclonal antibody (Biolegend, clone EH12.2H7) on day 0, 3 and 7.

Tumour growth is monitored via size measurement using digital callipers (formula: (Height x Length x Width)/2) and via bioluminescence imaging (BLI) of Luciferase+ cells. During imagine, mice are anaesthetised via isoflurane. Luciferase expression is detected using D-Luciferin (Melford Laboratories) which is injected IP at 200 mg/mouse, with subsequent BLI performed using the IVIS Imaging System 100 Series (Perkin Elmer) once a week for up to 4 weeks post CAR-T cell treatment. The photons emitted from fLuc-expressing cells in the animal body are quantified using Living Image software (Xenogen). Photon counts are normalised using the software ROI tools section before getting the images and calculating average luminescence. This is done by drawing a square to highlight the whole mouse. The same square is the copied and pasted to all other mice to ensure same surface area; the value we were interested in was Average Radiance Values [p/s/cm²/sr].

To check animal health pre and post treatment, animals are monitored daily for signs of pain or distress and weighted every 2-3 days to ensure that the animals did not surpass the limit of 10% weight loss.

Survival of animals was also monitored, and animals were sacrificed when they either reached a humane endpoint or when the tumour size reached the limit of our license (1.5cm total).

3.6.1 Ex-vivo TIL assessment

When mice were sacrificed, tumours and spleens were harvested for immunohistochemistry analysis or flow cytometry analysis. For flow cytometry analysis, tissues were finely cut and digested for 1h at 37°C with slow agitation with RPMI-10 containing DNAseI and CollagenaseI. After the hour, tissues are passed through a nylon cell strainer (70µm) to remove clumps and tissues, and washed 1x in PBS. To eliminate red blood cells, cells are incubated with 1xRBC Lysis buffer (BioLegend) following manufacturer's instruction. After additional wash, cells are counted and stained with viability dye and FITC-anti humanCD45 antibody (Biolegend, clone HI30). Samples are then analysed via flow cytometry and total CD45+mCherry+ cells are counted and normalised to the total #events recorded.

TILs were sorted for the Nanostring experiment. Briefly, once TILs were extracted by digested tumours collected at the same time, staining was performed for viable cells and human CD3. Sorting was performed at the Flow Cytometry Core facility for double positive CD3 and mCherry cells. Cells were lysed in RLT buffer and re-suspended at the same cell concentration prior storage at -80°C.

3.7 Immunohistochemistry

Organs and tumours were harvested and placed into pots containing 10% neutral buffered formalin (Cellpath). Sectioning, embedding and human CD8 staining was performed by Francesca Launchbury at the UCL Institute of Neurology. CD8 quantification, as well as mCherry staining and quantification were performed blindly by Dr Elena Miranda in the pathology department at UCL Rockefeller building. Detailed information will be in the figure legends.

Chapter 4 Development and characterisation of CAR-T cells secreting αPD-1 scFv

4.1 Introduction

We have successfully developed a fully humanized binder named F that targets a novel epitope on the membrane-proximal frizzled domain of ROR1, and previously reported its efficacy against a broad range of malignancies in a Bispecific T-cell engager (BiTE) and in a second-generation CAR format (324, 325).

Our CAR-T cells are generated via lentiviral transduction. To make functional viral particles, we use a third generation pCCL lentiviral expression vector in which the CAR and fluorescent protein mCherry (327) are cloned downstream of a PGK (phosphoglycerate kinase) promoter and are separated by a FMD2A peptide, making a bicistronic vector. We included mCherry for a simple flow cytometry-based method to delineate transduction efficiency without affecting T cell function; moreover, it allows easy normalization of different CAR preparation to obtain more meaningful comparisons between different constructs by decreasing bias introduced by variation in transduction efficiencies. Downstream of the CAR we have included a WPRE (Woodchuck Hepatitis Virus Posttranscriptional Regulatory Element) to enhance the transgene expression (328). The CAR is a second-generation structure containing the humanized F binder, an extracellular hinge and CD8 transmembrane domain, followed by 41BB and CD3ζ intracellular signalling domains (329) (Figure 4-1 adapted from (5).

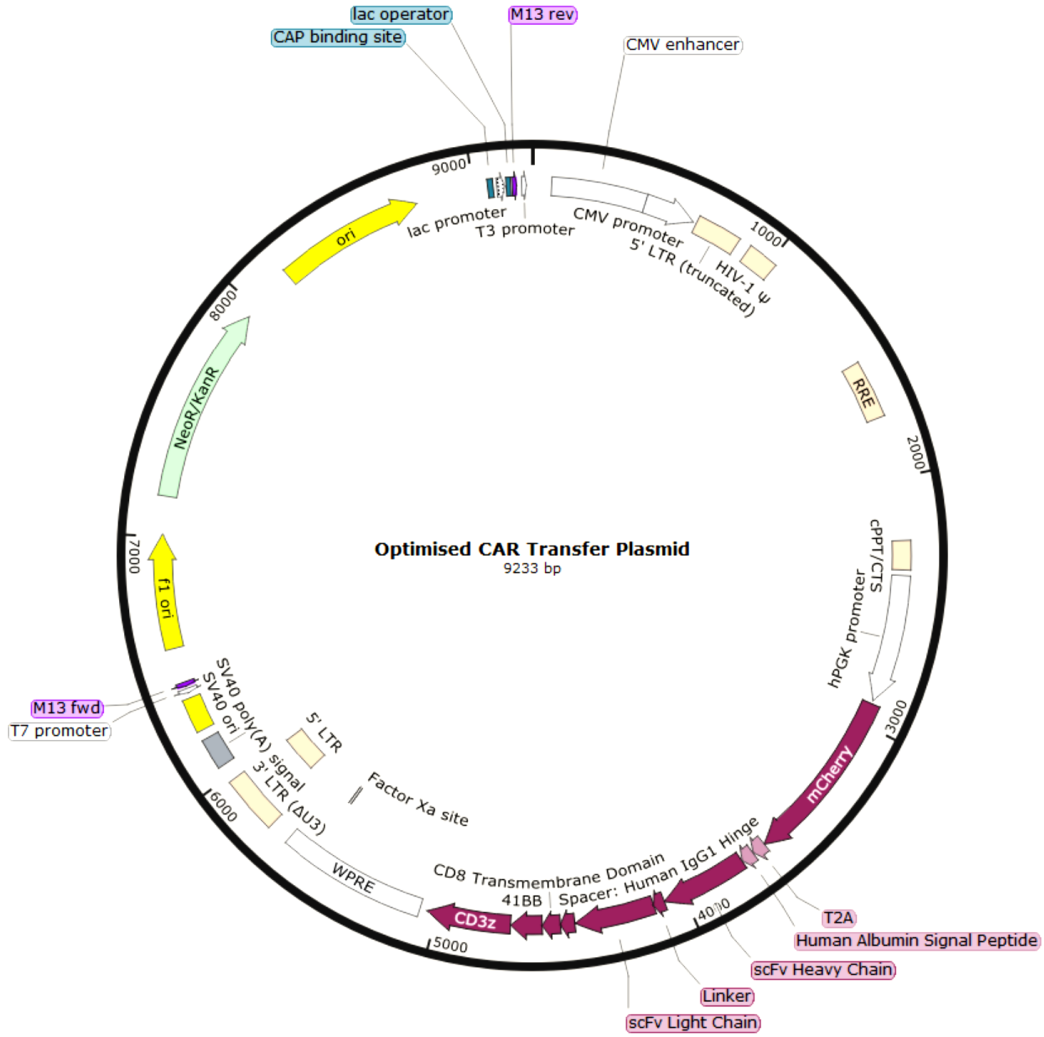

Figure 4-1: Optimised transfer plasmid for CAR-T cell production. The CAR sequence of choice was cloned into a 3rd generation lentiviral construct with a human PGK promoter. mCherry was used as a transduction marker and followed by a T2A ribosomal skipping element. The scFv sequence was placed in a heavy chain, linker, and light chain format and utilised the hinge spacer from human IgG1. This was followed by a CD8 transmembrane domain with 41BB and CD3 intracellular signalling arms. The design was modular such that each component could be switched with simple cut and paste cloning.

In this chapter we investigate the potential influence of immunological checkpoints on CAR-T cell function and use this information to develop a strategy that attempts to improve T cell function. The following table shows a summary of the constructs used in this chapter with transgene schematics, plasmid name and page where the plasmid is mentioned.

Table 5: Summary of transgene schematics of the plasmids used in this chapter. Schematics include corresponding plasmid name and page. Not included in the schematics is the WPRE sequence downstream of the last element (CAR, reporter gene or anti-PD-1scFv). PGK= Phosphoglycerate kinase; 2A= FMD2A peptide; mouseFc = murine Fc fragment; orange X represent stop codon, blue diamond represents signal peptide.

Transgene schematic	Plasmid name	Page text
	PL166	85
	PL182	89
	PL365	89
	PL191	93
	PL241	93
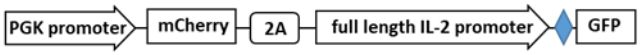	PL210	93
	PL268	96
	PL284	100
	PL315	100
	PL321	101
	PL344	103

4.1.1 ROR1 CAR-T cells upregulate surface PD-1 in the presence of the targeted antigen

As PD-1 is often upregulated on TILs and CAR-T cells, we assessed the surface expression of PD-1 on our ROR1 CAR-T cells via flow cytometry from several in vitro co-culture conditions to see if any difference could be observed. When ROR1 CAR-T cells were left in culture with recombinant IL-2 following transduction, we detected stable low surface PD-1 levels (average of 0-10% PD1+ CAR-T cells, *n*=3, day 0 in Figure 4-2). Similarly, surface PD-1 did not increase substantially when the CAR-T cells were co-cultured with the ROR1negative T-lymphoblastic leukaemia cell line SupT1 (black triangles). When co-cultured with ROR1+ cell lines MDA-MB-231 (TNBC) H1975 (NSCLC) and Kasumi2 (ALL), CAR-T cells showed rapid upregulation of surface PD-1 (7-9-fold increase, pink symbols) after 24h, which correlates with canonical T cell activation. PD-1 surface expression remained consistently high up to 96h of co-culture when target cells were still present, suggesting an acquired exhausted phenotype by CAR-T cells with long-term antigen stimulation.

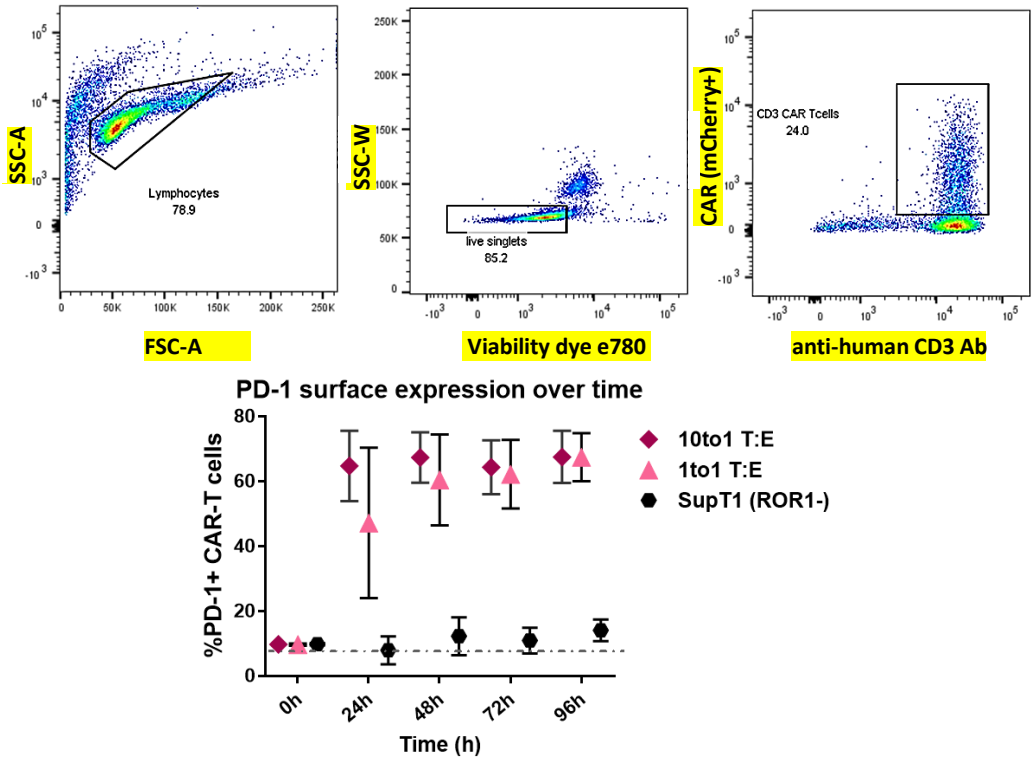

Figure 4-2 Gating strategy and surface PD-1 measurement via flow cytometry. Freshly isolated PMBCs from three healthy volunteers were transduced to express ROR1 CAR. After transduction, CAR-T cells were cultured is different settings and checked via flow cytometry for surface PD-1 expression at various time points: top panel: gating strategy for detection of surface PD-1 from CD3+ CAR-T cells (CD3+mCherry+ cells); bottom graph: %PD-1+CAR-T cells before co-culture (0h) and after co-culture with 4 different cell lines: ROR1+ Kasumi2, MDA-MB-231 and H1975 (pink symbols) and ROR1- cell line SupT1 (black symbol) at 10:1, 5:1 and 1:1 T:E ratios. Bars represent SD between the different cell lines and between the three donors at a given T:E ratio.

4.2 αPD-1 scFv manufacturing and characterisation

4.2.1 Cloning of PD-1 binders in a single chain variable fragment (scFv) format

Based on the marked and stable upregulation of the immune checkpoint PD-1 by our CAR-T cells, we developed a monotherapy approach that leads to secretion of anti-PD1 scFv upon activation of CAR-T cells using the NFAT inducible promoter (330). We hypothesize that a spatially targeted checkpoint blockade delivery will enhance CAR-T cell effectiveness whilst limiting off-tumour toxicities that often arise with systemic checkpoint blockade therapy (331, 332).

Variable chains from the commercial antibodies pembrolizumab and nivolumab were paired by a short amino-acid linker sequence to generate the respective antibodies in a single chain variable fragment (scFv) format. To facilitate detection and purification, an N-terminal hexa-histidine (His) tag was added. The resulting sequences were generated as g-Blocks and cloning was done to replace the reporter gene mCherry with the αPD1 scFv from either nivolumab or pembrolizumab:

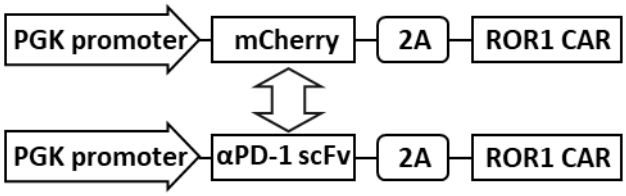

In his way, constitutive scFv production is driven by the PGK promoter (PL182), allowing us to easily produce the scFvs via transient transfection of HEK-293T cells. Material and methods section 3.4.2 contains more detailed protocols.

4.2.2 Production and binding assessment via flow cytometry

HEK 293T cells were transiently transfected with the two expression vectors to secrete αPD-1 scFv from either pembrolizumab or nivolumab. Supernatants were collected after 72h and were incubated with our engineered SupT1-PD1+ cell line (GFP+). To assess binding capacity, after a washing step to remove unbound material, an APC-conjugated anti-His antibody was added, and a further incubation step was performed before flow cytometry analysis. Figure 4-3 shows representative double positive populations of His-tagged αPD-1 scFv (*y* axis) bound to PD-1/GFP+ target cells (*x* axis) which were always above 90% showing specific binding of the scFv to surface PD-1

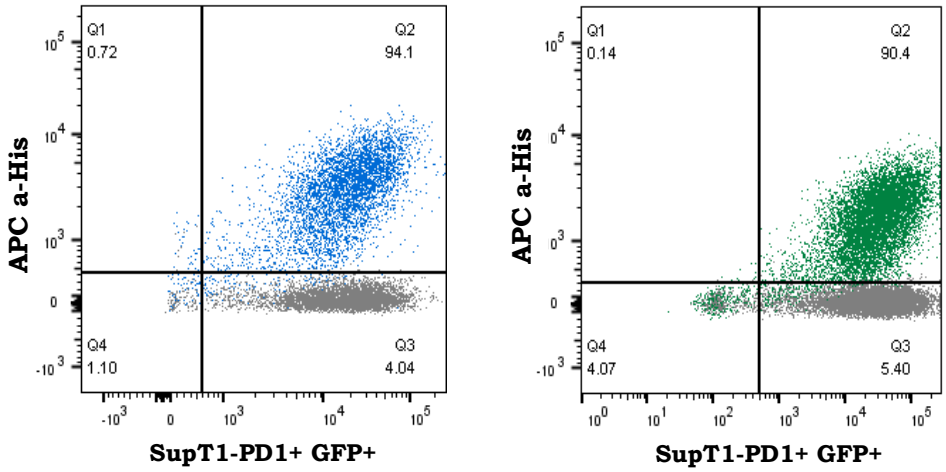

Figure 4-3 Binding assay via flow cytometry. scFv binding was assessed using our engineered SupT1-PD-1+ cells (GFP+) as targets. Negative control is target cells with detection antibody APC-anti His Tag only. Gates were set up based on negative control plots. Left panel: pembrolizumab scFv showed 94% of double positive population for GFP (targets) and APC (his-tagged scFv). Right panel: nivolumab scFv showed 90.4% double positive shift.

4.2.3 αPD-1 scFv binding kinetics using surface plasmon resonance (SPR)

Next, to better characterise the binding kinetics of the pembrolizumab-derived scFv, we undertook SPR experiments on a Biacore X-100 to define affinity constants for the interaction with recombinant PD-1 protein.

Cloning was performed to link the αPD-1 scFv from pembrolizumab to a mouse Fc stalk (PL365) to allow binding to the CM5 sensor Chip, coated with a mouse capture kit. Following transient transfection, supernatants containing the αPD-1 scFv-mFc were concentrated using Amicon Ultra centrifugal filter units. We made a total of four independent productions (roughly 15mL supernatant each) then supernatants were combined and concentrated into two separated stocks. The concentrated supernatants were tested via flow cytometry to confirm binding to PD-1 and via Western Blot to assess the product quality. Using an HRP-conjugated anti-mouse IgG mAb we detected the binders at the correct size (about 55kDa) for both supe#1 and supe#2, along with the full mIgG1 Ab control (2 bands as reducing conditions were used, Figure 4-4).

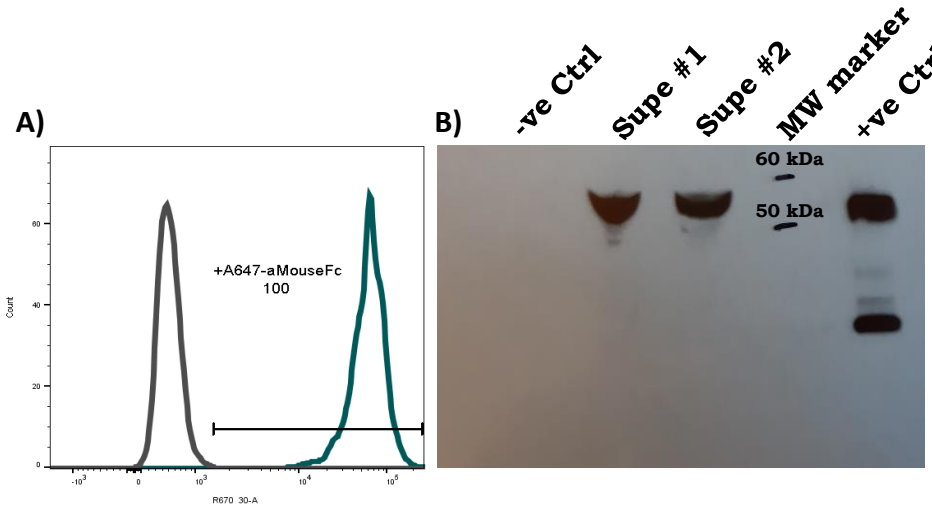

Figure 4-4 αPD-1 scFv binding assessment. The newly generated αPD-1 scFv linked to a mouse Fc stalk was generated via transient transfection of HEK-293T cells. Supernatant was then concentrated and tested as follow: A) flow cytometry binding assay against the same PD-1+ cell line using a A647-conjugated anti-mouse IgG to confirm no changes in binding to the target; B) concentrated supernatants from 3 independent productions were tested via Western Blot under reducing conditions to confirm presence of the correct product (expected band size: 55kDa) and similar amounts between batches. Positive control: purified mouse IgG1κ antibody, negative control: non-transfected concentrated media.

For the SPR experiment, we selected a single-step multi-cycle protocol where we coated sensor Chip (CM5) with the αPD-1 scFv-mFc, to which we then added increasing concentrations of the analyte, the PD-1 protein. We performed a total of 4 runs on the Biacore: 3 independent runs, of which a representative sensogram is showed in Figure 4-5 and a control run, where we used the same settings and reagents but on a human Fc capture sensor Chip. With this experiment we obtained the background/baseline of the binding. Dr Muczynski kindly performed the downstream analysis and calculated the affinity values, where representative values were: Ka (1/Ms) = $7.15e^{+05}$, Kd (1/s) = 0.00246 and K_D (M) = $3.54e^{-09}$. This means that the scFv retained very good affinity for PD-1. The K_D reported for pembrolizumab antibody is 29 pmol/L (333)

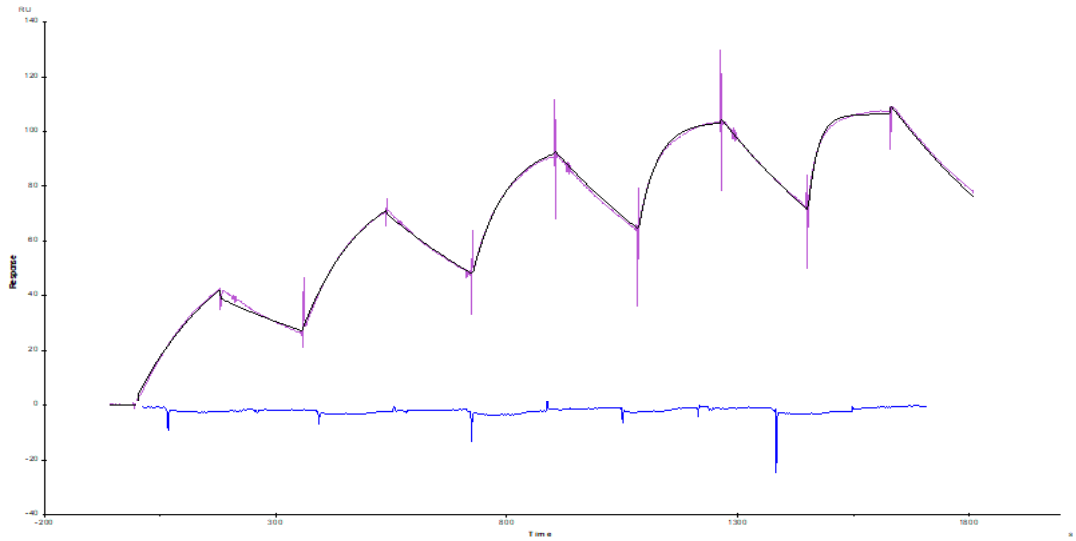

Figure 4-5 Representative SPR sensogram. (1 of three independent runs) showing binding to increasing concentrations of PD-1 protein (from 0µg/ml to 2.5µg/ml) in Response Units (=RU, *y* axis) with association/dissociation cycles over time (*x* axis). Baseline (blue line): No cross-linking of the aPD1scFv-Fc was expected and therefore no binding from the sensogram was detected. Experimental setup and downstream analyses were kindly performed by Dr Vincent Muczynski. ka = association rate constant, kd = dissociation rate constant and K_D = equilibrium dissociation constant.

4.3 Manufacturing of CAR T cells with inducible promoter

4.3.1 Generation of the inducible system cassette

The detailed cloning strategy is found in materials and methods section 3.1.2 and is based on the work by Hoojiberg and colleagues (334). Following their methodology, we first generated the pBS-$NFAT_6$-$IL2_{min}$ vector, containing the inducible cassette made of 6 repetition of NFAT followed by the minimal IL-2 promoter. The inducible expression cassette was then transferred into the backbone of a pCCL.PGK vector which was then named PL241. For the preliminary functional assays, we inserted the reporter gene GFP downstream the inducible system to allow for easy detection of the signal via flow cytometry. The schematic of the inducible system was the following:

4.3.2 Detection of induced GFP expression via flow cytometry

The first *in vitro* experiment to evaluate the functionality of the inducible system had the following settings:

Fresh T cells were co-transduced with viruses made using the following expression lentiviral vectors:

1- Vector for constitutive anti-ROR1 CAR expression with a BFP reporter gene ($CAR_{BFP,}$ PL191)
   And:
2- Plasmid 241: vector containing the inducible cassette (6xNFAT followed by the minimal IL-2 promoter) to drive GFP expression, plus constitutive expression of mCherry reporter gene *or*
3- Plasmid 210: vector containing a full-length IL-2 promoter followed by GFP and expressing mCherry as well

The reason for including vector 3 (PL 210) was to evaluate whether the full-length would give better induction than minimal IL-2 promoter in these settings. The negative controls were 'CAR only', or T cells transduced only with the CAR_{BFP} plasmid, or double-transduced CAR-T cells expressing the co-cultured with the ROR1- target cell line. These controls would generate total absence of GFP (former) and non-specific GFP induction (latter).

Before setting up the co-culture assay CAR-T cells were checked for transduction efficiency (% double positive for mCherry and BFP) and normalised to have the same transduction level. ROR1+ target cell line used was the mantle cell lymphoma Jeko1. Target and effector cells were seeded at 1:1 T:E ratio in a 96well-plate in triplicate (2 donors) and conditions were checked for GFP expression via flow cytometry at: 0h, 24h, 48h, and 72h. Figure 4-6 shows the gating strategy (top panels) and flow cytometry results. The gating strategy is showing GFP signal (panel on the right) from live double positive CAR-T cells. The background or baseline GFP signal was roughly 2-5% for both constructs (210 and 241) alone, suggesting minimal non-specific induction from both systems, but when CAR-T cells were co-cultured with

SupT1 cell line, we measured increased GFP signal over time. With the minimal IL-2 promoter, GFP expression increased up to 8% (peak at 48h), whereas for the full-length IL-2 promoter the signal went up to 16% at 72h (3 times more than the signal from effector cells without targets), suggesting a non-specific induction of GFP which was more marked for the 210-CAR-T cells; we hypothesise this might be due to the strength of the full-length IL-2romoter compared to minimal promoter of plasmid 241. Against the ROR1+ target Jeko-1, we observed induced GFP expression up to 23% and 15% for 210 and 241, respectively, which sustained for the whole 3 days of co-culture.

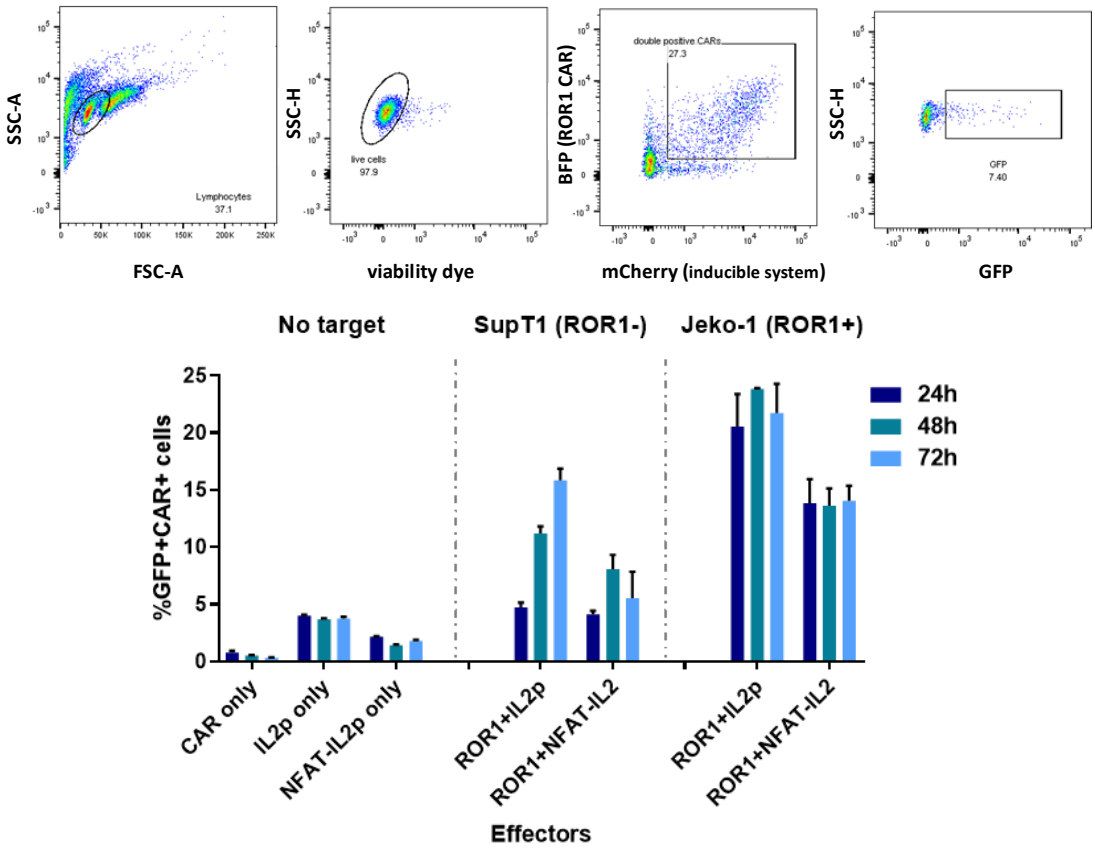

Figure 4-6 GFP expression is induced in the presence of the targeted antigen. Fresh human T cells from 2 donors were co-transduced with two lentiviruses to express a CAR (either GD2, nonspecific, or ROR1) and the inducible system (either NFAT-IL-2min or full-length IL-2 promoter). Co-cultures were set up with Jeko-1 (ROR1+) and SupT1 (ROR1-) cell lines and GFP expression was measured via flow cytometry over time (24h, 48h, and 72h). Top panel: flow cytometry gating strategy to obtain the %GFP from co-transduced CAR-T cells (gated on respective reporter genes mCherry and BFP); bottom graph: summary of GFP expression: background GFP is the average %GFP (5%) from co-transduced cells expressing the irrelevant CAR or co-transduced cells cultured without target (labelled 'only'). Results are mean+SD of 2 donors plated in triplicate.

From this preliminary assay we concluded that both inducible systems worked in the presence of ROR1 (induced GFP detected over time) and decided to proceed using the inducible system with the minimal IL-2 promoter because, despite showing weaker GFP signal compared to the full-length promoter, the leakage or non-specific induction was also much lower (almost half).

We therefore set up further *in vitro* experiments using only two plasmids for the effector cells: one for constitutive ROR1 CAR expression (PL166) and one for inducible GFP expression (PL241). Once freshly isolated human T cells were transduced, co-cultures were set up with several target cell lines with different ROR1 surface expression levels (Figure 4-8 for representative flow cytometry plots) to provide an insight into functional differences when targeting cell lines expressing different targeted antigen levels. CAR-T cells were checked for GFP expression up to 72h of co-culture: and we confirmed the mild leakage of the system (roughly 15% GFP, orange dotted line in Figure 4-8) when CAR-T cells were cultured with ROR1- target cells or alone. In terms of inducible expression, the peak was at 24h for all cell lines, with SKW 6.4 being the target cell line inducing the highest GFP expression (up to 52% versus an average of 40% for all other ROR1+ target cell lines). We assumed that this increased induction was likely due to the highest ROR1 expression compared to the other cell lines. GFP expression decreased an average of 10% over time, with almost no difference between 48h and 72h, demonstrating functional induction over time.

In summary, with these preliminary co-cultures we show that the inducible system, made of 6 repetitions of the NFAT molecules followed by either a minimal or a full IL-2 promoter, is functional as GFP expression was detected from activated CAR-T cells in the presence of the targeted antigen up to 72h of co-culture in two independent co-cultures and using 4 different donor-derived T cells.

As we were able to generate PD-1 binders in a scFv format and a functional inducible system, the following steps focused on the generation of ROR1 CAR-T cells able to secrete αPD-1 scFv through the inducible system.

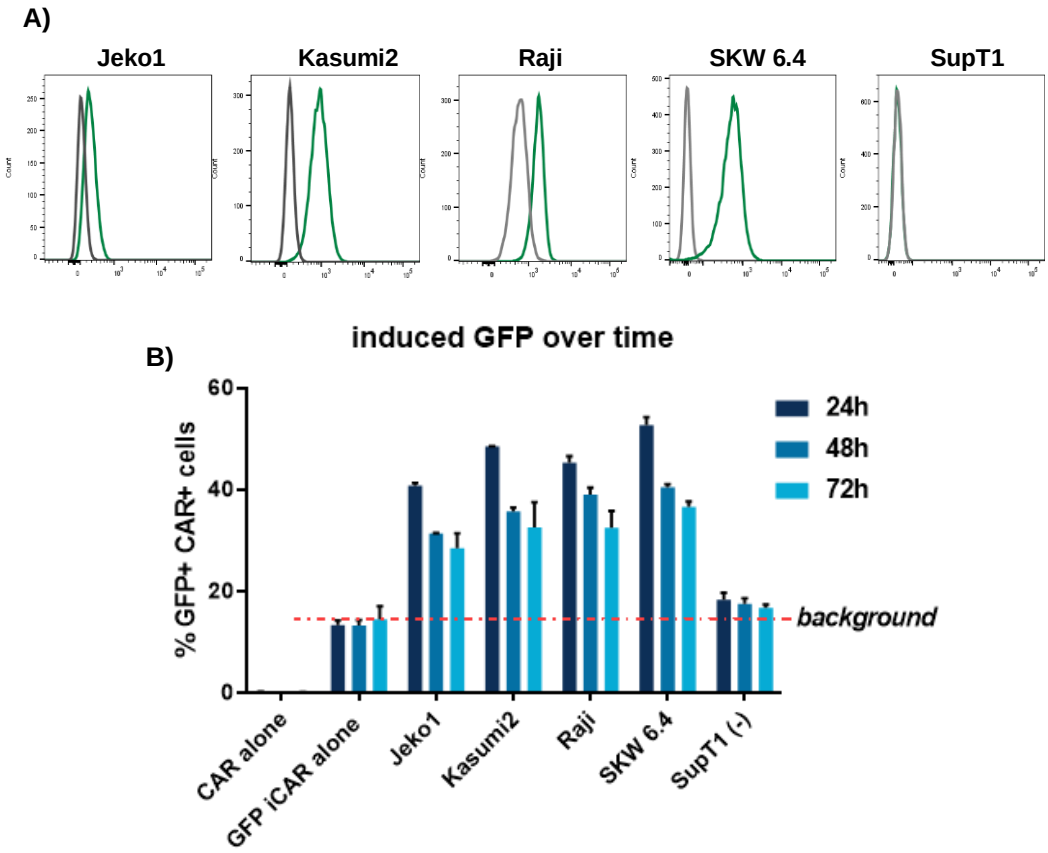

Figure 4-7 Second co-culture for i-GFP expression. A second co-culture was set up, this time with more ROR1+ cell lines and only using co-transduced T cells expressing ROR1 CAR and the NFAT inducible system; A) representative flow cytometry histograms showing ROR1 surface expression on target cell lines (green shift versus isotype control peak, in grey); B) %GFP+CAR-T cells: as control, T cells were transduced to express the CAR only, without the inducible GFP system. As before, cells were harvested at different time points and analysed via flow cytometry for GFP expression. Background line is the average signal from double transduced CAR-T cells alone in the absence of stimulus.

4.3.3 Generation of the single construct for inducible αPD-1 scFv secretion

Cloning was performed to replace the GFP with the αPD1 scFv and to place all the elements into one multicistronic expression vector. Shown below is the transgene schematics of PL268 (refer also to table 4-1 page 86):

To confirm the induced secretion of the scFv, we set up several *in vitro* co-cultures using freshly transduced T cells incubated with ROR1+ (Kasumi2) and ROR1- (SupT1) target cell lines at 5:1 T:E ratio. We collected supernatants after 24h to detect the secreted αPD-1 scFv labelled with His-tag using the flow cytometry-based binding assay to the SupT1 PD-1+ cell line. The negative control was ROR1 CAR-T cells only (lacking the inducible system), whereas CAR-T cells with constitutive secretion of anti-PD-1 scFv were used as positive control.

Figure 4-9 shows representative flow cytometry plots where, as expected, the highest binding or histogram shift from baseline is given by supernatant from constitutive secretion of αPD-1-scFv, followed by supernatant from CAR-T cells with the inducible system (from now on referred as i-CAR T cells) co-cultured with ROR1+ target cells. Negative histogram shifts (overlapping with the baseline from the APC-conjugated anti-His antibody) were always detected with supernatants from either ROR1 CAR-T cells only (control) or from i-CAR-T cells co-cultured with ROR1- cell lines (non-induced). The non-induced negative shift suggests that the mild leakage of the system, if still present, is not producing enough αPD-1 scFv to be detected via flow cytometry.

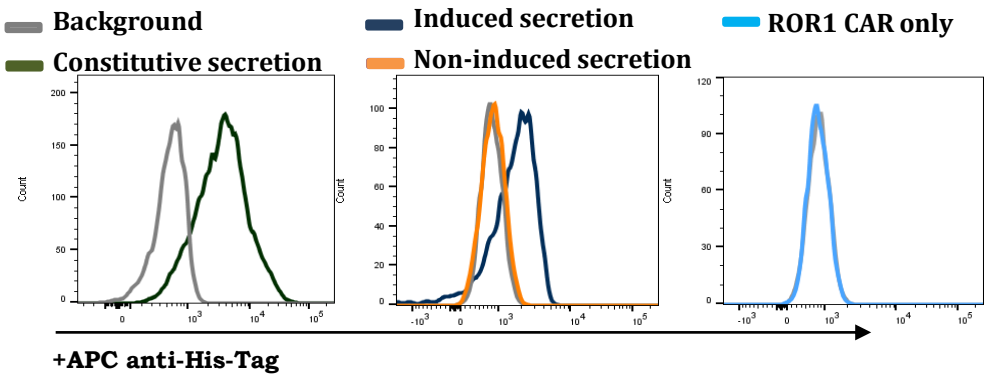

Figure 4-8: Representative plots for scFv binding to PD-1+ cell line upon CAR T cell activation. Co-cultures of ROR1 i-CAR-T cells with ROR1+ and ROR1- targets were set up to assess constitutive and inducible secretion of αPD-1 scFv at 1:10 E:T ratio. After 24h, supernatant was collected and assessed via flow cytometry for binding to the PD-1+ cell line. Binding was detected using an APC-conjugated anti-His-Tag antibody. Representative flow cytometry histograms show binding from either constitutive secretion or i-CAR-T cells with ROR1+ target (green and dark blue peaks, respectively, as opposed to grey baseline), whereas no shift of the histogram (no binding) were detected with either ROR1 CAR only (control, light blue histogram) or with ROR1 i-CAR-T cells without the targeted antigen (yellow histogram).

4.3.4 Troubleshooting for T cell transduction efficiency

Freshly isolated T cells from healthy volunteers are transduced with lentiviral particles made using the pCCL.PGK lentiviral expression vectors. Transduction using these vectors to express one of our second-generation CARs yields between 50% and 80% mCherry+ T cells, whereas the transduction levels using the new transgenes containing the inducible system are at best 40%, requiring sorting of mCherry+ T cells before performing functional experiments. As this process is time consuming and unpractical, not to mention the fitness variability of the sorted primary cells, we decided to assess several strategies to increase the transduction efficiency for these constructs to avoid the need for sorting.

4.3.4.1 Viral titre

We thought the first thing was to make sure that good titres of virus were made. To calculate viral titres, we set up infectious assays using HEK-293T cells. Briefly, HEK-293T cells are infected with the virus of interest which is titrated and combined with polybrene (5μg/mL) prior storing the cells in the incubator for 3 days. On the read-out day, cells are checked via flow cytometry for reporter gene expression (usually mCherry). Calculations are then made to assess total infectious units (IU, the number of cells transduced) per ml of viral supernatants. Figure 4-10 (table) shows representative infectious assay results. We consider viral titres to be good when they range between 5 and $10x10^6$ IU/mL. In this representative example, canonical ROR1 CAR viral titre is 8.9, whereas i-CAR viral titre is 2, which likely explains the very poor transduction efficiency. We concluded something in the transgene is dramatically lowering the virus titres.

In parallel, SupT1 cells and freshly isolated T cells were transduced with the same viruses. After transduction, SupT1 and T cells were analysed via flow cytometry for mCherry expression. Figure 4-10 shows flow cytometry plots: interestingly, when looked at SupT1 cells (top right panel), although they are all 100% mCherry positive compared to non-transduced cells, the shifts are less compared to ROR1 CAR (red histogram), suggesting that transduction

with the inducible cassette-containing plasmids seems affected even in SupT1 cells. When primary cells were assessed, as expected we measured much lower transduction levels compared to ROR1 CAR (69% versus 45% and 23%, from ROR1 CAR + inducible system only (all elements minus the PD-1 binder) and ROR1 i-CAR, respectively.

As first troubleshooting approach, we tried transducing cells using concentrated virus, but no improved transduction efficiency was observed (data not shown).

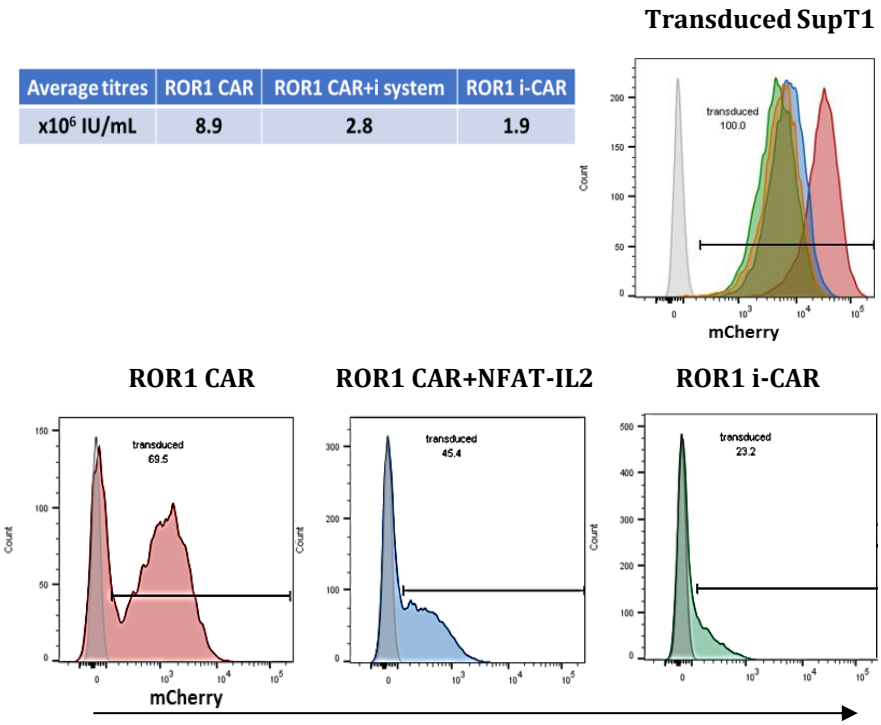

Figure 4-9 Representative viral titres (IU/ml) of virus and flow cytometry plots of transduced cells (mCherry+). Infectious assays were performed on 4 viruses: ROR1 CAR (positive control), ROR1 CAR+inducible system (+NFAT-IL2) and ROR1 i-CAR; a) representative viral titres expressed in IU/mL; b) flow cytometry plots show transduction efficiency of SupT1 (top right) and of freshly isolated T cells (bottom three) based on mCherry expression.

4.3.4.2 Transfer vector transgene size

We then hypothesised that the larger vector genome size, due to the additional elements, was causing the reduced transduction compared to the ROR1 CAR one. After removing roughly 1250bp of non-essential elements (reporter gene and IRES), transduction efficiencies were compared again but no difference was detected between the plasmid containing ROR1 CAR with constitutive αPD-1 (PL284) and same plasmid without reporter gene and IRES (PL315, Table 4-1 for transgene schematics and Figure 4-11 for flow cytometry plots). To measure transduction, cells were stained with a FITC-anti-human Fab antibody (that binds to the CAR extracellular domain), but no shift was observed for both 284 and 315 compared to the positive control (SupT1 expressing the same ROR1 CAR, Figure 4-11 top right panel). Interestingly, when secretion of anti-PD-1 scFv was compared between the same two plasmids we observed a shift of roughly 96% for both (two bottom flow cytometry plots), suggesting that the transduction issue might cause expression issues in region between the mCherry and the CAR on the transgene. This hypothesis was supported by a further experiment to assess binding to ROR1eFc protein, where we measured same binding (or shift) for both inducible systems, which was still much lower than control (top left panel).

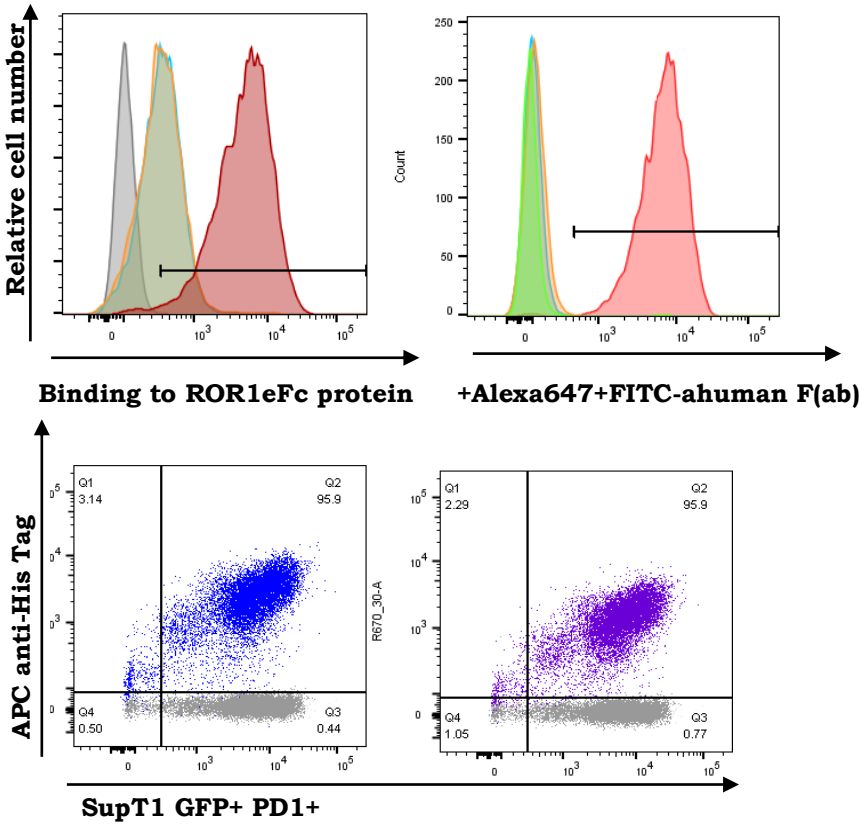

Figure 4-10 Functional comparison between PL284 and PL315 for transduction efficiency, ROR1 binding and scFv secretion. Binding to soluble ROR1eFc was assessed for SupT1-268 (+ve ctrl), T cells expressing ROR1 CAR+ *c* system (284) and smaller version plasmid (315). NT = NT T cells + ROR1eFc+ A647-anti-mouseFc antibody (for background signal). Second plot shows same cells tested with FITC-anti-human Fab antibody which binds to the ROR1 CAR extracellular domain; b) Flow cytometry of secreted scFv binding to the PD-1+ cells

4.3.4.3 Co-transduction

The next strategy was to separate the two expression cassettes (ROR1 CAR and inducible system) into two different expression vectors and compare the overall transduction efficiency after co-transduction. The first viral vector encoded for the canonical ROR1 CAR. The second vector, named PL321, contained the inducible αPD-1 scFv followed by eBFP reporter gene with a T2A peptide in between to allow co-translation. In this way, both pembrolizumab scFv and eBFP presence can be detected via flow cytometry only after CAR activation-mediated induction.

Subsequently, fresh T cells were transduced to express either ROR1 CAR, ROR1 i-CAR or ROR1 i-CAR via co-transduction. Transduction efficiencies were compared along with binding to ROR1eFc. Results (Figure 4-12) show that co-transduced cells had increased % of mCherry+ T cells compared to ROR1 i-CAR (38% versus 31%), but still not as good as ROR1 CAR (47%), likely because of the halved amount of virus used for transduction. ROR1eFc bindings were very similar between ROR1 CAR-T cells and co-transduced cells (44% and 35% double positive, respectively), so we assumed that ROR1 CAR from co-transduced T cells was more functional than i-CAR-T cells (mCherry+ but no shift from binding, top central panel).

Next, a co-culture was set up to assess inducible eBFP expression with ROR1+ targets only. Transduced cells have been co-cultured with SupT1 (ROR1-), Kasumi2 (ROR1++) and Raji (ROR1+) cell lines at 10:1 T:E ratio. Cells were checked for induced BFP expression via flow cytometry after 24h. Figure 4-12 (bottom panel) shows flow cytometry plots for double positive cells, confirming specific eBFP induction (no eBFP with SupT1 cells) which seems related to ROR1 expression on target cells (8% from Kasumi 2 versus 2.5% of eBFP from Raji).

Although promising, these results show transduction levels that are still too low for our standards, therefore we decided to explore other alternatives.

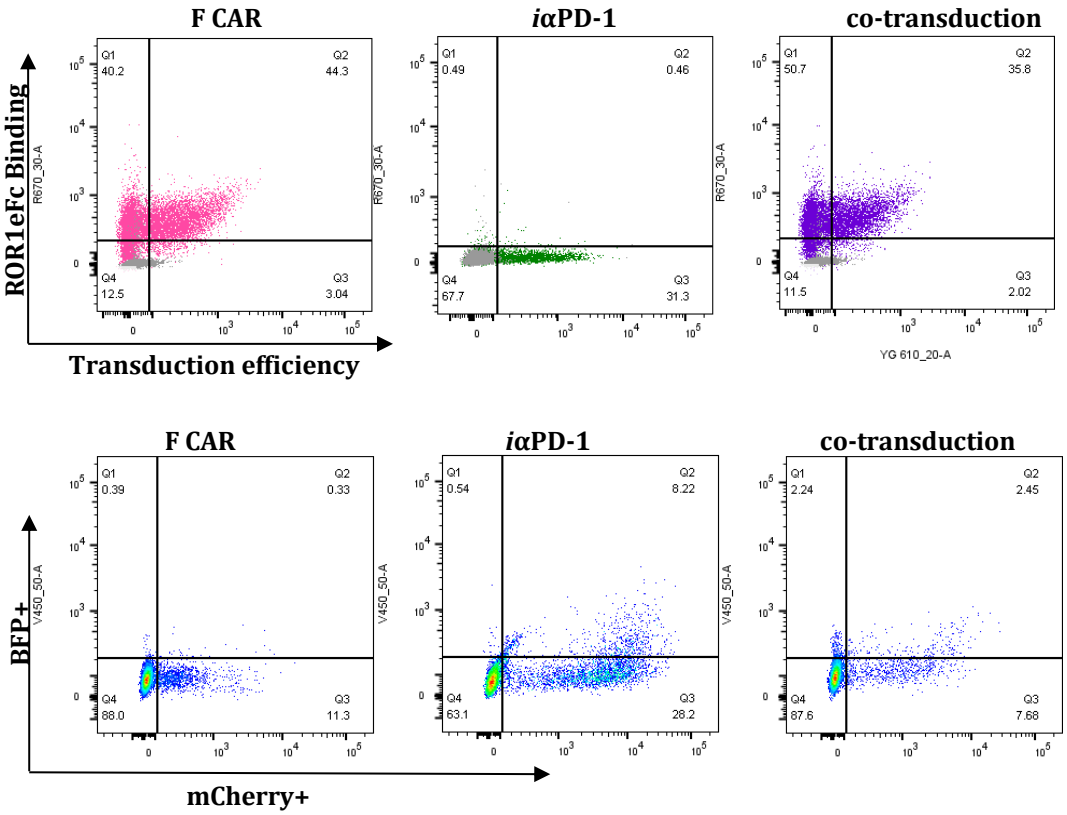

Figure 4-11 Flow cytometry plots to check co-transduced CAR-T cells. Top panel: transduction efficiency based on reporter gene expression (mCherry, *y* axis) and binding to ROR1eFc (*x* axis). Double positive population indicate CAR T cells binding to soluble ROR1eFc. Bottom panel: induction of BFP (*x* axis) gated on mCherry (*y* axis) via co-culture with SupT1 (first), Kasumi2 (middle) and Raji (last plot) cell lines.

4.3.4.4 3rd generation SIN-viral vector

Next, we hypothesised that the issue might be due to the presence of too many promoters into a single expression vector: the CMV promoter-enhancer of our third-generation expression vector, the minimal IL-2 promoter for the inducible system and the PGK promoter for reporter gene and CAR expression. This issue is often referred as promoter or transcriptional interference. We found a plasmid from Cheng L et al. (335) with the following features:

-3rd generation lentiviral (LV) vector with disabled viral promoter in the 3′ LTR of the vector genome following integration, also known as self-inactivating (SIN)

-Two internal promoters driving two transcriptional units: CMV for GFP expression and EF1-α for FasL surface ligand expression.

Interestingly and promising for my work, they showed that dual-promoter LV-transduced human CD34+ cells were 56% positive for GFP, which is the second (downstream) gene. Moreover, high expression at mRNA levels for both the GFP and the FasL transgenes were observed via qPCR.

We therefore purchased the plasmid from Addgene (https://www.addgene.org/17616/) aiming to insert both expression cassettes into this backbone and evaluate transduction efficiency using mCherry. The resulting 3rd generation SIN-LV, named PL344, contained the following transgene:

The following viruses were made in several independent experiments:

ROR1 CAR

ROR1 i-CAR *old* (old backbone with same transgene as new plasmid)

ROR1 i-CAR *new* (new SIN-backbone, plasmid named PL344)

After 48h, viruses were used to transduce freshly isolated T cells and HEK-293Ts for viral titre calculation. For the infectious assay, data from several independent tests are shown in Figure 4-13 and highlight that viral titres using the new vector are much higher than the ones generated with the previous backbone (7.5 versus 2.8x10^6 IU/ml). These results were confirmed by mCherry expression via flow cytometry (Figure 1-13 for flow cytometry plots), where transduction levels from new ROR1 i-CAR-T cells, although slightly lower than ROR1 CAR-T cells (55% mCherry+ versus 78%) were much

better than the ones using the i-CAR transgene with the previous backbone (15%).

Average viral titre	ROR1 CAR	Old ROR1 i-CAR	New ROR1 i-CAR
10x106 IU/mL	9.7	2.8	7.5

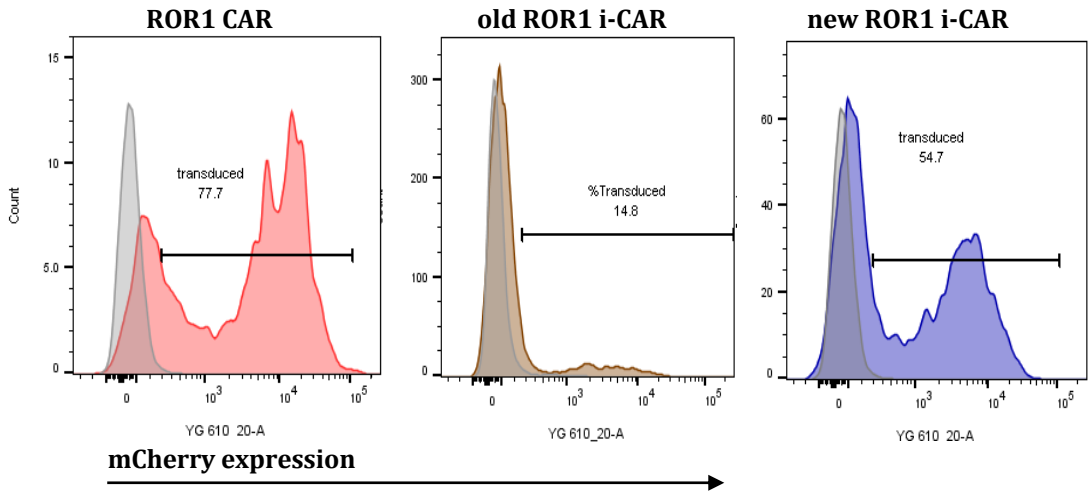

Figure 4-12 Viral IU and corresponding transduction efficiencies of freshly isolated T cells. Infectious assays as well as transduction efficiency of fresh T cells were performed independently several times to evaluate the quality and transduction efficiency of the new SIN-lentiviral plasmid (named New ROR1 i-CAR) versus the canonical ROR1 CAR (positive control) and the same transgene in the former lentiviral backbone, named old ROR1 i-CAR.

As these results were reproducible, we concluded I was able to generate a single lentiviral expression vector to generate functional virus to make ROR1 CAR T cells able to secrete upon activation blocking αPD-1 scFv.

4.4 Discussion

One of the most studied immunological checkpoints so far is the PD1/PD-L1 axis. Therapeutics interfering with this interactions showed remarkable beneficial effects to treat melanoma (336-338), lung cancer (339) and to a lesser extent breast cancer (255, 340). CAR-T cells are susceptible to inhibitory immune checkpoints and acquire a differentiated and exhausted phenotype resulting in loss of effector functions (341, 342). Substantial literature has showed that PD-1 pathway blockade combined with CAR-T

cells was able to enhance cytotoxicity (151, 343, 344) and to provide superior in vivo tumour eradication and survival in murine models (156, 157, 345). Moreover, combination therapy is being actively investigated in the clinic, despite the severe toxicities that may arise from systemic administration of checkpoint inhibitors.

In line with this work, we aimed at combining ROR1 CAR-T cell therapy with a localized delivery of PD-1 blockade to overcome the immunosuppressive TME whilst limiting off-target toxicity that often arise with systemic administration of checkpoint blockade (238, 346). We selected an inducible system for the secretion of the scFv. This is based on the nuclear factor of the activated T cell (NFAT)-responsive expression cassette, where the CAR-derived CD3ζ signalling induces the activation of the NFAT minimal promoter which in turns leads to production and secretion of the molecule of choice. This approach was first reported by Chmielewski and Abken with their redirected CAR-T-cells secreting IL-12 upon activation (72). They reported increased efficacy and better tumour eradication at much lower dose than second-generation CAR-T cells.

We started by assessing PD-1 expression by our CAR-T cells and confirmed stable ROR1-specific upregulation of PD-1 up to 96h of co-culture in the presence of the targeted antigen (mean of 80% using three different target cell lines and three different donor-derived T cells). Without antigen, no upregulation was observed, confirming that the overexpression is due to CAR-T cell activation.

We then successfully cloned two blocking scFv binding to human PD-1 derived from two commercially available antibodies, nivolumab and pembrolizumab. The latter was tested for binding kinetics via SPR and we measured high binding affinity for its ligand with consistent K_D values in the nanomolar range.

For the inducible system, we set up preliminary co-cultures to assess the induction of GFP via flow cytometry for an easier and direct evaluation. In parallel we also assessed the full-length IL-2 promoter to see whether it would

confer stronger induction: although we did see that ROR1-induced GFP signal was higher at almost two-fold, so it was the non-specific (or leaking) induction in the presence of the ROR1- target cell line. Potential leakage of the NFAT promoter independently of CAR signalling is a concern for this and any other promoter which is also induced by TCR-derived signalling (330) . For this reason, we decided to continue with the minimal IL-2 promoter as we were concerned by such high levels of uncontrolled release which may cause more systemic or non-specific adverse events.

A second set of co-culture assays confirmed the induction of GFP in the presence of several target cell lines which expresses different levels of ROR1 at higher T:E ratio (5:1 instead of 1:1) as we hypothesised that more targets would induce higher GFP signal. Induced GFP signal was indeed much higher than the previous co-culture and similar across all ROR1+cell lines (average of 40%) but was still detected when CAR-T cells were either cultured with a ROR1- target cell line or left alone, suggesting mild leakage of the inducible system.

Once confirmed the functionality of the inducible system, we cloned it into our canonical 3rd generation lentiviral expression vector downstream the CAR expression cassette. In this way, we would have one single expression vector to make virus to efficiently transduce freshly isolated T cells. Unfortunately, this vector was not efficient given the very low viral titres that resulted in poor transduction efficiency (measured via mCherry expression) and lower antigen binding efficacy by the ROR1 CAR.

We tested several strategies to solve this problem, from concentrating the virus to reducing the size of the transgene, as well as co-transducing the T cells with two expression vectors. None of these approaches showed remarkable improvements in viral titres or in transduction efficiency.

We then assumed the issue was related to promoter or transcriptional interference, which can be defined as the perturbation of one transcription unit by another(347). The interference we observed seemed to primarily affect the expression of the mCherry-2A-CAR transgene, via PGK promoter.

The potential transcriptional interference between the LTR activity and an internal promoter driving the transgene can be prevented by the SIN design. For this reason we opted for a self-inactivating (SIN)-lentiviral vector, which has a deletion in the 3'LTR region of the viral genome (348). With the new backbone, we were able to recover both viral titres (7.5 versus 2 IU/ml from previous backbone) and transduction efficiency (50% versus 15%).

Overall, with this chapter we report the generation of a functional lentiviral expression vector that can be used to generate ROR1-targeted CAR-T cells bearing an inducible system that becomes operational upon CAR-T cell activation.

Chapter 5 Functional assays: *in vitro* validation of CAR-T cells in the context of solid malignancies

After successfully generating the lentiviral construct to make functional ROR1 targeted CAR-T cells secreting αPD-1 scFv, we validated the system primarily in the context of solid malignancies. This chapter will therefore describe in detail the *in vitro* functional features of the ROR1 CAR-T cells. The overall aim was to compare ROR1 i-CAR-T cells with the parental ROR1 CAR-T cells lacking inducible system for parameters such as targeted cytotoxicity, T cell fitness and phenotype.

5.1 Detection and quantification of αPD-1 scFv produced by activated CAR-T cells

5.1.1 Production, purification and quantification of αPD-1 scFv

Based on the preliminary flow cytometry data showing specific secretion of αPD-1 scFv by i-CAR-T cells, we set up further and more sensitive assays to confirm the specificity of the NFAT-inducible system and, at the same time, to quantify the produced scFv. We first developed an in-house PD-1 ELISA, where ELISA plates were coated with recombinant PD-1 protein, to which αPD-1 scFv-containing supernatant was added and the scFv, which is His-tagged, was detected using an HRP conjugated anti-His antibody.

In order to quantify the detected scFv in the supernatant, we used a standard curve made of purified αPD-1 scFv. The scFv was purified from supernatant of HEK-293T producing cells following transient transfection using the Akta FPLC system. Figure 5-1A shows the elution trace with the elution peaks highlighted. The fractions corresponding to the 2 elution peaks were then tested via western blot to confirm presence and purity of the scFv. According to the western blot (Figure 5-1B), both peaks contained the purified His-tagged protein at the right molecular weight (27kDa), with the second peak-related fractions showing brighter bands which translates to higher concentration of the His-tagged protein. Moreover, the second peak bands showed a higher His-tagged band at approximately 55KDa, which suggests dimerization of the scFv.

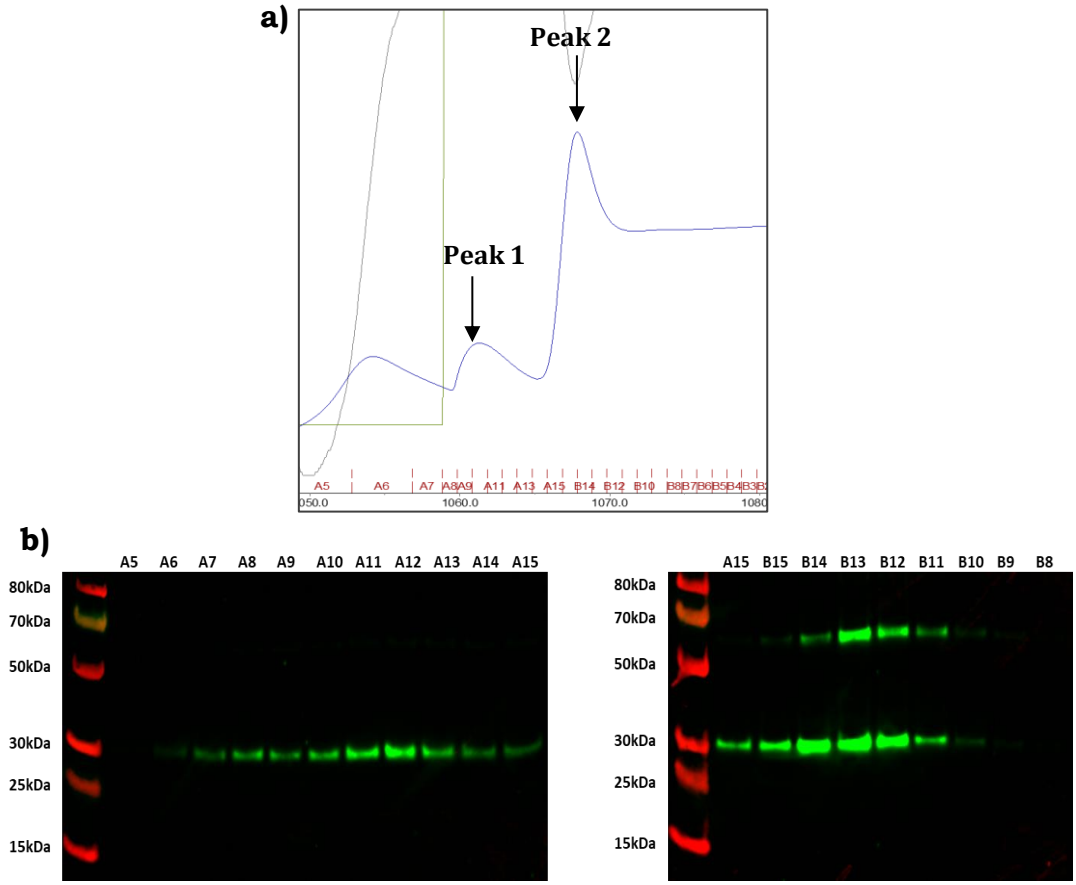

Figure 5-1 scFv purification: a) UV chromatography (blue line) of the elution phase of purification with two peaks; the green line corresponds to the Imidazole concentration and dashed red lines at the bottom the fractions collected; b) Western blot using an anti-His-HRP secondary shows band at the correct size for both peaks, with second peak fractions (B15-B12) having higher concentration of protein; despite the presence of a possible dimer, there is significant purity.

After combining the fractions with the brightest bands (A11-A13 + B14-B12), dialysis in PBS was performed overnight. The purified scFv was quantified using a standard curve with a purified His-tagged protein (ROR1xCD3 BiTE) of known concentration (Figure 5-2a for western blot). To note, the putative dimer band is still present but in much lower amounts than before dialysis. The purified scFv was stored at -20°C. To ensure the PD-1 ELISA was specific and sensitive enough for our scFv binder, we performed a preliminary run with serial 1 in 2 dilutions of the purified scFv starting at 4µM. The standard curve (Figure 5-2b) confirmed specific detection of the αPD-1 scFv, with lowest detectable concentration being 0.0078 nM corresponding to an OD value of 0.0088 mOD.

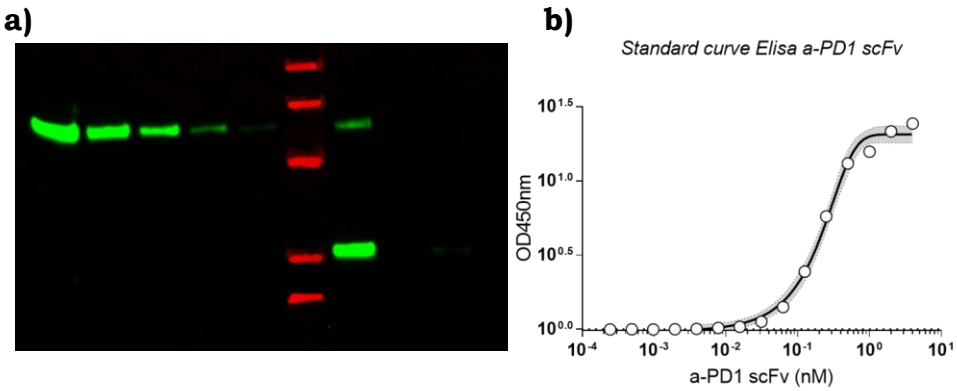

Figure 5-2 scFv quantification and ELISA assessment. a) Following dialysis overnight, the purified scFv was quantified via western Blot using a purified His-tagged scFv serially diluted for the standard curve and ImageJ software was used to generate a standard curve and exact quantification; b) once concentration was determined, an in-house ELISA was set up: serial 1in2 dilutions of the purified scFv were tested for binding to recombinant PD-1 (coated on the plate) and detected using the same HRP anti-His antibody used for western blot. Signal from OPD substrate was detected using a plate reader.

5.1.2 PD-1 ELISA show targeted and long-lasting scFv production

We set up co-cultures using freshly transduced ROR1 i-CAR-T cells incubated with ROR1+ target cells MDA-MB-231 and H1975 (TNBC and NSCLC, respectively) and with ROR1- cell line SupT1 (T lymphoblast). Co-culture supernatant was collected at different time points and stored at -20°C to test all samples at the same time via PD-1 ELISA.

Results (Figure 5-3) confirmed the flow cytometry data: we detected secreted scFv only in the presence of the targeted antigen (3 donors average+SD), as early as 5h and up to 96h of co-culture. The quantity of scFv produced was roughly the same between the two different target cell lines, suggesting that the levels of released scFv might be due to intrinsic features of the CAR-T cell rather than correlated with ROR1 surface expression levels. 4pM was the average concentration detected for the whole duration of the experiment, with peak at 24h against both target cell lines (4.15±2.47 pM). This confirms the presence of the scFv in the supernatant up to 96h of co-culture, and we hypothesize that the stable level is the result of a balance between production and scFv binding to PD-1 (therefore not collected in the supernatant) or scFv

degradation. Importantly, no signal was detected in the supernatant from co-cultures with the ROR1- target cell line, confirming specificity of the system.

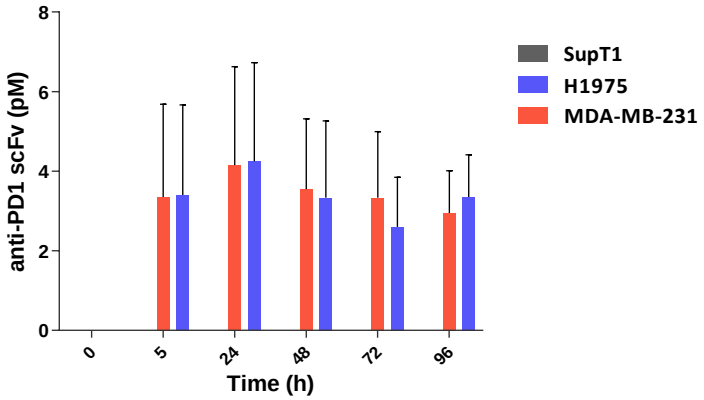

Figure 5-3 Quantification of secreted scFv via PD-1 ELISA. In-house PD-1 ELISA was set up coating plates with recombinant PD-1 protein. Co-culture supernatants (1:1 T:E ratio used) were incubated, washed and bound αPD-1 scFv was detected with an HRP conjugated anti-His antibody. Standard curve was made of serially diluted purified scFv, which also served as positive control. Negative controls were supernatant harvested pre-coculture (time point 0h). Results shown are mean+SD of 3 donors in triplicate against each target cell line.

5.1.3 scFv labelling with Gaussia Luciferase and detection confirm specific and long-lasting scFv secretion

We then performed a third experiment to detect the secreted αPD-1 scFv. This time cloning was performed to swap the His-tag with a Luciferase tag (gaussia Luciferase, gLuc). Freshly isolated T cells from three healthy volunteers were transduced to express ROR1 i-CARgLuc before setting up the same co-culture protocol we used for the ELISA quantification.

Supernatants were collected at different time points and gLuc substrate was added to detect the scFv-gLuc. Bioluminescence signal was read via plate reader, with minimal signal detection from supernatants with ROR1- target cells (Figure 5-4). This confirms once again that the secretion of the scFv is specific. When ROR1+ targets were present, CAR-T cells released αPD-1 scFv-gLuc as early as 6h, with peak at 24h for both targets. Bioluminescence

signal was again detected up to 96h, which is in agreement with the ELISA results. This approach gave greater detection sensitivity and we were able to more accurately assess target cell and time dependence. We detected a higher signal from MDA-MB-231 compared to H1975 (peak values 547±385 and 366±163, respectively). The differences were small and not significant, and the overall trend was similar in the two ROR1+ target cell lines.

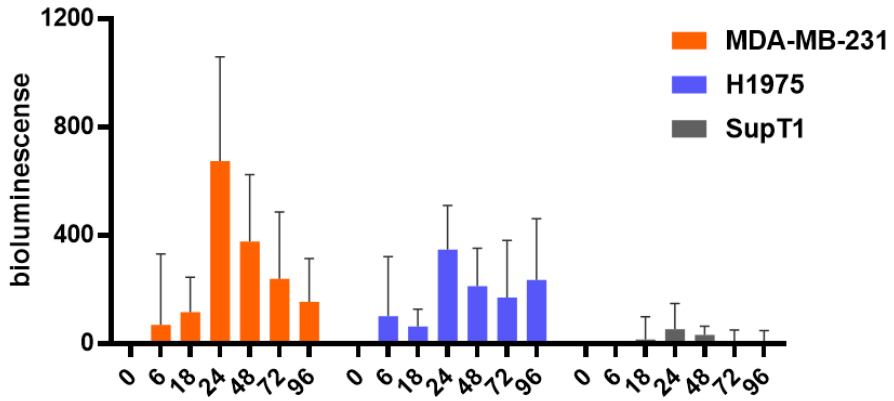

Figure 5-4 Detection of produced scFv via plate reader. The same co-cultures were set up using CAR-T cells secreting the αPD-1 scFv tagged with a Gaussia Luciferase (gLuc). Supernatants were harvested at the indicated time points and coelenterazine, the gLuc substrate, was added prior bioluminescence reading via plate reader. Negative control: supernatants from CAR-T cells alone (time point 0h); positive control (not showed): CAR-T cells constitutively expressing gLuc. Results show mean+SD of 3 donor-derived CAR-T cells plated in triplicate against each target cell line.

In summary we were able to confirm secretion of the scFv as early as 5-6h of co-culture and up to 96h in the presence of ROR1+ target cell lines; we quantified the scFv produced via in-house ELISA (average of 4pM) and most importantly we demonstrated the specificity of our ROR1 i-CAR-T cell system by showing that co-culture with ROR1- target cells does not induce release of αPD1-scFv.

5.2 *In vitro* cytotoxicity

5.2.1 Preliminary killing assay and cytokine secretion assessment show potential of PD-1 blockade on CAR-T cells

We next aimed to assess the efficacy of our i-CAR-T system as opposed to parental ROR1 CAR-T system; we set up co-cultures to quantify cytotoxicity of ROR1-targeted CAR-T cells constitutively secreting the scFv (+scFv) versus parental CAR, versus combination therapy with a blocking anti-PD1 mAb (+mAb) from Biolegend (clone EH12.2H7). The first co-culture had the following conditions: 1:2 T:E ratio, with cytotoxicity and pro-inflammatory secretion measured after 24h against the TNBC cell line MDA-MB-231. We did not measure significant differences in targeted cytotoxicity when we compared ROR1 CAR alone versus ROR1 CAR with checkpoint blockade (either combination therapy with mAb or secreted scFv). However, we measured increased pro-inflammatory cytokine production (IL-2 and IFNγ) in the presence of checkpoint blockade, which was especially marked with the secreted αPD-1 scFv (average of 2-fold increase for both IFNγ and IL-2 production compared to ROR1 CAR only, $p<0.0001$, Figure 5-5). Combination therapy with the commercial antibody (mAb) showed IFNγ production levels comparable to the scFv condition but very similar IL-2 levels compared to ROR1 CAR alone.

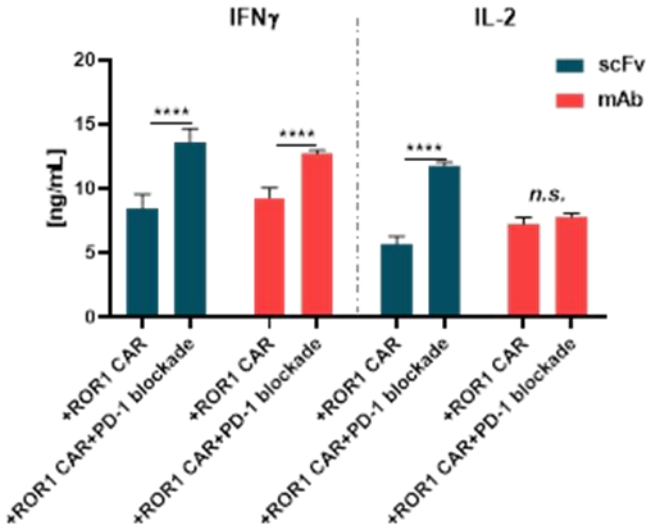

Figure 5-5 Pro-inflammatory cytokine production. A preliminary co-culture assay was set up to assess and IFNγ IL-2 release by our CAR-T cells against the target cell lines MDA-MB-231 and SKOV-3, either alone or in the presence of PD-1 blockade in the form of the αPD-1 scFv (dark green bars)or a commercial antibody (red bars). Results show mean+SD of two donor-derived CAR-T cells against both target cell lines. 2way ANOVA was performed using ROR1 CAR alone as comparator arm.

5.2.2 Optimised killing assays: long-term co-culture show superior efficacy of i-CAR-T cell versus parental CAR

There are contrasting results in the literature regarding the ideal E:T ratio and co-culture length in order to detect the best PD-1 blockade-mediated effect on cytotoxicity. Two independent studies highlighted that killing with checkpoint inhibitors resulted enhanced in prolonged co-cultures (up to 4-5 days) and with a high T:E ratio, possibly to generate a more suppressive microenvironment via upregulation of PD-1/PD-L1: Krupka and colleagues used a CD33:CD3 BiTE against a range of acute myeloid leukaemia (AML) cell lines and reported that the E:T ratio and the CD33 expression level significantly influenced lysis kinetics in long-term cultures of primary AML cells: specifically, the PD-1/PD-L1 blockade-mediate increased cytotoxicity was most prominent in cultures with low E:T ratios (1:5), which may be linked to the considerably enhanced T cell proliferation observed. Tanoue and colleagues showed that their combination of an oncolytic adenovirus with a helper-dependent Ad expressing a PD-L1 blocking mini-antibody was able to

enhance CAR T-cell killing of two HER2+ tumour cell lines at 1:20 E:T ratio after 120h (349, 350).

With these examples in mind, we set up co-cultures against the non-adherent cell line Kasumi2 at various high T:E ratios and assessed killing after 3 days of co-culture. This time the ROR1 CAR+/- anti-PD1 mAb were compared to ROR1 i-CAR (inducible secretion). The results (Figure 5-6 from 2 representative donors) show that PD-1 blockade enhanced cytotoxicity at all T:E ratios, but only at 10:1 T:E ratio the cytotoxicity was significantly higher than ROR1 CAR-T cells only (half live targets left, p=0.02). We therefore selected this co-culture condition for the following co-culture assays.

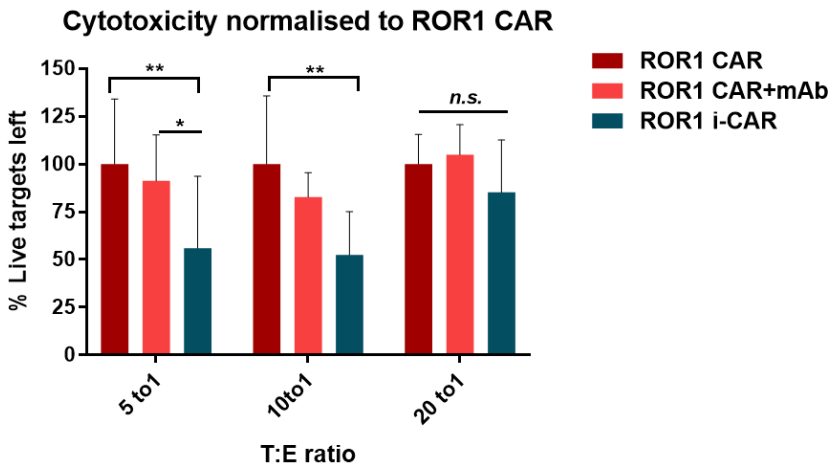

Figure 5-6 Co-culture test to find best condition. Co-cultures were set up using freshly transduced T cells to express ROR1 CAR or ROR1 i-CAR. Target cell line used was AML Kasumi2. Cells were plated at various T:E ratios with a further condition: ROR1 CAR+mAb, a commercial anti-PD-1 antibody. Killing was assessed after 72h. 2way ANOVA was performed using ROR1 CAR as comparator arm, p<0.05.

We set up co-cultures using multiple donor-derived CAR-T cells against the ROR1+ cell lines MDA-MB-231 (TNBC), H1975, A549 (both NSCLC) and Kasumi2 (AML). The aim was to confirm the results observed so far: using multiple donors and target cell lines we aimed to ensure the PD-1 mediated increased cytotoxicity was not donor- nor target cell line-dependent. As controls we used ROR1- SupT1 and MCF-7 (BC) cell lines. Co-culture of

ROR1 CAR-T cells with H1975 and MDA-MB-231 cell lines demonstrated specific T cell activation as evidenced by clustering and expansion, which was not seen with CD19 CAR-T cells under the same conditions (Figure 5-7).

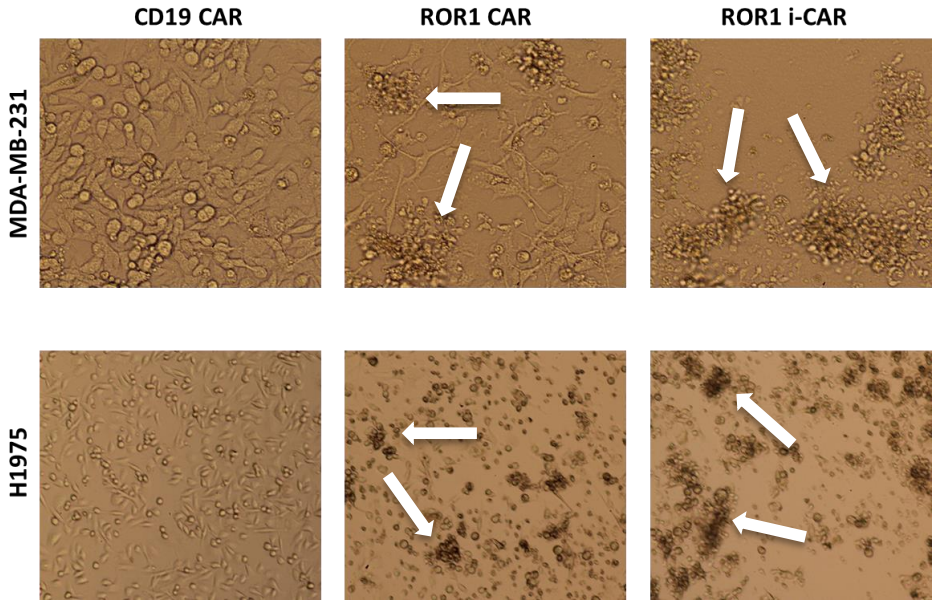

Figure 5-7 Antigen-specific activation of CAR-T cells in vitro. Representative photographs of co-cultures with ROR1+ target cell line MDA-MB-231 (top, 10x objective) and H1975 (bottom, 4x objective) show specific clustering and expansion of activated CAR-T cells with loss of target cells in the background, compared to irrelevant CD19 CAR (1st column on the left).

When we performed the flow-cytometry based killing assay, no increased killing of ROR1- targets was detected when we compared target survival with control irrelevant CAR (CD19 CAR, Figure 5-8A). Against the panel of ROR1+ cell lines (MDA-MB-231 and H1975, Figure 5-8B; A549 and Kasumi2, Figure 5-8C) we observed enhanced and reproducible cytotoxicity with >80% killing of target cells at a target to effector cell ratio of 1:1. As the number of ROR1 positive tumour target cells was increased it become apparent that ROR1 i-CAR-T cells were more efficient at killing tumour targets compared to ROR1 CAR-T cells with the difference being significant at a T:E ratio of 10:1 for all target cell lines ($p<0.005$ to $p<0.001$).

We hypothesise that this increased cytotoxicity might be due to the more immunosuppressive/tumorigenic environment given by higher numbers of PD-L1-expressing tumour cells, which would make the PD-1 blockade-effect more evident.

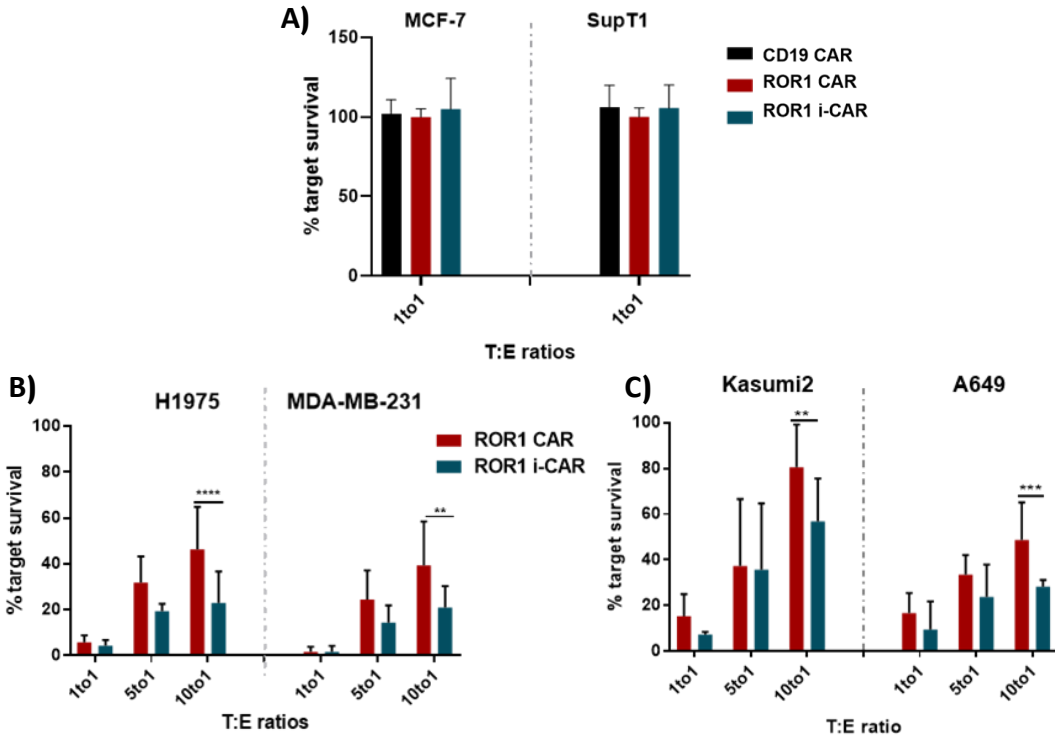

Figure 5-8 Extended co-cultures to assess cytotoxicity. Several co-cultures were set up using multiple donor-derived CAR-T cells against several targets at three T:E ratios. Cytotoxicity was assessed via flow cytometry after 72h of co-culture, results show mean+SD of at least 3 donor-derived CAR-T cells, assessed at least in two independent experiments. A) Non-targeted cytotoxicity by ROR1 CAR-T cells was assessed against the ROR1- target cell lines SupT1 and MCF-7. % target survival was compared to control: 100% target survival from co-culture with the irrelevant CD19-targeted CAR, black bars; for targeted cytotoxicity, % of B) H1975, MDA-MB-231, C) Kasumi2 and A649 survival compared to control (irrelevant CAR, not included) is shown for parental CAR (red bars) and ROR1 i-CAR (dark green bars). 2way ANOVA was performed using ROR1 CAR as comparator arm, $p<0.005$ – $p<0.0001$.

5.2.3 Additional co-cultures with combination therapy confirm PD-1 mediated enhanced cytotoxicity

In order to confirm that this observed increased cytotoxicity is because of PD-1 blockade, we set up additional co-cultures including the combination therapy as control: ROR1 CAR-T cells with 1µg/mL of αPD-1 mAb.

Cytotoxicity and pro-inflammatory cytokine secretion were assessed. Once again, we measured consistently lower % H1975 and MDA-MB-231 survival in the presence of PD-1 blockade (significantly lower MDA-MB-231 survival for i-CAR versus ROR1 CAR at 1:2 and 1:1 T:E ratios, Figure 5-9A), confirming that the disruption of PD-1/PD-L1 interaction is indeed increasing our ROR1 CAR-T cell-mediated cytotoxicity. Interestingly, combination therapy was not as effective as our i-CAR-T cells, suggesting that superior blockade can be achieved by the spatial regulation of PD-1 blockade from the i-CAR system. For cytokine secretion, we confirmed once more a PD-1 blockade mediated increased secretion for both IL-2 and IFNγ (up to 30% more, Figure 5-9B), with very similar production levels between induced scFv production and commercial mAb.

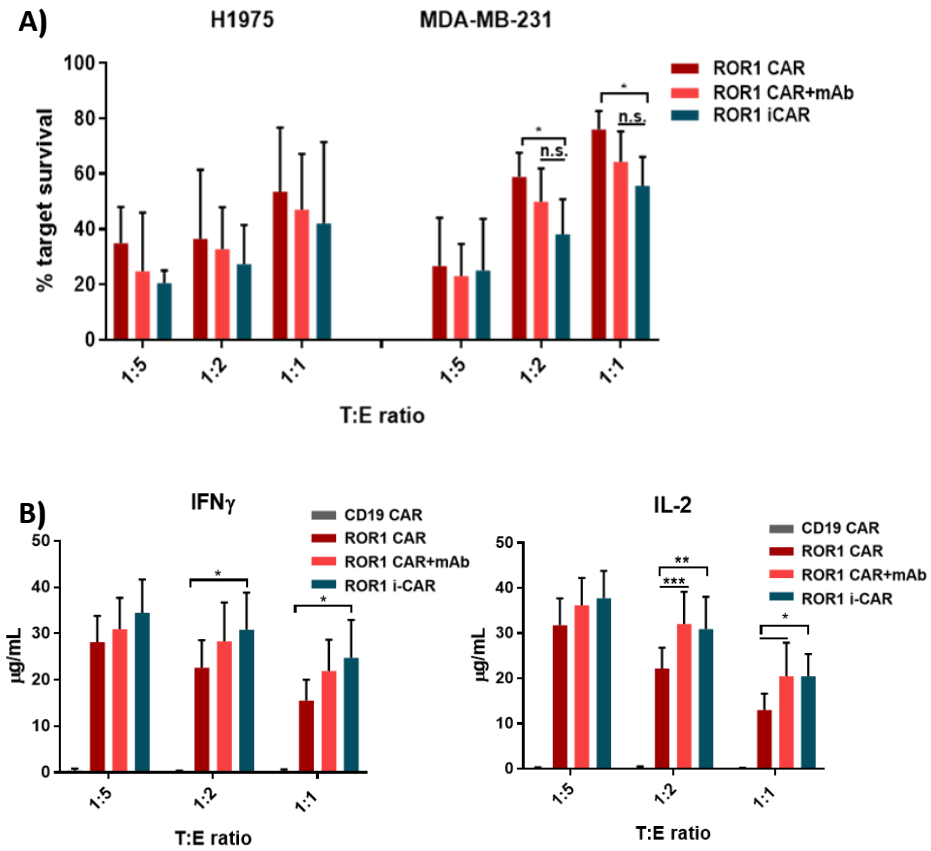

Figure 5-9 PD-1 blockade mediated cytotoxicity and pro-inflammatory cytokine secretion. Further co-cultures were set up including the control of combination therapy to confirm that the increased cytotoxicity was a result of PD-1 blockade. From the same co-culture, supernatants were also assessed for pro-inflammatory cytokine production via ELISA: A) % live H1975 and MDA-MB-231 left normalised to control (100% live targets left with irrelevant CD19 CAR); B) pro-inflammatory cytokine secretion was measured. Results are mean+SD of at least 3donor-derived CAR-T cells assessed at two different times; 2way ANOVA was performed with ROR1 CAR as comparator arm: p<0.05 - <0.001.

5.2.4 PD-L1 blockade diminishes effect of PD-1 mediated increased cytotoxicity

Next, a further set of co-cultures was set up where the target cells (PD-L1+) were pre-incubated with a commercial αPD-L1 antibody overnight prior CAR-T cell addition. There were two aims:

1. To make sure with an additional condition that we are disrupting the PD-1/PD-L1 interaction

2. To determine the efficiency of this disruption by comparing presence versus absence of additional PD-L1 blockade

After 24h, we performed the killing assays. The results show that with additional PD-L1 blockade, the percentages of live targets left for both cell lines were roughly the same regardless of the effector used (parental CAR versus i-CAR versus combination, condition +aPD-L1, Figure 5-10). These findings suggest that the presence of PD-L1 is needed to have a noticeable PD-1 blockade effect on CAR-T cell efficacy. Moreover, when we compared %live targets left with and without PD-L1 blockade for each CAR, the greatest difference was observed for parental ROR1 CAR ($p<0.001$ and $p<0.05$ against MDA-MB-231 and H19675, respectively). This lack of increased efficacy with additional PD-L1-blockade for all conditions but ROR1 CAR-T cells only, confirms that PD-1 disruption is indeed happening, and that the additional PD-L1 blockade does not significantly improve combination or i-CAR-T cell potency versus parental CAR-T cells.

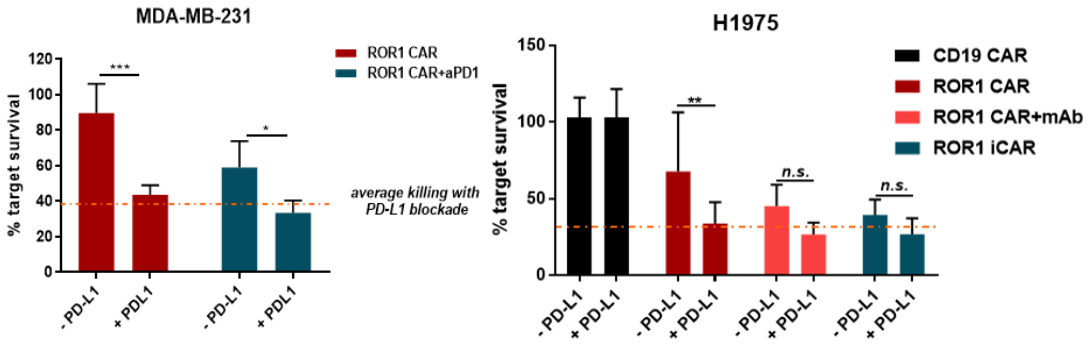

Figure 5-10 PD-L1 blockade effect. Co-cultures were set up to address the effect of pre-PD-L1 blockade on CAR-T cell mediated effector functions. Target cells were seeded with or without anti-PD-L1 antibody before adding the effector functions. The next day, cytotoxicity was assessed.One way ANOVA was performed to compare, for each effector, the presence or absence of PD-L1 blockade (- and +aPDL1, respectively). Results are mean+SD of 3 donor-derived CAR-T cells.

Having confirmed superior effector functions by our i-CAR-T cells compared to the parental version in the presence of PDL1, we proceeded with a phenotypic characterisation of the two CAR-T cell populations. We wanted to find markers that could either clarify or be a consequence of the observed PD-1 blockade-mediated increased cytotoxicity.

5.3 CAR-T cell characterisation

5.3.1 i-CAR-T cells show increased actin accumulation at the immunological synapse site

We started by looking at mechanistic features of the CAR-T cells, particularly at immunological synapse (IS) formation on the tumour cell. We set up co-cultures using the cell line MDA-MB-231 seeded at 1:1 T:E ratio and fixed the cells after 24h. Cells were stained to visualise actin polarisation and accumulation at the IS site: this mechanism is part of the sustained interaction between cells that allows polarized cytotoxic granule release and effective T cell-mediated killing. We therefore used the quantification of actin accumulation from CAR-T cells as a readout of IS strength and stability (351).

Representative confocal images show MDA-MB-231 target cells (red) with the much smaller T cells on top (blue and yellow for CD3). As expected, compared

to UT T cells, both ROR1-targeted CAR-T cells showed actin accumulation at the IS site (green, Figure 5-11 top panel).

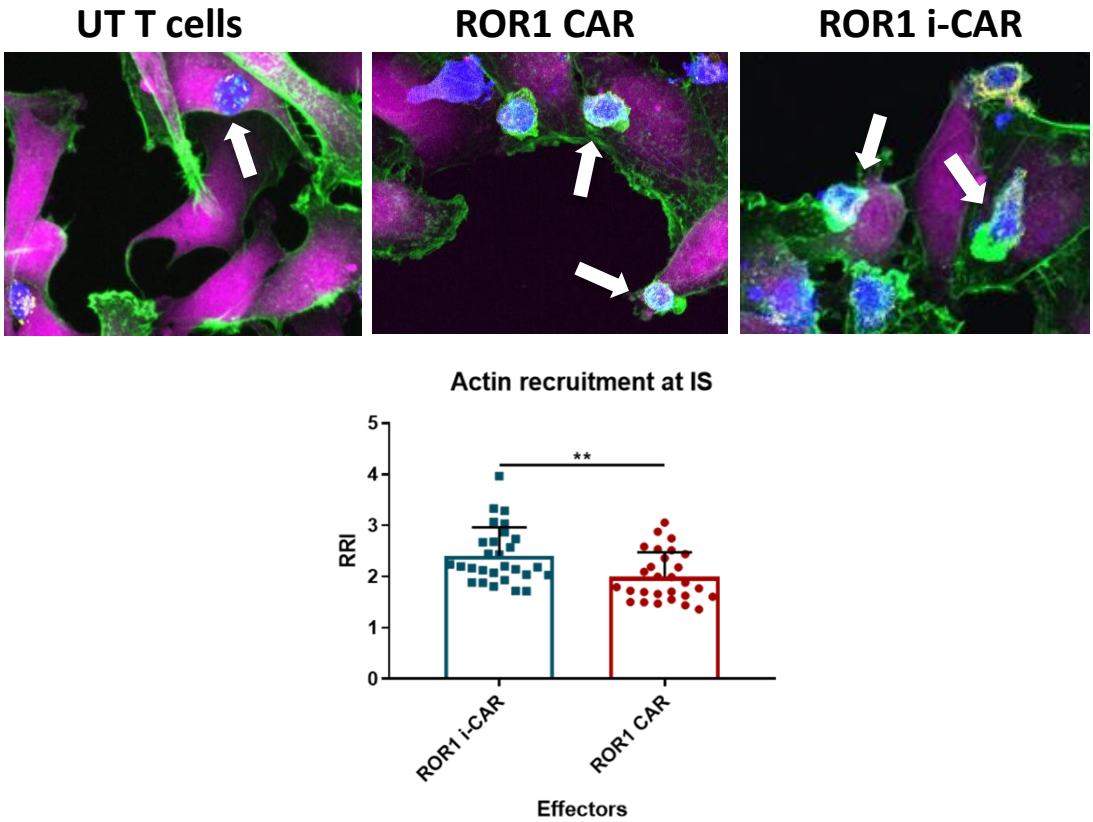

Figure 5-11: IS formation and actin RRI from CAR-T cells. Co-cultures of CAR-T cells (3 donors) were co-cultured with labelled MDA-MB-231 target cells for 24 h then fixed. Cells were stained with CD3-AF647 and phalloidin-AF488 before mounting and imaging by confocal microscopy (Zeiss LSM880, 960 oil objective; Zeiss, Oberkochen, Germany). Example CAR-T cells (blue and arrows) show actin accumulation at the IS site (green), scale bar = 10 mm. Cell conjugates were identified manually and phalloidin recruitment quantified using mean fluorescence intensity in an area of cell contact and normalized against phalloidin signal in a non-contact area of the T cell plasma membrane. ImageJ was used for phalloidin recruitment quantification, with a total of 28 quantifications/CAR used. Student *t* test (Welch correction) was performed, p=0.043.

This approach revealed that i-CAR-T cells exhibit enhanced actin recruitment to the IS site, with a significantly higher RRI of actin compared to ROR1 CAR-T cells (2.4±0.55 versus 1.99±0.47, mean+SD of 28 calculations). This suggests that the increased i-CAR efficacy that we observed is partly mediated through stronger IS formation compared to parental CAR-T cells.

To note, as we fixed the cells at 24h from setting up the co-culture, we speculate that a time course might reveal more striking differences in RRI considering that in terms of cytotoxicity we can see the best PD-1 blockade-mediated effect after 72h of co-culture.

5.3.2 CAR-T cell phenotyping show differences between the two constructs

We then assessed the two CAR constructs, along with the respective untransdued (UT, mCherry-) T cells, for several markers via flow cytometry after 24h or 72h of co-culture with MDA-MB-231 and H1975 cell lines. We included UT T cell analysis to see whether the CAR-T cells would influence the phenotype of the untrandusced counterpart.

For i-CAR-T cells, we measured increased granzyme B (GZB) production (20% versus 12% after 24h of co-culture) and same levels of CD107α (~20%). Interestingly, combination therapy showed lower GZB production (12%) but higher CD107α than i-CAR-T cells (23%, Figure 5-12). UT T cells had much lower levels of both cytotoxic markers, likely due to their more inactive state compared to their ROR1-targeted transduced counterpart.

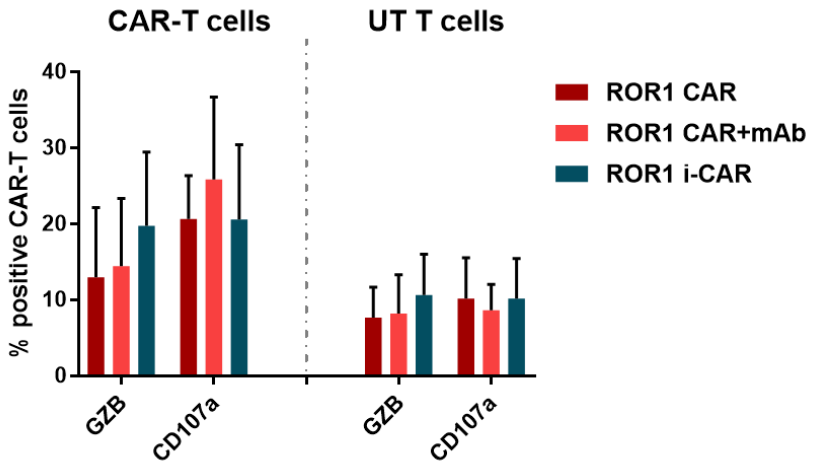

Figure 5-12 Cytotoxic markers. Co-cultures were set up to measure cytotoxic markers from CAR+ and CAR- T cells. After 24h of co-culture with MDA-MB-231 and H1975, cells were stained for granzyme B (GZB) and a degranulation assay was performed for CD107a. Results are mean+SD of 3 donors against both target cell lines. No significant differences were found.

From the same co-cultures, we stained transduced and untransduced (UT) T cells for the following markers: CD4/8, CCR7, CD45RO and CD45RA. When we assessed CD4/8 ratio, we found a significant increase in cytotoxic CD8+ CAR-T cells in the presence of PD-1 blockade: 31% versus 50% from combination therapy (p=0.01) and 56% from i-CAR-T cells (p=0.0003, Figure 5-13). This suggests that PD-1 blockade mediates a preferential expansion of cytotoxic T cells, either with or without expression of the CAR, highlighting a possible paracrine effect on bystander cells. When we looked at central memory markers (CD45RO+ CCR7+), no difference was observed in CD4/CD8+ central memory T cells between the CAR-T cell constructs (average of 20%). This indicates that PD-1 blockade may not influence the T cell stage *in vitro*.

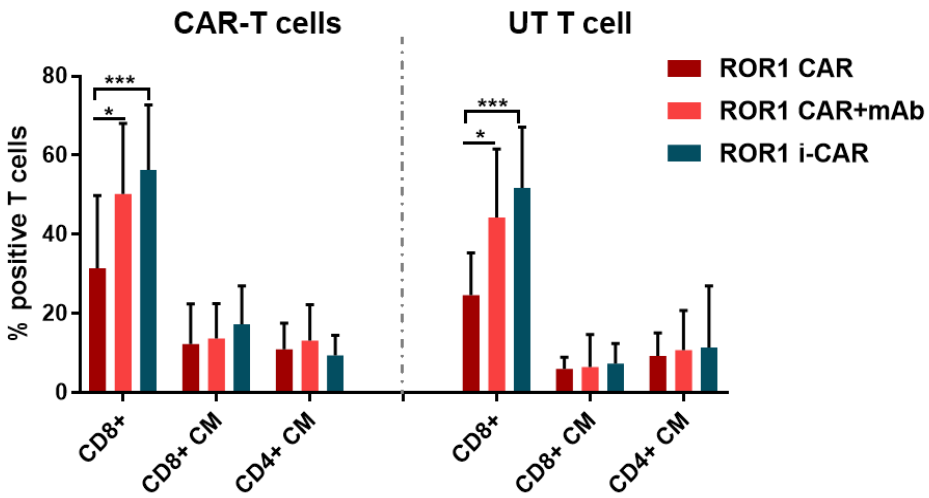

Figure 5-13 T cell markers. CAR-T cells were co-cultured as before, followed by staining for CD4/8 and phenotype markers prior flow cytometry analysis. Results shown are % positive cells for a given marker compared to parental population (CD3+ T cell or CAR-T cell) and are mean+SD of three donors against both target cell lines. 2way ANOVA performed with ROR1 CAR as comparator arm: p<0.05-0.001.

Next, we looked at the surface expression of the most common exhaustion markers: we measured similar expression levels for Tim3 (average 24% for all CAR-T cells and UT T cells) and LAG-3 (average of 38% for all CAR-T cells and UT T cells). Notably, CTLA-4 was expressed at low levels by all CAR-T cells but was doubled on parental CAR-T cells (7% versus 3% average for both combination and i-CAR-T cells). PD-1 expression, either total or on CD8+ T

cells, was much lower on i-CAR-T cells and CAR-T cells with mAb treatment compared to ROR1 CAR-T cells only (5-9% versus 7-15% versus 18-27%, Figure 5-14), suggesting competitive binding by the blocking αPD-1 reagents (mAb or secreted scFv). Roughly the same expression levels were measured on the respective UT T cells, potentially confirming the PD-1 blockade effect on bystander immune cells.

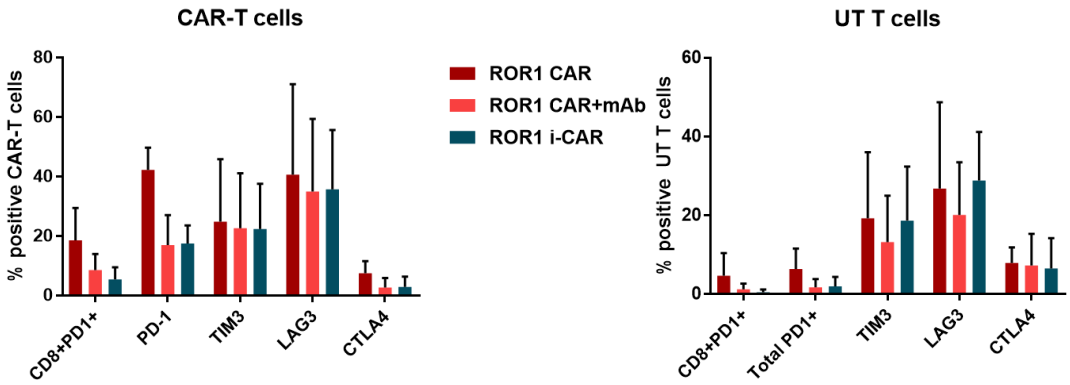

Figure 5-14: Exhaustion markers on T cells. Transduced (CAR expressing) and untransduced (UT) T cells were assessed, after co-culture, for common exhaustion markers via flow cytometry. Results are mean+SD of 3 donor-derived CAR-T cells co-cultured with both target cell lines.

Lastly, to assess antigen-specific proliferation, we co-cultured ROR1+ target cells with CAR-T cells that were previously labelled with CellTrace™ Violet. We monitored proliferating CAR-T cells via assessment of dye dilution (and therefore signal reduction) via flow cytometry after 24h. As expected, the positive signal of all ROR1 CAR-T cell conditions was significantly lower than the control CD19 CAR-T cells ($p<0.0001$), indicating higher proliferation rate for ROR1 CAR-T cells. For each ROR1 CAR-T cell condition, combination therapy had lowest percentage of labelled cells measured (10%) compared to i-CAR (20%) and parental CAR (40.8%, $p<0.0001$, and $p<0.05$ for parental versus i-CAR, Figure 5-15), suggesting a PD-1 blockade effect also on CAR-T cell proliferation in the presence of the targeted antigen.

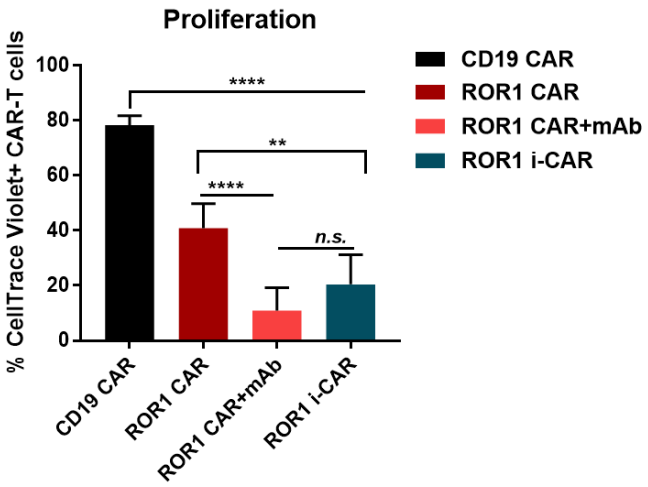

Figure 5-15 Proliferation assay. Co-culture with labelled CAR-T cells was set up to measure ROR1-mediated CAR-T cell proliferation. Control was irrelevant CD19 CAR-T cells. Results show mean+SD of 3 donors plated in triplicate at 1:1 E:T ratio. One-way ANOVA with multiple comparison was performed.

Overall, with this phenotyping analysis we were able to compare the surface expression of multiple markers between several donor-derived CAR-T cells after co-culture with ROR1+ target cells. We found a PD-1 blockade-mediated effect on: granzyme B production, cytotoxic CD8+ T cell expansion, proliferation (all increased) and lower surface PD-1 expression. We conclude that all these features are likely causing the increased effector functions of ROR1 i-CAR-T cells compared to parental CAR-T cells.

5.4 Discussion

Immune-checkpoint inhibitors release the immune system's brakes to enhance anti-tumour immune responses. As CAR-T cells frequently turn into a terminally differentiated and exhausted phenotype associated with increased expression of immune checkpoint molecules such as PD-1/PD-L1, using checkpoint blockade to bolster the potency of CAR-T cells revealed impressive effects in the context of certain solid malignancies (151, 345, 352).

With this in mind, we developed a monotherapy where ROR1 CAR-T cells secrete, upon activation, blocking anti-PD-1 scFv that would protect the cells from PD-1-mediated suppression in the confines of the TME.

As the constitutive production of anticancer molecules such as checkpoint inhibitors might cause systemic side effects, we first started with the validation of the inducible system, where *in vitro* functional assays showed CAR activation-mediated secretion of αPD-1 scFv which was rapid (5h) and long lasting (up to 96h), with minimal or no detection in the absence of ROR1. This confirms the previous findings for endurance and specificity of our inducible system, which are in line with the study by Uchibori and colleagues, where they used the same inducible promoter reporting targeted and enduring expression both *in vitro* and in mouse studies (353).

We then assessed PD-1-blockade effect on several CAR-T cell features via multiple *in vitro* functional assays.

Preliminary *in vitro* co-cultures with ROR1+ target cell lines showed a sharp increase in pro-inflammatory cytokine production by CAR-T cells (either combination therapy or scFv secretion) after 24h, which is in line with other studies (150).

We then set up co-cultures with high T:E ratios to find the condition where the PD-1 blockade effect was more pronounced. We assessed the killing after 72h and found that the 10:1 T:E ratio was the only one showing significant reduction in target survival. The 20:1 T:E ratio showed the least target survival difference between conditions, as overall targeted efficacy was decreased.

We then set up co-cultures using multiple donor-derived CAR-T cells and assessed cytotoxicity against a range of ROR1+PDL1+ cell lines. Compared to ROR1 CAR-T cells only, we measured consistently higher cytotoxicity by i-CAR-T cells, which was significant at 10:1 T:E ratio. This confirms the findings reported by others (349, 350), and suggest that a more hostile microenvironment with increased PD-L1 triggers a more pronounced PD-1 blockade-mediated efficacy.

In the context of breast cancer, there is a well-established correlation between high TIL infiltrate (especially in the stroma) and long-term positive outcomes for patients. However, a study by Buisseret et al highlighted that TIL density and PD-L1 expression were correlated with more aggressive tumour characteristics such as higher proliferation and hormone receptor negativity; they therefore suggest the extent, the type and location of the immune infiltrate should all be considered when assessing antitumor immunity and the potential for benefit from immunotherapies (354, 355).

Importantly, i-CAR-T cell potency was more effective than combination therapy with a blocking αPD-1 mAb and was only marginally improved by additional PD-L1 blockade, highlighting the high efficiency of the inducible system.

In order to better elucidate the differential effector functions of our CAR-T cells, we performed a detailed characterisation of the two constructs following *in vitro* co-culture with ROR1+ target cell lines. The key differences that we observed are overall emphasizing a more cytotoxic and active phenotype of i-CAR-T cells compared to parental. These include increased proliferation and preferential CD8+ T cell expansion, higher IL-2 and IFNγ production and lower expression of some exhaustion markers. These findings suggest that, compared to i-CAR-T cells, parental CAR-T cells exhibit impaired effector functions (356, 357), which may hint at some degree of exhaustion. We did observe an increase in LAG-3 expression, which has been reported following checkpoint blockade treatment on T cells (358). Importantly, combination therapy showed the same features as i-CAR-T cells, suggesting that these features are likely a consequence of PD-1 blockade.

Overall, as proof of concept, we believe that our i-CAR-T cell possesses the cytotoxic potential and key phenotypic features that would make it a much more promising candidate for *in vivo* antitumor activity compared to its parental version, which constitutes a canonical CAR-T cell therapy approach. The following chapter will therefore cover the *in vivo* and *ex-vivo* experiments and findings.

Chapter 6: Validation of ROR1 CAR-T cells in a pre-clinical TNBC mouse model

6.1 Introduction to *in vivo* studies

Breast cancer is the most common malignant disease in women in developed countries. The TNBC subtype, which accounts for roughly 15% of breast cancers, presents a highly aggressive and metastatic phenotype; this, combined with the lack of effective treatment, makes the prognosis dismal (154, 359). High levels of ROR1 expression on breast cancer cells and clinical activity with PD-1 blockade therapy have been reported (360), with the FDA recently approving PD-L1 blockade therapy in combination with chemotherapy for PD-L1+ TNBC patients (361). Phase I clinical trials evaluating CAR-T cell therapy in TNBC showed safe administration but modest therapeutic efficacy (322, 359).

We therefore selected a TNBC orthotopic model for our in vivo studies using the PD-L1+ ROR1+ cell line MDA-MB-231 which we implanted into immunodeficient mice (362). Despite missing valuable information such as the role of other immune components and potential checkpoint blockade-derived systemic side effects, for this proof-of concept study we focused on evaluating PD-1 blockade effect specifically on CAR-T cell-mediated antitumor effect. We also wanted to evaluate long-term effects and survival of the animals, which would have not been possible with the use of immunocompetent mice. Moreover, this model can be used to study metastases given their consistent development without the need for resection of the primary tumour (362). The aim for this section was to assess ROR1 CAR-T cell therapy in a xenograft model to identify differences between treatments.

6.1.1 Pilot study with orthotropic TNBC model in NSG mice show engraftment and no treatment-related toxicity

First, we engineered the TNBC cell line MDA-MB-231 to express firefly luciferase (Ffluc) to allow easy and more accurate detection of low tumour burden and eventual lymph node metastasis via bioluminescence imaging

(BLI). MDA-MB-231-Ffluc tumour cells were generated via transduction of tumour cells with a vector encoding the FfLuc-eBFP fusion gene, followed by sorting of BFP+ cells (Figure 6-1 top panel, representative flow cytometry plot post sort).

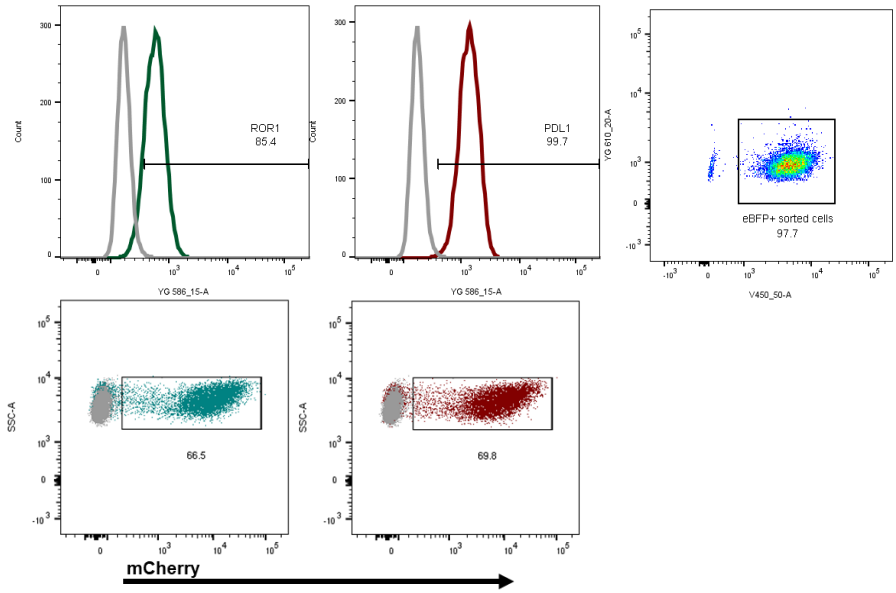

Figure 6-1 Flow cytometry assessment of tumour cells and CAR-T cells. Prior injections into mice, tumour cells were assessed for BFP expression (%transduced cells expressing Luciferase) and for ROR1 and PD-L1 expression via flow cytometry. Similarly, CAR-T cells were checked for transduction efficiency to calculate how many T cells to administer.

To assess ROR1 CAR-T cell response to a TNBC tumour, we established an orthotopic breast cancer xenograft by injecting $2x10^6$ MDA-MB-231-Ffluc cells into the mammary fat pad of NSG (NOD.Cg-PrkdcSCID Il2rgtm1Wjl/SzJ) mice (Charles River). The first objective was to make sure the tumours would engraft and grow. We performed bioluminescence imaging (BLI) using the IVIS system 6 days post tumour inoculation, confirming successful engraftment.

We therefore proceeded with CAR-T cell treatment. Prior to CAR-T cell administration, the cells were assessed for % mCherry+ T cells via flow cytometry (example of ~65% transduction efficiency, Figure 6-1 bottom panel) for eventual normalisation and to determine dosage; as control, the equivalent total number of UT T cells were injected.

The aim for this pilot study was to carefully monitor the mice for eventual toxicity in terms of behaviour, weight loss or distress. Additionally, as no symptoms for side-effects were observed, we assessed the potential effectiveness of the treatment via BLI. When we imaged the mice for tumour size over a 3-week period, the i-CAR-T cell treated mouse showed a 3fold reduction in tumour size ($1.16x10^7$ versus $3.44x10^7$ average radiance) compared to parental CAR-T cell treated mouse (Figure6-2 for BLI results and average radiance). This suggests a more effective control of tumour growth by i-CAR-T cells.

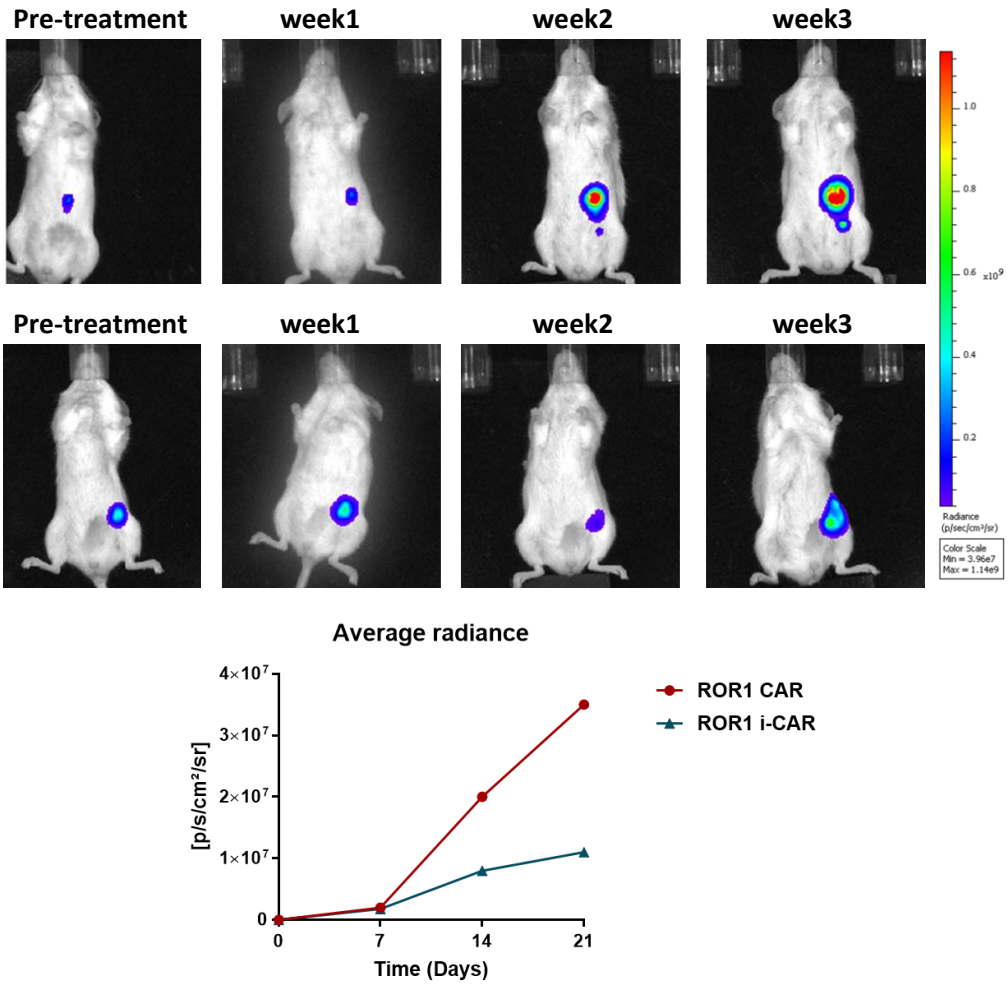

Figure 6-2 Pilot TNBC xenograft in NSG mice. 6-8weeks old NSG mice were implanted with $2x10^6$ MDA-MB-231Ffluc cells in 100µl of PBS in the mammary fat pad, with one injection/mouse. 6 days later, mice were imaged to confirm engraftment (left panel). The following day, mice were treated with a single i.v. injection of $4x10^6$ CAR-T cells. Mice were imaged for additional 3 weeks post treatment. Data showed are normalised using the IVIS software. Top panel: ROR1 CAR-T cell treated mouse. Bottom panel: ROR1 i-CAR-T cell treated mouse. Average radiance calculated using the IVIS Living Image software.

Overall, with this pilot experiment we were able to show consistent tumour engraftment in mice and safe CAR-T cell administration, as animals did not show any symptoms. While this is a pilot study where the treatment effectiveness was not a priority, we were positively impressed by these preliminary results, therefore we set up a full study to properly assess CAR-T cell effectiveness and its impact on animal survival.

6.1.2 TNBC model in NSG mice: first study shows superior activity of i-CAR

For the first study, treatment groups were as follow: ROR1 CAR-T cells only (n=6), ROR1 i-CAR-T cells (n=6), combination therapy with the mAb clone used for in vitro studies (Biolegend, 3x doses of 250µg/mouse, n=6) and untransduced (UT) CAR-T cells (control, n=3), all from the same donor and normalised for transduction efficiency before injection. Mice received one intravenous dose of $4x10^6$ CAR-T cells and tumours were monitored via BLI and digital calliper. As observed with the pilot studies, a single dose of i-CAR-T cells resulted in superior tumour control compared to CAR-T cells only, with significantly smaller tumours from week 4-5 post treatment (p<0.0001). Specifically, at day 28 we measured almost half signal from tumours either with combination therapy or with i-CAR-T cell therapy (averages of $1.67e^7$ versus $2.89e^7$, p<0.005, Figure 6-3 top panel).

Similar observations were made with the digital calliper measurements, where tumour volumes were more than doubled in ROR1 CAR-treated mice at day 28 compared to the two other treatment groups (p<0.0001). Interestingly, from week 5 post treatment (day 35), we observed a significant decrease in efficacy of combination therapy as tumours reached almost the same average size as ROR1 CAR treatment group (0.85±0.39cm^3 and 1.1±0.41cm^3, respectively), while i-CAR-T cells were still able to control tumour growth (0.4±0.31cm^3, p<0.0001, Figure 6-3 bottom graph). We were surprised to see this substantial decrease in anti-tumour effect by combination therapy over time.

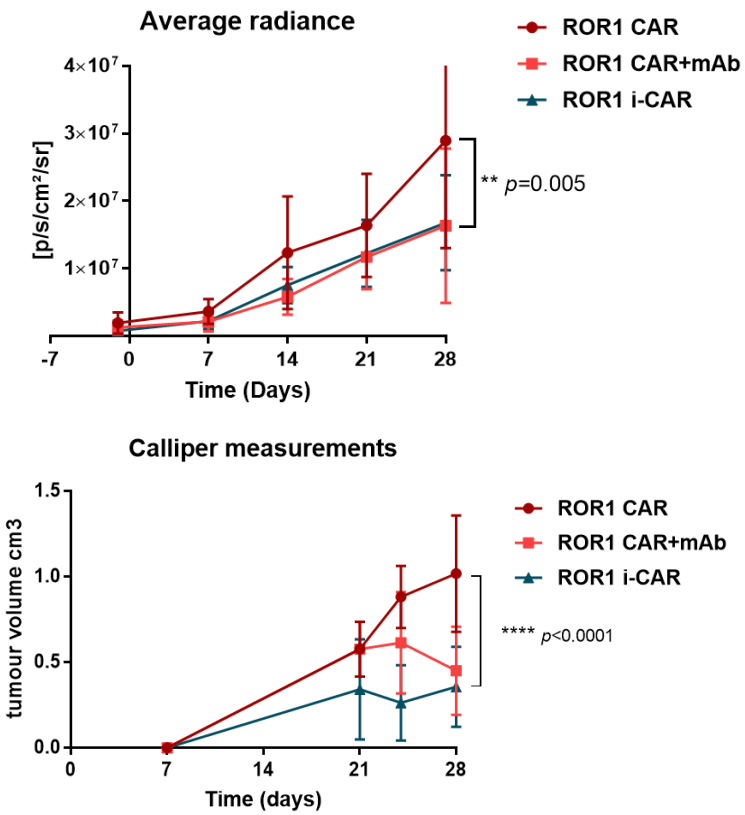

Figure 6-3 Tumour measurements via BLI and digital calliper. Tumours were monitored via BLI imaging once a week for 4 weeks total. Data were normalised and the average radiance is showed for all mice (mean+SD of n=6/treatment). 2way ANOVA was performed using ROR1 CAR as comparator arm, p<0.005 for both treatment groups. Bottom graph is showing parallel measurements using a digital calliper. 2way ANOVA performed with multiple comparisons, p<0.0001.

6.1.2.1 αPD-1 mAb plasma levels drop weeks after the last treatment

We therefore decided to investigate this long-term loss of efficacy by combination therapy. We set up a parallel experiment where one mouse received the same mAb treatment as combination therapy, followed by blood collections at multiple time points to monitor the presence of αPD-1 mAb in the plasma. We wanted to monitor the antibody plasma levels over time for a possible correlation with the observed reduced anti-tumour activity. Plasma from multiple time points was assessed via in-house anti-PD-1 ELISA, where

we found a sharp decrease in concentration at week 4 post last injection, which corresponds to 5 weeks post CAR-T cell treatment and to when combination therapy seems unable to control tumour growth. We therefore hypothesise a correlation between the sharp loss in plasma levels and the inability of combination therapy to control tumour growth (Figure 6-4).

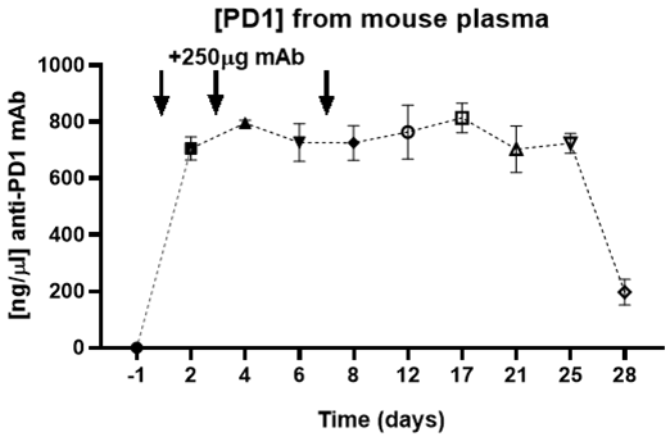

Figure 6-4 Plasma concentration of the αPD-1 antibody. One mouse was injected i.p 3x with 250µl of anti-PD1 mAb (clone EH12.2H7) on days 0, 3 and 7. Blood samples were collected at the time points showed in the graph. Plasma was analysed via in-house PD-1 ELISA with the standard curve made of the same purified mAb used for the treatment.

6.1.2.2 Survival monitoring show significant benefit for i-CAR-T cell treatment group

When we looked at survival, we observed a correlation with the superior antitumor activity of i-CAR-T cell treatment. All mice were sacrificed due to endpoint or tumour size limit (1.5cm) by day 61 (median survival: 56 days and 58 days for ROR1 CAR-T cell and combination therapy groups), while 1/3 of i-CAR-treated mice were still alive up to 95 days post treatment (median survival 71 days, Figure 6-5, p=0.0138). Combination therapy did not improve survival of mice compared to ROR1 CAR-T cells only, suggesting that despite the initial promising anti-tumour effect, a long-lasting therapeutic effect is needed to positively impact survival.

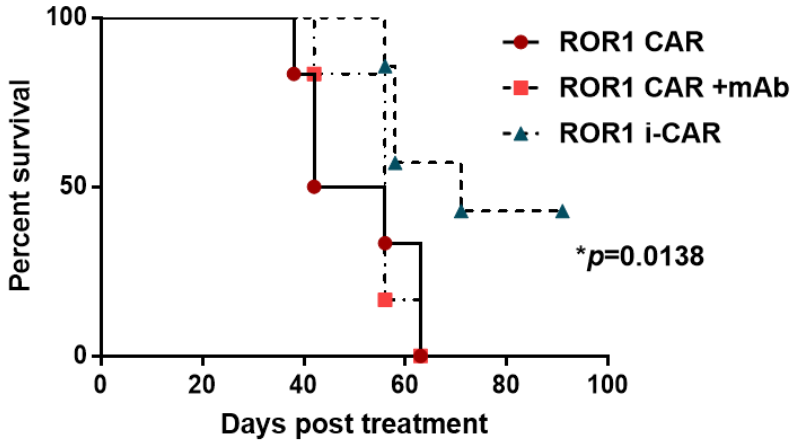

Figure 6-5 Survival of treated mice. Survival was assessed using GraphPad Prism, where survival tables were generated with Log-rank (Mantel-Cox) test used to compare survival curves.

We concluded that our ROR1 CAR-T cell therapy is showing anti-tumour effect, which is remarkably enhanced with PD-1 blockade as observed with *in vitro* studies. Given the significant superior activity of i-CAR-T cells especially from week 5 post treatment, we hypothesise that local and potentially long-lasting production of checkpoint blockade is offering superior effects, such as extended i-CAR-T cell persistence, compared to systemic administration, where no remarkable therapeutic effect was seen at late stage compared to monotherapy. This is in line with the study by Cherkassky and colleagues where by adding a second cycle of anti-PD-1 mAb treatment they restored the anti-tumour efficacy of mesothelin-directed CAR-T cells, suggest that CAR-T cell efficacy was short lived and reliant upon repeated αPD-1 mAb administration (78).

6.1.3 Second TNBC xenograft study with a different donor confirms preliminary results

In order to confirm that these findings were not donor-specific, we set up a second study with the same protocols and settings, using a different donor-derived CAR-T cells. This time we used CAR-T cells expressing the irrelevant CD19 CAR as control.

As confirmed with all our *in vivo* studies, no treatment-related toxicities were observed (Figure 6-6 for lack of substantial variations in mouse weight).

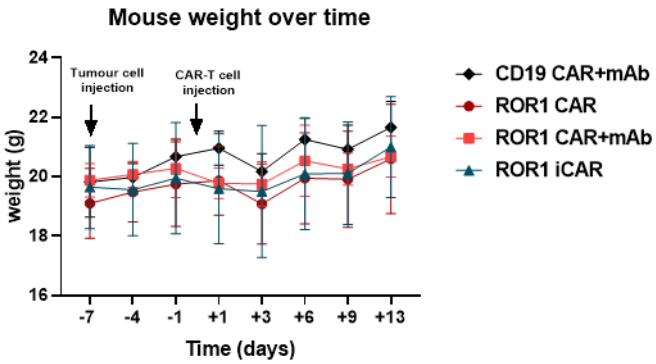

Figure 6-6 Mouse weight over time. Mice were weighted before and after treatment (arrow for CAR-T cell injection) to assess eventual treatment-derived toxicity resulting in weight loss higher than 10%.

In terms of tumour growth over time, we observed the same trend as the previous study via BLI imaging (Figure 6-7) and via calliper measurements, with smaller tumours measured 5 weeks post treatment in mice receiving PD-1 blockade (averages of 0.6±0.42cm from combination and 0.35±3cm from i-CAR-T cells) compared to ROR1 CAR-T cells (0.79±0.45cm, Figure 6-8). These findings correlated with the previous study outcomes, particularly in confirming the reduced efficacy of combination therapy over time.

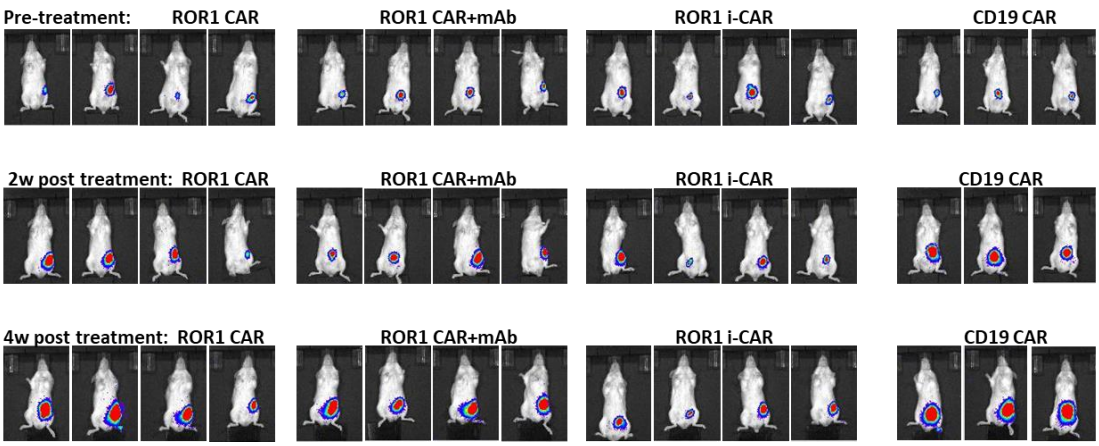

Figure 6-7 BLI of tumour bearing mice over time. BLI imaging up to 4weeks post treatment and overall normalisation were performed. Top row is showing pre-treatment images of 3-4 representative mice/treatment group. Second and third rows are showing 2week and 4week time points, respectively.

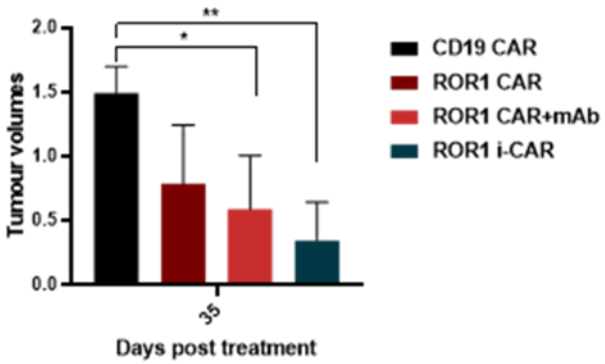

Figure 6-8 Tumour volumes 5 weeks post treatment. 35 days post-treatment timepoint is showed with mean+SD of 6mice/treatment (3 for control). 1way ANOVA was performed with multiple comparisons, p=0.0175 and p=0.0026

In terms of survival, we confirmed significant benefit only for the i-CAR-T cell treated group, where once again at day 82 only a fraction of i-CAR-T cell-treated mice were still alive (p=0.0025, Figure 6-9).

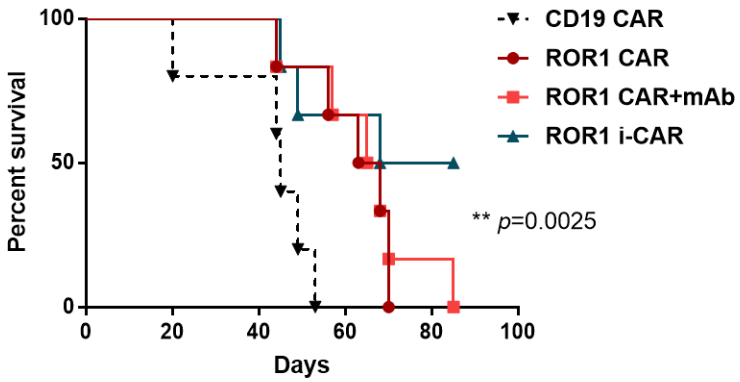

Figure 6-9 Survival of mice. Kaplan-Meyer survival curve of second study, n=6 mice/treatment group.

Overall, the TNBC xenograft models show superior activity of the i-CAR-T cell treatment over combination and monotherapy ROR1 CAR-T cell therapy, where with a single dose we were able to control tumour growth especially long-term after treatment. This resulted in significantly improved survival for these mice compared to all other treatment groups where no difference was

observed. We hypothesise that the observed lack of long-term efficacy by combination therapy is correlated to the drop in circulating antibody levels in the plasma; we assume that this might reflect a decreased intratumoral mAb level, which in turn may negatively impact CAR-T cell fitness and function. One possible explanation for this hypothesis, or an alternative mechanism for the observed poor efficacy, was showed by the recent study from Arlauckas and colleagues, where they used live imaging to show that αPD-1 mAbs that effectively bind PD-1+ tumour-infiltrating CD8+ T cells are captured within minutes from the T cell surface by PD-1- tumour-associated macrophages, unveiling a new mechanism of resistance to checkpoint blockade therapy (363).

6.2 *Ex-vivo* validation: Immunohistochemistry of tumour sections

When mice were sacrificed, tumours and spleen were collected. Tumours were then paraffin embedded, sectioned and stained (Institute of Neurology). We aimed at assessing the tumour infiltrating CAR-T cells to find potential differences between treatment groups that can support or explain the significant anti-tumour effect by i-CAR-T cells compared to the other treatments.

6.2.1 ROR1 staining reveals expression after ROR1 CAR-T cell treatment

We started with ROR1 expression. A few studies reported ROR1 expression in patient derived TNBC tissues, with the study from the Riddell group measuring ROR1+ on 57% of their samples, of which 56% expressing high levels and 74% showing homogenous staining (306). As antigen downregulation is a key mechanism of tumour escape, and we observed that all mice eventually became refractory to ROR1 CAR-T cell treatment, we wanted to see whether tumours downregulated ROR1 expression. We confirmed that, regardless of the treatment and the time the tumour was collected (e.g. 5 versus 9 weeks post treatment), ROR1 was still expressed homogenously although not at high level by all tumours (Figure 6-10 for representative snapshots). This suggests that other mechanisms are likely hampering CAR-T cell anti-tumour activity.

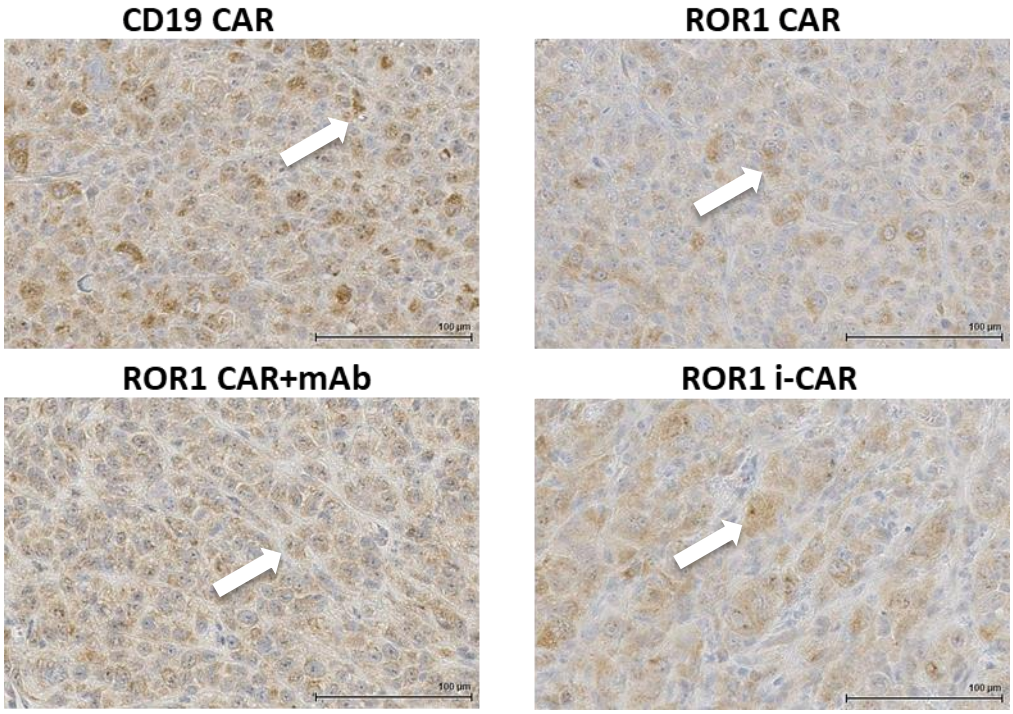

Figure 6-10 IHC staining for human ROR1 expression on tumours. Staining for ROR1 was performed on paraffin-embedded tumour tissues. Representative sections from each treatment group are showed at 20x magnification with white arrows pointing at positive staining.

6.2.2 Human CD8 staining and quantification

We then focused our attention on the CAR-T cells. We checked the expression of human CD8 to assess the infiltration levels of cytotoxic T cells in the tumours. We confirmed positive staining on multiple tumour sections from all treatment groups (Figure 6-11 for representative images), with visible greater positivity from PD-1 blockade-treated mice that was confirmed by manual counting of positive staining (233±180cells/mm^2 from i-CAR-T treated, 208±110cells/mm^2 from combination-treated and 161±106 cells/mm^2 from ROR1 CAR-T treated, Figure 6-11).

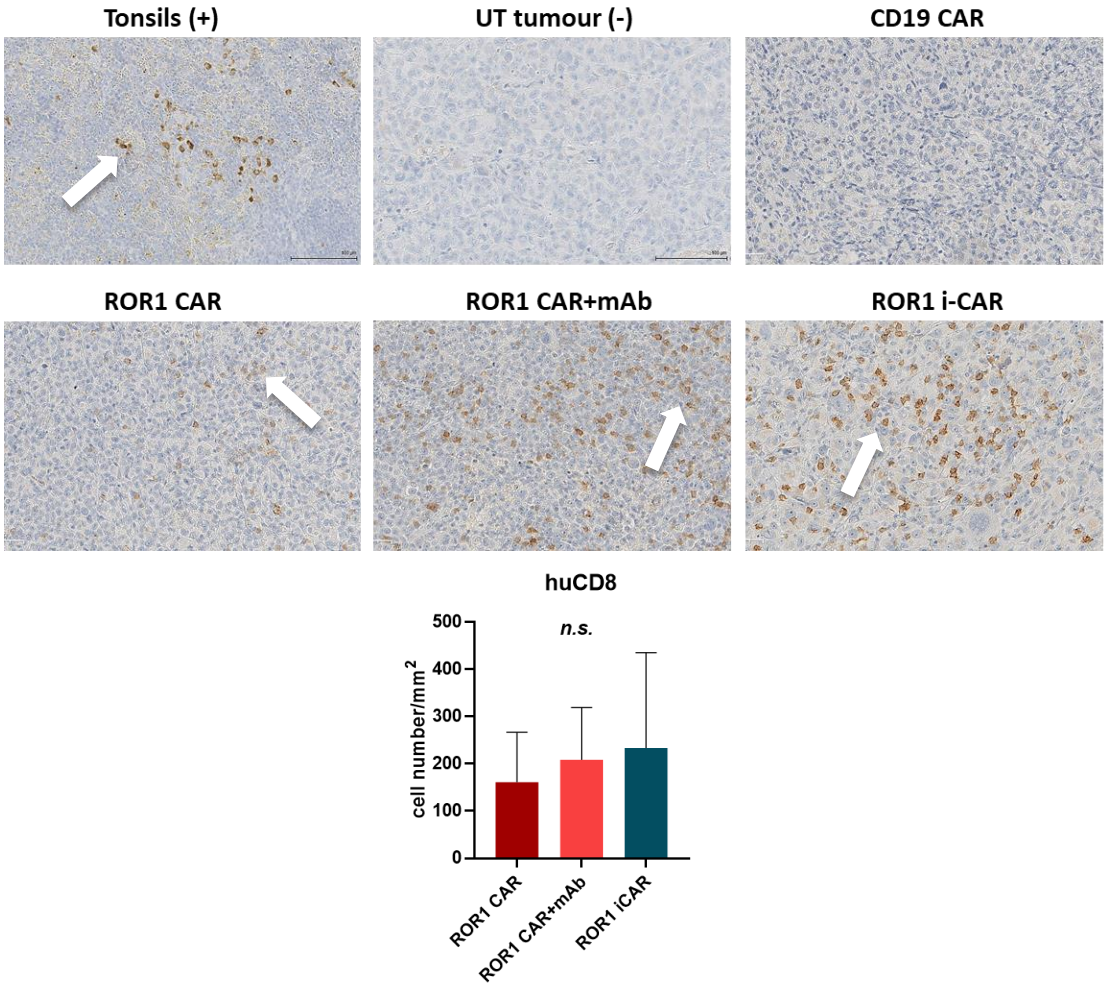

Figure 6-11 IHC staining and quantification for human CD8. Staining was performed on paraffin embedded tumour tissues. Representative snapshots from all treatment groups show positive staining (white arrows) for ROR1 CAR-treated mice compared to negative control (untreated tumour). CD19-treated tumours showed very low positivity. Staining was performed on 5 areas/tumour, 5-6 tumours/treatment group and quantified blindly by a collaborator. Results are mean+SD of all staining, expressed in cell number/mm^2.

These findings suggest a PD-1 blockade mediated increase in cytotoxic T cell infiltration in the tumours, but as the increased infiltration is not significant, we hypothesise that other factors are influencing the CAR-T cell-mediated anti-tumour effect. For instance, we do not know the status of these CD8+T cells (e.g. fitness, cell stage), nor the relative percentage of CAR-T cells versus untransduced T cells.

6.2.3 mCherry and FOXP3

We therefore assessed the expression of two additional markers: mCherry (CAR-T cells) and FOXP3 (Tregs). Staining for FOXP3 revealed a small number of positive cells, with most tumours being negative. This suggests that, if TILs are exhausted or hypofunctional, it may not be through Treg mechanisms.

Regarding CAR-T cell detection, mCherry+ staining was observed in all tumours, although at lower amounts than CD8. This suggests that both CAR-T cells and non-transduced T cells can infiltrate the tumours. Next, for mCherry, the quantification was performed blindly by our collaborator Dr Elena Miranda (UCL Pathology). Using the positive cell counting algorithm (QuPath image analysis software) on the whole section, she counted a significantly higher infiltration of i-CAR-T cells compared to ROR1 CAR-T cells only (44 versus 12 cells/mm^2, p<0.5, Figure 6-12). Quantification of tumours from the combination therapy group was 22cells/mm^2, which is twice the count of CAR-T cells only; this suggests that even if the PD-1 blockade-mediated effect was more transient than the induced secretion from the i-CAR, it was still able to increase CAR-T cell infiltration.

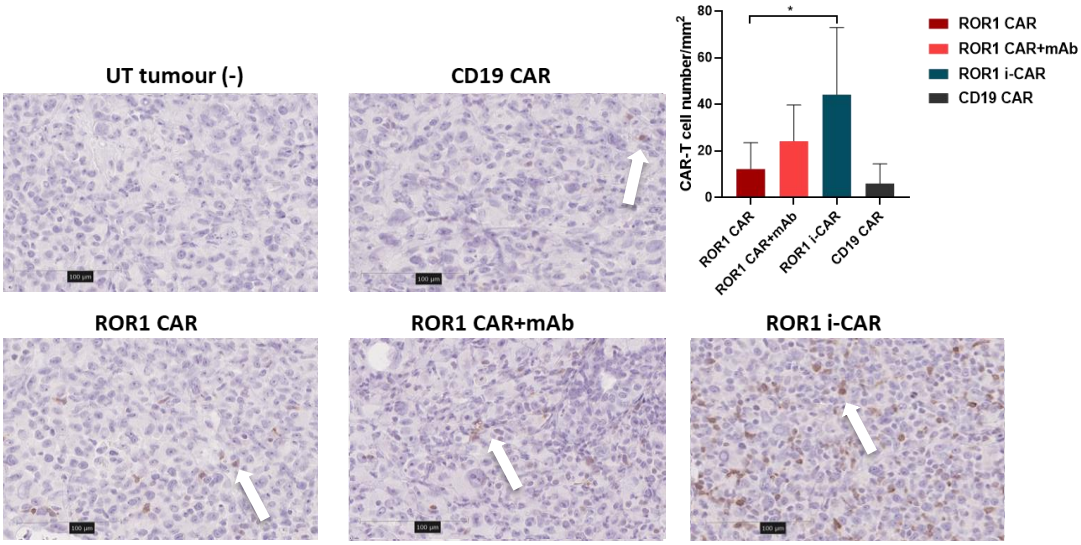

Figure 6-12 IHC showing staining for mCherry. The same tumour sections (1 section/tumour, 5 tumours/treatment group) were stained for mCherry to assess CAR-T cell infiltration. Representative snapshots show positive staining for ROR1 CAR-treated tumours (bottom panels). Quantification was performed and is sowed as positive cell number/mm^2.

Overall, the IHC staining revealed the presence of high numbers of TILs in all ROR1 CAR-treated tumours, with much lower numbers in the CD19-treated ones. Specifically, we looked at key markers such as CD8 for cytotoxic T lymphocytes, FOXP3 for Tregs and mCherry for CAR-expressing cells. The only significant difference was in the numbers of infiltrating CAR-T cells, which for the i-CAR-treated tumours were almost 4 times than ROR1 CAR-T cells only. Similarly, CD8+ TILs were increased in both i-CAR- and combination-treated tumours. Tregs were barely detected in all tumours. This suggests that in these *in vivo* settings, the injected Tregs, if present in higher amounts at the time of administration, somehow failed to infiltrate the tumour and/or to engraft and survive long-term. Overall, these findings highlight the presence of an effector T cell-based immune response against these tumours, which is likely increased by PD-1 blockade.

6.3 Ex-vivo analysis via Flow cytometry reveal higher numbers of i-CAR-T cells

After reaching endpoint, we collected the spleens from the treated mice, to which we extracted the T cells for downstream assessment via Flow

Cytometry. The aim was once again to address any difference between treatment groups. To note, spleens were processed fresh, therefore at different time points depending on when the animals were sacrificed. This means that direct comparisons between treatment groups are difficult to make as time can impact results (e.g. spleens collected on day 55 versus day 85).

The first parameter we measured was CAR-T cell numbers extracted from the spleens. The spleen is often considered as reservoir of large quantities of lymphocytes, and their status in the spleen has been shown to correspond with their function *in vivo* (364). We measured more than doubled CAR-T cell numbers in the i-CAR-treated spleens compared to ROR1 CAR-T cells only, which suggests better engraftment in these mice, especially considering that some spleens were processed up to 80+days post- CAR-T cell treatment (Figure 6-13C). We then stained the CAR-T cells for the following surface markers: CD4, CD8, PD-1, CCR7, and CD45RO. Results, in line with the IHC staining for the tumours, show increased %CD8+ CAR-T cells (60% versus 42%) and slight decrease in PD-1+ CAR-T cells (48% versus 41%) compared to parental CAR treatment (Figure 6-13A for gating strategy and 6-13B, mean+SD of four spleens/treatment).

When we looked at T central memory (TCM, CD45RO+CCR7+) versus T effector memory (TCM, CD45RO+CCR7-) we did not find any remarkable difference between treatments, with about 50/50 ratio between the two. We specifically looked at the TCM phenotype as it has been showed to be more long-lived, to better control tumours and to engraft better than effector memory cells (365, 366).

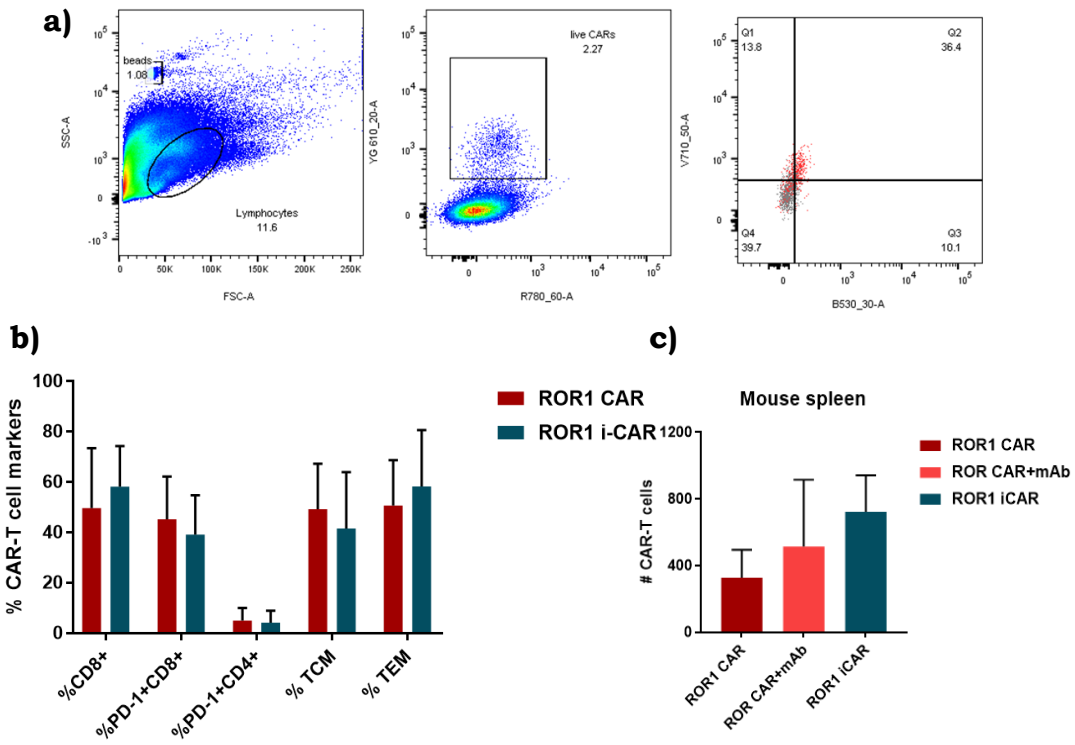

Figure 6-13 Flow cytometry gating and assessment of spleen-derived CAR-T cells. Spleens were harvested, digested and lymphocytes were extracted on the same day, with staining for surface markers. a) Gating strategy for %live mCherry+ cells; b) %positive cells based on CAR-T cell population, mean+SD of 4-5spleens from 2 donor-derived CAR-T cells with total *n*=7/treatment group; c) CAR-T cell numbers normalised to recorded counting beads, *n*=4 spleens/treatment group.

For downstream analysis using Nanostring technology (next section), we isolated TILs from fresh tumours which were harvested at the same time (4-weeks post treatment). Cells were collected at this time point as it previously showed noticeable differences between the two therapeutics in mice. TILs were sorted for CAR-T cells (mCherry and CD3 expression). We observed that the numbers of sorted cells were substantially different between treatment groups, where the average of sorted i-CAR-T cells was more than double compared to ROR1-CAR-T cells (33,000 versus 15,000 CAR-T cells, mean of two donor-derived CAR-T cells, Figure 6-14). This suggests better engraftment and/or homing to the tumour by i-CAR-T cells compared to monotherapy.

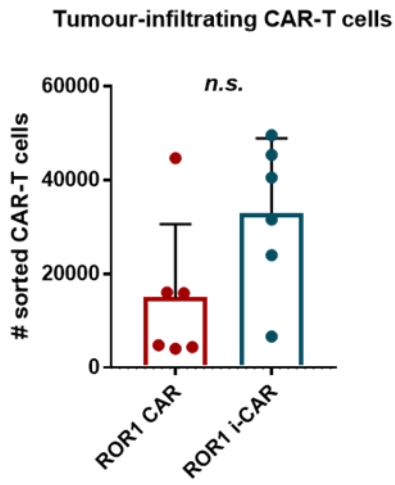

Figure 6-14 Tumour infiltrating CAR-T cell numbers. CAR-T cells were extracted from fresh tumours and sorted based on mCherry expression. Cells were needed for further experiment and therefore precise counts of sorted cells (2 donor-derived CAR-T cells) were noted. Student *t* test was performed.

6.4 Ex-vivo validation: Nanostring technology

In order to obtain a high-throughput and robust immune profiling analysis, we used the Nanostring technology which allows for direct single mRNA molecule counting to assess variations in gene expression. We used the CAR-T Characterization Gene Expression Panel to compare tumour-derived i-CAR-T cells versus parental ROR1 CAR, and to compare the *in vivo* versus *in vitro* setting (*ex-vivo* CAR-T cells versus CAR-T cells from 72h co-culture).

We focused on cell type abundance measurements (Figure 6-15), where genes previously shown to be characteristic of specific cell populations are used to measure these populations' abundance. Results, summarized as heat map, show linear cell type scores.

When we compared *in vitro*-derived CAR-T cells versus TILs, the most striking differences were in the CD4+ Th1 (4.4. versus 14.4), Treg (3.1 versus 18.8) and exhausted T cell (1.3 versus 20.7 linear score) compartments, which were close to absence compared to the TIL counterpart. The difference in Treg

presence between gene expression and IHC might be due to the different time points the cells were assessed (3 weeks post infusion versus 5-10 weeks, respectively). We were expecting to find a more exhausted phenotype with an increase in inhibitory cells, given the very different environments and times these cells were exposed to (*in vitro* for 72h, versus *in vivo* for 3 weeks). Specifically, we assume that the TME in live and growing tumours would be much more immunosuppressive due to the additional components such as stroma and suppressor cells. This, combined with the much more extended exposure time to inhibitory cells, is likely hampering the persistence and fitness of the CAR-T cells. However, some cells were expanded in the TILs group compared to *in vitro:* NK CD56dim cells (16.4 versus 3.2) which are reportedly cytotoxic, CD8+ T cells (33 versus 18) and cytotoxic T cells (22 versus 9), suggesting a potentially stronger cytotoxic anti-tumour response *in vivo.*

When we compared i-CAR-T cells versus parental CAR-T cells, we found several striking differences: for instance, despite having slightly less CD8+ T cells (23.5 versus 28.9 from ROR1 CAR), the T cells are more cytotoxic (19.7 versus 14.4) and much less exhausted (8.5 versus 15.14), which may be linked to the increased Treg population in ROR1 CAR-T cell samples (17.2 versus 13 from i-CAR-T cells). These results, which combine both *ex-vivo* and *in vitro* CAR-T cells, suggest that both CAR-T cells can mount an effective cytotoxic response at early stages. However, after long-term antigen exposure, parental CAR-T cells seem to be more exhausted and hypo functional than i-CAR-T cells. We hypothesise that, especially *in vivo*, the CAR-T cell tendency towards a hypo functional state is developing at much faster rates compared to the i-CAR-T cell counterpart. This would explain the significant improvements in long-term tumour growth management and increased survival by i-CAR-T cell treated mice versus ROR1 CAR-T cell-treated mice, as well as the increased infiltration observed with the IHC staining.

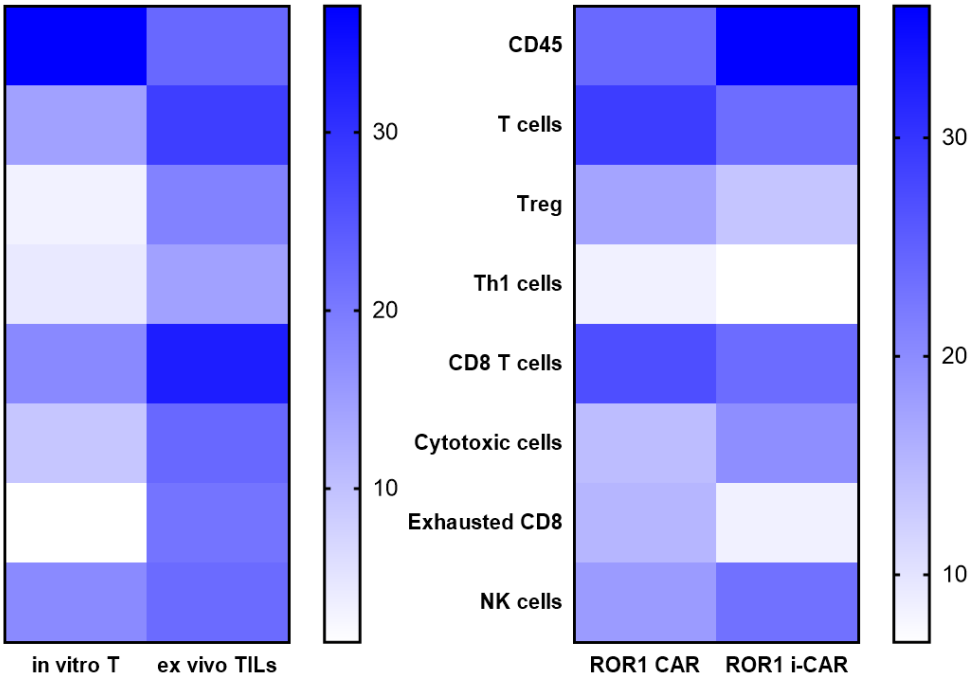

Figure 6-15 Summary of raw cell type abundance measurements via nSolver advanced analysis. Briefly, for TILs we harvested tumours at the same time (3tumours/CAR-treatment, 2 donors), extracted TILs and double positive cells for CD3 and mCherry were sorted at the Core Facility. Cells were immediately lysed in RLT buffer prior storage at -80°C. CAR-T cells were run on the cartridge using the CAR-T Characterization Panel codeset from Nanostring. For CAR-T cells from in vitro co-cultures, we did the same sorting and downstream procedure (3 donors used). After the advanced analysis report was generated, we selected specific information (cell type abundance) and compared ROR1 CAR versus ROR1 i-CAR (left heat map, *n*=9samples/condition), and in vitro T cells versus ex vivo TILs (right heat map, *n*=9samples/condition). QC flagged samples were excluded from the analysis.

Our assumptions are supported by the increased expression we observed in key genes in i-CAR-T cells compared to parental CAR-T cells (baseline, Table 5): IL2 receptors (p=0.002), granzyme B (p=0.006), IFN receptors (p=0.04), CD45RO (p=0.008) and CCR7 (p=0.02) receptor and several chemokines such as CCL1, CCL4, CXCR5 and CCL5 (Table 5). In terms of exhaustion markers, we found upregulated expression of genes for CTLA-4 (p=0.005), LAG3 (p=0.02) and Tim3 (p=0.008) in i-CAR-T cells compared to CAR-T cells. We hypothesise that because of the increased expression of many genes involved in activation, co-stimulation and metabolism, a percentage of these markers may be functioning as activation markers during early-stage activation, rather than exhaustion markers with inhibitory function.

Table 6: List of representative genes with significant increase in fold change. Comparison of i-CAR-T cell gene expression versus baseline of ROR1 CAR-T cells.

Gene	Linear fold change	*p* value	Function
FOSB, CD45R0, CXCR5	11.3, 5.11	0.001	Activation, TCR signalling
IL2RB	6.1	0.002	Activation, Interleukin Signalling, JAK-STAT, MAPK and PI3K Signalling, Phenotype, Th2, Toxicity
FOXP3	6.77	0.005	Cell Types, Phenotype, Th17, Treg
CTLA4, TNFRSF18, CTSW	4.99	0.005	Activation, Costimulatory Molecules, Exhaustion, T-cell exhaustion markers, TCR signalling
IL16, CCL1, DOCK2	4.25	0.005	Activation, Interleukin Signalling, Toxicity
GZMB	5.31	0.006	Apoptosis, Cell Types, Cytotoxicity, Exhaustion, Innate-like T-cells, Notch, Phenotype, Toxicity
GRK2, CCR7	3.21	0.007	Activation, Chemokine Signalling, Toxicity
HAVCR2 (TIM3)	2.62	0.008	Activation, Costimulatory Molecules, Exhaustion, T-cell exhaustion markers
IL10RA	3.2	0.009	Activation, Interleukin Signalling, JAK-STAT, Phenotype, Toxicity, Treg
GADD45B, CARD10, FKBP1A	3.54	0.012	Activation, Apoptosis, Cell Cycle, Exhaustion, MAPK and PI3K Signalling, Metabolism, NF-kB, Toxicity
PTPN6, OAS2, EGR1, IFNGR2/R1	3.2	0.013	Activation, Toxicity, Type I interferon signalling, Type II interferon signalling
LAG3	3.05	0.02	Activation, Antigen processing & presentation, Cell Types, Costimulatory Molecules, Exhaustion, T-cell exhaustion markers
STAT4/1, SOCS4	1.87	0.023	Activation, JAK-STAT, Phenotype, Th1
BCL6	2.52	0.026	Phenotype, Tfh, Th1
LCK and LTB	1.99	0.027	Activation, Cytotoxicity, NF-kB, TCR signalling, Toxicity
CCL4/L1, CCL22, TRAF5	3.6	0.03	Activation, Chemokine Signalling, Innate-like T-cells, NF-kB, Phenotype, Toxicity
PRKCB, RAC2, HLA-E	1.53	0.031	Activation, Cell Cycle, MAPK and PI3K Signalling, Metabolism, mTOR, NF-kB, Persistence, Phenotype, T-cell migration, Toxicity
IL12RB2, CCL5	1.85	0.036	Activation, Interleukin Signalling, JAK-STAT, Phenotype, Th1, Toxicity
ITGAM, CD38, CDC42	2.65	0.038	Persistence, T-cell migration

6.5 Conclusion

Currently there are several strategies that involve the use of checkpoint inhibitors combined with CAR-T cell therapy. Two promising examples include the work by Gargett et al, where they showed that PD-1 blockade enhanced survival of their GD-2-redirected CAR-T cells and promoted killing of PD-L1+ tumour cell lines (150); additionally, Tanoue and colleagues document the superiority of local versus systemic production of PD-L1 mini-

body combined with an oncolytic adenovirus and administration of tumour-directed CAR-T cells to control the growth of solid tumours in a HER2+ prostate cancer xenograft model (350).

Additionally, two independent studies showed that by engineering CAR-T cells to constitutively secrete checkpoint blockade they achieved significant tumour eradication and survival of the animals compared to monotherapy in multiple mouse models (156, 367).

Our approach was to combine our anti-ROR1 CAR-T cell therapy with anti-PD-1 blockade through inducible secretion of a blocking scFv. In this way, we aim to boost the CAR-T cell responses against solid tumours by interfering with the PD-L1-mediated local immunosuppression while reducing the risk of unwanted cell activation and side effects that could arise from the constant release of checkpoint inhibitors, especially in an *in vivo* setting.

For the *in vivo* studies we selected the breast cancer cell line MDA-MB-231 that has been engineered to express Luciferase. The aim was to establish a TNBC orthotopic model via subcutaneous injection of tumour cells in the mammary fat pad of NSG mice (Charles River). This mouse strain was chosen for its feasibility to engraft tumour xenografts and for allowing long-term analysis such as survival of the animals treated with human T cells. These assessments would have not been possible in a humanised model, such as the CD34 humanised mouse where CD34+ stem cells seed into the BM after adoptive transfer. T progenitor cells originating from these CD34+ cells migrate into the thymus and undergo positive selection and negative selection (under mouse MHC, instead of human HLA) in mouse thymus. After injecting human breast cancer cells into CD34 humanised mice, the T cells might reject them even before correct engraftment (xenogeneic response), and may also reject the inoculated human CAR T cells. An alternative would be to perform a PBMC humanisation (with the same donor as the CAR-T cells that will be used), however GvHD would become a concern. Additionally, as proof of concept, we were interested in looking at the PD-1 blockade effect specifically on T cells, which would have not been possible in an immunocompetent model.

Overall, with pilot studies and subsequent studies, we succeeded in establishing consistent xenografts and confirmed no treatment-related side effect manifestations in weight drop, behaviour and visible signs. This was particularly important given the homology between mouse and human ROR1, and the antigen expression on healthy tissues (368, 369).

We compared treatment efficacy between parental ROR1 CAR, combination therapy and ROR1 i-CAR in two independent studies with two donor-derived T cells. Results were reproducible and showed that with a single dose, ROR1 i-CAR-T cells were able to significantly slow down tumour growth when compared to either ROR1 CAR or, to a less extent, combination therapy. While there are many examples of checkpoint blockade-mediated increased efficacy of CAR-T cells in vivo, some reports showed no significant advantage in tumour reduction or survival (154, 350, 370), highlighting that factors such as tumour target, CAR-T cell construct and protocols such as continuous mAb injections throughout the experiment can influence the checkpoint blockade effect on anti-tumour activity. Moreover, CAR-T cells harbouring the CD28 costimulatory domain showed to respond better to checkpoint blockade therapy as opposed to 41BB constructs (78) which is likely due to the activated PD-1 inhibitory effect on CD28-mediated signalling (371). This may explain further the marginal improvement we observed with our 41BB CAR constructs with combination therapy.

Compared to all other treatment groups, we also detected increased i-CAR-T cell numbers in the spleens and increased CD8+T cells and CAR-T cells (mCherry+) within the tumours, suggesting better persistence of the i-CAR-T cells which also resulted in significantly prolonged survival of i-CAR-treated mice.

We then performed additional CAR-T cell profiling using the targeted gene expression screening technology from Nanostring. We observed a more exhausted phenotype for parental CAR-T cells with increased exhausted CD8+ T cells and regulatory T cells. These findings were confirmed by differential gene expression measurements, where i-CAR-T cells showed significantly higher expression of several genes related to activation, survival

and effector functions such as IL-2 and IFN receptors, granzyme B, CCL1 and CD45RO. These results confirm our assumption that, compared to parental ROR1 CAR-T cells, the i-CAR-T cells have increased effector functions which ultimately lead to better and longer anti-tumour effect resulting in significant survival benefit for the treated mice.

Chapter 7 Summary and future work

Adoptive transfer of T cells expressing chimeric antigen receptors (CARs) is an innovative form of immunotherapy in which autologous T cells are genetically modified to express synthetic receptors enabling recognition of cancer cells in an HLA-independent manner. CAR T cells raise the possibility of achieving long term disease control even after a single infusion, as it has been showed in the context of CD19+ haematological malignancies (94, 133).

The lack of efficacy observed in the context of solid tumours paved the way to multiple approaches to bolster CAR-T cell therapy. Some promising strategies include: CAR-T cells harbouring two scFv targeting two different tumour antigens at the same time, making the response more targeted and decreasing chances of tumour escape via downregulation of one targeted antigen (101, 141); combination therapy with therapeutic antibodies (150) or oncolytic viruses (350); and CAR-T cells secreting therapeutics such as pro-inflammatory cytokines (136) and checkpoint blockade molecules to bolster the anti-tumour response from infiltrating immune cells (367).

Like canonical T cells, CAR-T cells are also susceptible to immunoregulatory checkpoints and acquire a differentiated and exhausted phenotype resulting in loss of effector functions (78, 150, 372). PD-1/PD-L1 blockade, either in combination or directly secreted by CAR-T cells has shown to enhance cytotoxicity (78, 151), and to improve survival in murine models (156, 367, 370). Combination therapy is actively investigated in the clinic despite the side effects that may arise from systemic administration of checkpoint inhibitors (238, 346).

We believe that a spatially targeted checkpoint blockade delivery may enhance CAR-T cell effectiveness against solid tumours whilst limiting off-target toxicity (238, 332). We therefore combined CAR-T cell therapy with a localized delivery of PD-1 blockade to overcome the local immunosuppression. To our knowledge, this is the first evaluation of the checkpoint blockade effect on CAR-T cell therapy in the context of ROR1.

ROR1 is an attractive therapeutic target due to its overexpression on a wide range of aggressive tumours with unmet therapeutic need including breast and lung cancers, as well as cancer initiating cells. Given its low expression on several healthy tissues, careful monitoring for on-target off-tumour side effects will be fundamental. So far, clinical evaluation showed safe administration but limited efficacy using either CAR-T cells or a therapeutic antibody (373), with the report by Specht and colleagues highlighting the upregulation of inhibitory receptors in expanding ROR1 CAR-T cells (322).

7.1 Previous results

We have previously reported the generation of a fully humanized ROR1-targeted scFv and showed superior activity compared to the other two binders tested in the clinic, both in a BiTE and in a second-generation CAR formats. This enhanced efficacy might be due to our targeted epitope (Frizzle versus Ig-like), as a more-proximal position on the membrane of the epitope has been shown to activate CAR-T cells more efficiently (374). When we tested the same three binders in the context of solid tumours, we observed the same trend but overall lower effectiveness, which is in line with the reported poor performance of CAR-T cells in the context of solid malignancies (150, 367, 375).

7.2 Summary of this project findings

Overall, with this work we show the generation of a new and improved ROR1-targeted therapeutic, made of CAR-T cells secreting αPD-1 scFv upon activation. Through a thorough and extended in vitro characterisation, we first demonstrated the safety and efficiency of the inducible system; this was followed by showing a PD-1 blockade-mediated effect on improved targeted cytotoxicity, pro-inflammatory cytokine secretion and proliferation using a panel of ROR1+ and PD-L1+ cell lines.

Due to the limitations of *in vitro* characterisation using cell lines, it would be interesting and more informative to use better translational models such as 3D tumorspheres (376), patient-derived samples and organoid technology (377, 378).

Finally, when we tested this system in a TNBC xenograft mouse model, we confirmed the preliminary *in vitro* findings as we observed a significant benefit for mice receiving a single dose of i-CAR-T cells compared to ROR1 CAR-T cells only or combination therapy. We showed that this increased efficacy is due to better i-CAR-T cell engraftment, better tumour infiltration and a less inhibited/exhausted phenotype compared to ROR1 CAR-T cells only.

7.3 Further preclinical assessments

7.3.1 In vitro

As we successfully generated a robust, long-lasting and specific inducible system, our platform gives the possibility to pair CAR-T cell therapy with other therapeutics including other targeted scFvs, cytokines, chemokines, enzymes and so on.

A feature of exhausted T cells versus activated, memory-like CD8+ T cells is their altered long-term survival: in the absence of the targeted antigen, exhausted T cells are unable to proliferate and to persist long term (24). While we do observe increased proliferation by i-CAR-T cells *in vitro*, the comparison of proliferative capacities long-term and following removal of ROR1 might provide valuable information.

The anti-inflammatory cytokine IL-10 is often induced in chronic infections and cancer (23). It has been shown that IL-10 blockade can prevent and/or reverse T cell exhaustion (25). Although we did not perform any screening for this cytokine, if present, as combination strategy it would be interesting to pair PD-1 blockade with IL-10 blockade to evaluate the effect on CAR-T cell effector functions. This approach has already been tested in the context of chronic viral infection, where robust effector responses, functional memory T cells, and effective control of viral replication were reported (23, 379).

At the same time, we are planning to further increase the strength of the promoter, for example via codon-optimisation of the coding sequence for the scFv and using a different minimal promoter. In case of unwanted/non-

specific activation of the inducible promoter, we could test pharmacological inhibitors FK506 (tacrolimus) and cyclosporin A (CsA) to block activation and secretion as reported by Uchibori and colleagues (353).

7.3.2 *In vivo*

One of the preliminary experiments that should follow should be testing the CAR-T cells in a different tumour model (e.g. NSCLC) to confirm that the effect is not limited to the model and cell line that we used. Moreover, as for the *in vitro* assessment, cell lines may not necessarily represent the complexities of the original tumours, including heterogeneity in terms of clonal evolution leading to differential antigen expression (positive or negative), absolute expression levels, mutated antigens and differences in immune cell infiltrate (380, 381). One solution could be the use of patient-derived tumour samples (382), which would provide more robust evidence of the therapeutic effect of ROR1-targeted CAR-T cells. Moreover, it would be interesting to assess whether a single dose with more CAR-T cells, or multiple injections of CAR-T cells would increase the anti-tumour effect which may lead to tumour eradication.

Despite the very promising findings, we are aware of some limitations of the NSG strain: firstly, the lack of a functional immune system, despite allowing monitoring of long-term survival, prevented the assessment of the PD-1 blockade effect on other immune cells exploiting this pathway. One clear example is given by the report from Lin et al., where they demonstrated a loss of therapeutic effect by PD-L1 blockade in immunodeficient mice, suggesting that PD-L1+ macrophages and dendritic cells may play a role in shaping and predicting clinical efficacy of PD-1/PD-L1 blockade (383). This may also explain the lack of efficacy by combination therapy that we observed.

The use of wild type mouse models is excluded, considering that our ROR1 binder is humanized and therefore could cause allergic reactions; moreover, the PD-1 binder recognises human PD-1 but may not recognise murine PD-1, considering that the two genes share 60% homology at the amino acid level (384).

Humanised mouse models could offer an attractive alternative to observe the broader effect that our therapy would have, specifically on other cells of the immune system. Moreover, humanised models offer a better recapitulation of the TME, as well as using donor-matched conditions (CD34+ stem cells and CAR-T cells derived from the same donor). One example of a strain that could be utilised is the SGM3 mouse (JAX), also to see enhanced myeloid engraftment including PD-1 expressing macrophages.

7.3.3 Toxicology assessments

To further characterise the CAR-T cell effect *in vivo,* it will be fundamental to perform toxicology studies with dose-escalating CAR-T cell infusions to assess potential on-target off-tumour toxicity in mice which has been reported by other groups (369, 385, 386). In case toxicity is observed (such as in the liver and lungs), H & E staining could be performed to quickly assess tissue damage.

The other two published ROR1 binders, cirmtuzumab (mAb) and R12 CAR-T cells, have been tested in non-human primates with reported lack of toxicity, which is at odds given the presence of ROR1 on healthy tissues such as adipocytes (306). In the case of cirmtuzumab, this may be due to its primary function as signalling inhibitor instead of mediating cytotoxicity. Additionally, CAR T cell administration in nonhuman primates, which present an ROR1 expression pattern in normal tissues similar to humans, showed no evidence of toxicities (319). Poor trafficking of CAR T cells to these ROR1 positive healthy tissues and/or insufficient level of antigens to trigger CAR-T cell trafficking and activation might explain the lack of toxicity.

Ongoing clinical trials with both reagents reported safe profile: for cirmtuzumab, Kipps' group recently reported preliminary results of the clinical trial where 26 CLL patients received the mAb (up to 20 mg/kg) with no dose-limiting toxicities observed (373). Regarding the CAR-T cell trial, clinical reports show lack any significant on-target, off-tumour toxicities such as severe neurotoxicity, severe CRS, or tumour lysis syndrome in the 7 ROR1-expressing TNBC patients that were treated (387). Importantly, they reported

an exhausted phenotype for the engrafted second-generation ROR1 scFv-4-1BB-CD3ζ cells. Further results with a wider treated population are awaited from both trials as they would be very informative especially for the toxicity profile.

It is important to remember that CAR-T cell-derived toxicities may be confined to a specific construct and/or binder, as demonstrated by independent studies (114, 388). Nevertheless, we will have to carefully plan and assess our constructs for potential on-target off-tumour cytotoxicity to allow for a low-risk and successful ROR1-targeted therapy, as well as anticipation and management of the potential side effects.

7.3.4 Ex-vivo characterisation

Regarding the *ex-vivo* characterisation, one of the first important assessments to perform is the quantification of the released scFv and the mAb in the TME of treated mice. This could be done via IHC, ELISA or via labelling of the PD-1 blockers. Our attempt to detect via BLI the scFv tagged with a luciferase in mice had failed, possibly due to weak signal; alternatively, other ways for live tracking such as radiolabelling could be explored via collaborat6ion with the CABI imaging facility at the Cancer Institute. In determining the intra-tumoral mAb concentration, we could assess for potential poor trafficking into the tumour as the plasma concentration drops, or potentially determine the mAb uptake by tumour-associated macrophages via their FcγR as our mAb is a mouse IgG. For the scFv, it would be interesting to confirm the hypothesised long-lasting production by long-lived and engrafted i-CAR-T cells.

Additionally, we could also label and track CAR-T cells, to determine useful information such as where else the infused T cells might go (lung, etc.), the duration of tumour infiltration, overall CAR-T cell persistence or engraftment and so on (389, 390).

For the *in vivo* settings, an interesting point of discussion is whether the targeting of the PD-1:PD-L1 pathway is truly reversing exhaustion, since in

mouse tumour models injections are usually performed at early stages of treatment, when full T cell exhaustion may not have developed yet. Instead, what may be happening is that PD-1 blockade is impacting priming and/or preventing the development of exhaustion (24).

This scenario may be happening in our TNBC xenograft model, where the combination therapy treatment group received 3 injections of PD-1 blockade only at beginning of treatment (day 3, 7 and 10 post treatment). We could evaluate the exhaustion profile of tumour infiltrating CAR-T cells: in case of exhaustion signatures on parental CAR-T cells only, we could hypothesise that combination therapy at such early stage is impairing exhaustion development. We can perform this ex-vivo experiment via multicolour flow cytometry or DNA/RNA sequencing.

Moreover, in the in vivo settings, it remains unclear whether PD-1 blockade is directly impacting intratumoral T cells or it may also reinvigorate T cells in the secondary lymphoid organs (24). We could therefore consider characterising T cells from the tumour draining lymph nodes via ex-vivo multicolour flow cytometry.

Moreover, given the powerful Nanostring technology in assessing for gene expression, it would be interesting to use a different kit, such as the PanCancer IO 360 Gene Expression Panel which allows for a multifaceted characterization of cancer biology and interrogation of the mechanisms of immune evasion. This analysis would be particularly informative in the setting of a CAR-T cell-treated PDX.

Following on from the superior i-CAR efficacy that we observed compared to parental CAR-T cells and confirming the lack of limiting toxicities, we would be much more confident of the potential to safely administer ROR1 i-CAR T cells to generate long-lived and effective responses against ROR1+ solid malignancies difficult to treat such as TNBC and NSCLC.

1. Roybal KT, Lim WAJAroi. Synthetic immunology: hacking immune cells to expand their therapeutic capabilities. annual review of immunology. 2017;35:229-53.
2. Dunn GP, Old LJ, Schreiber RD. The three Es of cancer immunoediting. Annu Rev Immunol. 2004;22:329-60.
3. Grivennikov SI, Greten FR, Karin MJC. Immunity, inflammation, and cancer. 2010;140(6):883-99.
4. Malissen B, Gregoire C, Malissen M, Roncagalli RJNi. Integrative biology of T cell activation. 2014;15(9):790.
5. Iwai Y, Hamanishi J, Chamoto K, Honjo T. Cancer immunotherapies targeting the PD-1 signaling pathway. Journal of Biomedical Science. 2017;24(1):26.
6. Lonberg N, Korman AJ. Masterful Antibodies: Checkpoint Blockade. Cancer Immunology Research. 2017;5(4):275-81.
7. Dyck L, Mills KH. Immune checkpoints and their inhibition in cancer and infectious diseases. European Journal of Immunology. 2017.
8. Mueller DL, Jenkins MK, Schwartz RHJAroi. Clonal expansion versus functional clonal inactivation: a costimulatory signalling pathway determines the outcome of T cell antigen receptor occupancy. Annual review of immunology. 1989;7(1):445-80.
9. Schumacher TN, Schreiber RDJS. Neoantigens in cancer immunotherapy. 2015;348(6230):69-74.
10. Palucka K, Coussens LM, O'shaughnessy JJCj. Dendritic Cells, Inflammation and Breast Cancer. 2013;19(6).
11. Restifo NP, Dudley ME, Rosenberg SAJNRI. Adoptive immunotherapy for cancer: harnessing the T cell response. 2012;12(4):269.
12. Sieh M, Batzer A, Schlessinger J, Weiss AJM, Biology C. GRB2 and phospholipase C-gamma 1 associate with a 36-to 38-kilodalton phosphotyrosine protein after T-cell receptor stimulation. 1994;14(7):4435-42.
13. Boise LH, Minn AJ, Noel PJ, June CH, Accavitti MA, Lindsten T, et al. CD28 costimulation can promote T cell survival by enhancing the expression of Bcl-XL. 1995;3(1):87-98.
14. Gajewski TF, Schreiber H, Fu Y-XJNi. Innate and adaptive immune cells in the tumor microenvironment. 2013;14(10):1014.
15. Pardoll DM. The blockade of immune checkpoints in cancer immunotherapy. Nature Reviews Cancer. 2012;12(4):252-64.
16. Varn FS, Mullins DW, Arias‐Pulido H, Fiering S, Cheng CJI. Adaptive immunity programmes in breast cancer. 2017;150(1):25-34.

17. Gattinoni L, Powell Jr DJ, Rosenberg SA, Restifo NPJNRI. Adoptive immunotherapy for cancer: building on success. 2006;6(5):383.
18. Klebanoff CA, Gattinoni L, Restifo NPJIr. CD8+ T - cell memory in tumor immunology and immunotherapy. 2006;211(1):214-24.
19. Hinrichs CS, Borman ZA, Cassard L, Gattinoni L, Spolski R, Yu Z, et al. Adoptively transferred effector cells derived from naive rather than central memory CD8+ T cells mediate superior antitumor immunity. 2009;106(41):17469-74.
20. Klebanoff CA, Gattinoni L, Torabi-Parizi P, Kerstann K, Cardones AR, Finkelstein SE, et al. Central memory self/tumor-reactive CD8+ T cells confer superior antitumor immunity compared with effector memory T cells. 2005;102(27):9571-6.
21. Berger C, Jensen MC, Lansdorp PM, Gough M, Elliott C, Riddell SRJTJoci. Adoptive transfer of effector CD8+ T cells derived from central memory cells establishes persistent T cell memory in primates. 2008;118(1):294-305.
22. Blank CU, Haining WN, Held W, Hogan PG, Kallies A, Lugli E, et al. Defining 'T cell exhaustion'. Nature Reviews Immunology. 2019;19(11):665-74.
23. McLane LM, Abdel-Hakeem MS, Wherry EJ. CD8 T cell exhaustion during chronic viral infection and cancer. Annual review of immunology. 2019;37:457-95.
24. Pauken KE, Wherry EJ. Overcoming T cell exhaustion in infection and cancer. Trends in immunology. 2015;36(4):265-76.
25. Zarour HM. Reversing T-cell dysfunction and exhaustion in cancer. Clin Cancer Res. 2016.
26. Thommen DS, Schumacher TN. T cell dysfunction in cancer. Cancer cell. 2018;33(4):547-62.
27. Sawant DV, Yano H, Chikina M, Zhang Q, Liao M, Liu C, et al. Adaptive plasticity of IL-10+ and IL-35+ T reg cells cooperatively promotes tumor T cell exhaustion. Nature immunology. 2019;20(6):724-35.
28. Takeuchi A, Saito T. CD4 CTL, a cytotoxic subset of CD4+ T cells, their differentiation and function. Frontiers in immunology. 2017;8:194.
29. Nakayamada S, Takahashi H, Kanno Y, O'Shea JJJCoii. Helper T cell diversity and plasticity. 2012;24(3):297-302.
30. Hung K, Hayashi R, Lafond-Walker A, Lowenstein C, Pardoll D, Levitsky HJJoEM. The central role of CD4+ T cells in the antitumor immune response. 1998;188(12):2357-68.
31. Nishimura T, Nakui M, Sato M, Iwakabe K, Kitamura H, Sekimoto M, et al. The critical role of Th1-dominant immunity in tumor immunology. 2000;46(1):S52-S61.
32. Bos R, Sherman LAJCr. CD4+ T-cell help in the tumor milieu is required for recruitment and cytolytic function of CD8+ T lymphocytes. 2010;70(21):8368-77.

33. Antony PA, Piccirillo CA, Akpinarli A, Finkelstein SE, Speiss PJ, Surman DR, et al. CD8+ T cell immunity against a tumor/self-antigen is augmented by CD4+ T helper cells and hindered by naturally occurring T regulatory cells. 2005;174(5):2591-601.
34. Zhu J, Paul WEJB. CD4 T cells: fates, functions, and faults. 2008;112(5):1557-69.
35. Mahnke K, Johnson TS, Ring S, Enk AHJJods. Tolerogenic dendritic cells and regulatory T cells: a two-way relationship. 2007;46(3):159-67.
36. Swain SL, McKinstry KK, Strutt TM. Expanding roles for CD4+ T cells in immunity to viruses. Nature Reviews Immunology. 2012;12(2):136.
37. Trapani JA, Darcy PK. Immunotherapy of cancer. Australian Family Physician. 2017;46(4):194.
38. Fridman WH, Zitvogel L, Sautes-Fridman C, Kroemer G. The immune contexture in cancer prognosis and treatment. Nat Rev Clin Oncol. 2017.
39. Bianchini G, Balko JM, Mayer IA, Sanders ME, Gianni LJNrCo. Triple-negative breast cancer: challenges and opportunities of a heterogeneous disease. 2016;13(11):674.
40. Dudley ME, Yang JC, Sherry R, Hughes MS, Royal R, Kammula U, et al. Adoptive cell therapy for patients with metastatic melanoma: evaluation of intensive myeloablative chemoradiation preparative regimens. 2008;26(32):5233.
41. Rosenberg SA, Yannelli JR, Yang JC, Topalian SL, Schwartzentruber DJ, Weber JS, et al. Treatment of patients with metastatic melanoma with autologous tumor-infiltrating lymphocytes and interleukin 2. journal of the National Cancer Institute. 1994;86(15):1159-66.
42. Rosenberg SA, Restifo NP, Yang JC, Morgan RA, Dudley MEJNRC. Adoptive cell transfer: a clinical path to effective cancer immunotherapy. Nature Reviews Cancer. 2008;8(4):299.
43. Mackinnon S, Papadopoulos E, Carabasi M, Reich L, Collins N, Boulad F, et al. Adoptive immunotherapy evaluating escalating doses of donor leukocytes for relapse of chronic myeloid leukemia after bone marrow transplantation: separation of graft-versus-leukemia responses from graft-versus-host disease. Blood. 1995;86(4):1261-8.
44. Zhou J, Dudley ME, Rosenberg SA, Robbins PF. Persistence of multiple tumor-specific T-cell clones is associated with complete tumor regression in a melanoma patient receiving adoptive cell transfer therapy. J Immunother. 2005;28(1):53-62.
45. Turcotte S, Gros A, Hogan K, Tran E, Hinrichs CS, Wunderlich JR, et al. Phenotype and function of T cells infiltrating visceral metastases from gastrointestinal cancers and melanoma: implications for adoptive cell transfer therapy. The Journal of Immunology

2013;191(5):2217-25.

46. Hall M, Liu H, Malafa M, Centeno B, Hodul PJ, Pimiento J, et al. Expansion of tumor-infiltrating lymphocytes (TIL) from human pancreatic tumors. Journal for immunotherapy of cancer. 2016;4(1):61.
47. Billingham RE. The biology of graft-versus-host reactions. Harvey Lect. 1966;62:21-78.
48. Tolar J, Villeneuve P, Keating A. Mesenchymal stromal cells for graft-versus-host disease. Hum Gene Ther. 2011;22(3):257-62.
49. Paczesny S, Choi SW, Ferrara JL. Acute graft-versus-host disease: new treatment strategies. Curr Opin Hematol. 2009;16(6):427-36.
50. Wanko SO, Chao NJ. Non-pharmacologic approaches to graft-versus-host prevention. Blood Rev. 2005;19(4):203-11.
51. Shlomchik WD. Graft-versus-host disease. Nat Rev Immunol. 2007;7(5):340-52.
52. Archbold JK, Macdonald WA, Burrows SR, Rossjohn J, McCluskey J. T-cell allorecognition: a case of mistaken identity or deja vu? Trends Immunol. 2008;29(5):220-6.
53. Amrolia PJ, Muccioli-Casadei G, Huls H, Adams S, Durett A, Gee A, et al. Adoptive immunotherapy with allodepleted donor T-cells improves immune reconstitution after haploidentical stem cell transplantation. Blood. 2006;108(6):1797-808.
54. Koreth J, Matsuoka K, Kim HT, McDonough SM, Bindra B, Alyea EP, 3rd, et al. Interleukin-2 and regulatory T cells in graft-versus-host disease. N Engl J Med. 2011;365(22):2055-66.
55. Vago L, Oliveira G, Bondanza A, Noviello M, Soldati C, Ghio D, et al. T-cell suicide gene therapy prompts thymic renewal in adults after hematopoietic stem cell transplantation. Blood. 2012;120(9):1820-30.
56. DembiĆ Z, Haas W, Weiss S, McCubrey J, Kiefer H, von Boehmer H, et al. Transfer of specificity by murine α and β T-cell receptor genes. nature. 1986;320(6059):232.
57. Morris EC, Stauss HJJB. Optimizing T-cell receptor gene therapy for hematologic malignancies. Blood. 2016;127(26):3305-11.
58. Robbins PF, Kassim SH, Tran TL, Crystal JS, Morgan RA, Feldman SA, et al. A pilot trial using lymphocytes genetically engineered with an NY-ESO-1–reactive T-cell receptor: long-term follow-up and correlates with response. Clin Cancer Res. 2015;21(5):1019-27.
59. Valitutti S, Müller S, Cella M, Padovan E, Lanzavecchia A. Serial triggering of many T-cell receptors by a few peptide–MHC complexes. nature. 1995;375(6527):148.
60. Bendle GM, Linnemann C, Hooijkaas AI, Bies L, de Witte MA, Jorritsma A, et al. Lethal graft-versus-host disease in mouse models of T cell receptor gene therapy. Nat Med. 2010;16(5):565-70, 1p following 70.
61. Linette GP, Stadtmauer EA, Maus MV, Rapoport AP, Levine BL, Emery L, et al. Cardiovascular toxicity and titin cross-reactivity of

affinity-enhanced T cells in myeloma and melanoma. Blood. 2013;122(6):863-71.
62. Kunert A, Straetemans T, Govers C, Lamers C, Mathijssen R, Sleijfer S, et al. TCR-engineered T cells meet new challenges to treat solid tumors: choice of antigen, T cell fitness, and sensitization of tumor milieu. Frontiers in immunology. 2013;4:363.
63. Romero JM, Jimenez P, Cabrera T, Cozar JM, Pedrinaci S, Tallada M, et al. Coordinated downregulation of the antigen presentation machinery and HLA class I/beta2-microglobulin complex is responsible for HLA-ABC loss in bladder cancer. Int J Cancer. 2005;113(4):605-10.
64. Gross G, Waks T, Eshhar ZJPotNAoS. Expression of immunoglobulin-T-cell receptor chimeric molecules as functional receptors with antibody-type specificity. Proceedings of the National Academy of Sciences. 1989;86(24):10024-8.
65. Goverman J, Gomez SM, Segesman KD, Hunkapiller T, Laug WE, Hood LJC. Chimeric immunoglobulin-T cell receptor proteins form functional receptors: implications for T cell receptor complex formation and activation. Cell. 1990;60(6):929-39.
66. Eshhar Z, Waks T, Gross G, Schindler DGJPotNAoS. Specific activation and targeting of cytotoxic lymphocytes through chimeric single chains consisting of antibody-binding domains and the gamma or zeta subunits of the immunoglobulin and T-cell receptors. Proceedings of the National Academy of Sciences. 1993;90(2):720-4.
67. Marcus A, Eshhar Z. Allogeneic chimeric antigen receptor-modified cells for adoptive cell therapy of cancer. Expert opinion on biological therapy. 2014;14(7):947-54.
68. Wang X, Riviere I. Manufacture of tumor-and virus-specific T lymphocytes for adoptive cell therapies. Cancer gene therapy. 2015;22(2):85-94.
69. Hudecek M, Lupo-Stanghellini M-T, Kosasih PL, Sommermeyer D, Jensen MC, Rader C, et al. Receptor affinity and extracellular domain modifications affect tumor recognition by ROR1-specific chimeric antigen receptor T cells. Clin Cancer Res. 2013;19(12):3153-64.
70. Cheadle EJ, Gornall H, Baldan V, Hanson V, Hawkins RE, Gilham DE. CAR T cells: driving the road from the laboratory to the clinic. Immunological reviews. 2014;257(1):91-106.
71. Hegde UP, Mukherji B. Current status of chimeric antigen receptor engineered T cell-based and immune checkpoint blockade-based cancer immunotherapies. Cancer immunology, immunotherapy : CII. 2017.
72. Chmielewski M, Abken H. TRUCKs: the fourth generation of CARs. Expert opinion on biological therapy. 2015;15(8):1145-54.
73. Stoiber S, Cadilha BL, Benmebarek M-R, Lesch S, Endres S, Kobold S. Limitations in the Design of Chimeric Antigen Receptors for Cancer Therapy. cells. 2019;8(5):472.

74. Savoldo B, Ramos CA, Liu E, Mims MP, Keating MJ, Carrum G, et al. CD28 costimulation improves expansion and persistence of chimeric antigen receptor–modified T cells in lymphoma patients. The Journal of clinical investigation. 2011;121(5):1822.
75. Kim M-G, Kim D, Suh S-K, Park Z, Choi MJ, Oh Y-K. Current status and regulatory perspective of chimeric antigen receptor-modified T cell therapeutics. Archives of pharmacal research. 2016;39(4):437-52.
76. Maher J, Brentjens RJ, Gunset G, Rivière I, Sadelain MJNb. Human T-lymphocyte cytotoxicity and proliferation directed by a single chimeric TCRζ/CD28 receptor. Nature biotechnology. 2002;20(1):70.
77. Imai C, Mihara K, Andreansky M, Nicholson I, Pui C, Geiger T, et al. Chimeric receptors with 4-1BB signaling capacity provoke potent cytotoxicity against acute lymphoblastic leukemia. Leukemia. 2004;18(4):676.
78. Cherkassky L, Morello A, Villena-Vargas J, Feng Y, Dimitrov DS, Jones DR, et al. Human CAR T cells with cell-intrinsic PD-1 checkpoint blockade resist tumor-mediated inhibition. J Clin Invest. 2016;126(8):3130-44.
79. Long AH, Haso WM, Shern JF, Wanhainen KM, Murgai M, Ingaramo M, et al. 4-1BB costimulation ameliorates T cell exhaustion induced by tonic signaling of chimeric antigen receptors. Nat Med. 2015;21(6):581-90.
80. Sha H-h, Wang D-d, Yan D-l, Hu Y, Yang S-j, Liu S-w, et al. Chimaeric antigen receptor T-cell therapy for tumour immunotherapy. Bioscience reports. 2017;37(1):BSR20160332.
81. Till BG, Jensen MC, Wang J, Qian X, Gopal AK, Maloney DG, et al. CD20-specific adoptive immunotherapy for lymphoma using a chimeric antigen receptor with both CD28 and 4-1BB domains: pilot clinical trial results. Blood. 2012;119(17):3940-50.
82. Pule MA, Straathof KC, Dotti G, Heslop HE, Rooney CM, Brenner MK. A chimeric T cell antigen receptor that augments cytokine release and supports clonal expansion of primary human T cells. Mol Ther. 2005;12(5):933-41.
83. Koneru M, Purdon TJ, Spriggs D, Koneru S, Brentjens RJJO. IL-12 secreting tumor-targeted chimeric antigen receptor T cells eradicate ovarian tumors in vivo. Oncoimmunology. 2015;4(3):e994446.
84. Caruana I, Savoldo B, Hoyos V, Weber G, Liu H, Kim ES, et al. Heparanase promotes tumor infiltration and antitumor activity of CAR-redirected T lymphocytes. nature medicine. 2015;21(5):524.
85. Abken H. Adoptive therapy with CAR redirected T cells: the challenges in targeting solid tumors. Immunotherapy. 2015;7(5):535-44.
86. Serganova I, Moroz E, Cohen I, Moroz M, Mane M, Zurita J, et al. Enhancement of PSMA-Directed CAR Adoptive Immunotherapy by PD-1/PD-L1 Blockade. Mol Ther Oncolytics. 2017;4:41-54.
87. Khalil DN, Budhu S, Gasmi B, Zappasodi R, Hirschhorn-Cymerman D, Plitt T, et al. The New Era of Cancer Immunotherapy:

Manipulating T-Cell Activity to Overcome Malignancy. Adv Cancer Res. 2015;128:1-68.
88. Brentjens RJ, Riviere I, Park JH, Davila ML, Wang X, Stefanski J, et al. Safety and persistence of adoptively transferred autologous CD19-targeted T cells in patients with relapsed or chemotherapy refractory B-cell leukemias. Blood. 2011;118(18):4817-28.
89. Mann R, Mulligan RC, Baltimore DJC. Construction of a retrovirus packaging mutant and its use to produce helper-free defective retrovirus. cell. 1983;33(1):153-9.
90. Naldini L, Blömer U, Gallay P, Ory D, Mulligan R, Gage FH, et al. In vivo gene delivery and stable transduction of nondividing cells by a lentiviral vector. Science. 1996;272(5259):263-7.
91. Dull T, Zufferey R, Kelly M, Mandel R, Nguyen M, Trono D, et al. A third-generation lentivirus vector with a conditional packaging system. journal of virology. 1998;72(11):8463-71.
92. Xu J, Melenhorst JJ, Fraietta JA. Toward precision manufacturing of immunogene T-cell therapies. Cytotherapy. 2018.
93. Gill S, Maus MV, Porter DL. Chimeric antigen receptor T cell therapy: 25 years in the making. Blood reviews. 2016;30(3):157-67.
94. Davila ML, Riviere I, Wang X, Bartido S, Park J, Curran K, et al. Efficacy and toxicity management of 19-28z CAR T cell therapy in B cell acute lymphoblastic leukemia. Science translational medicine. 2014;6(224):224ra25.
95. Maude SL, Frey N, Shaw PA, Aplenc R, Barrett DM, Bunin NJ, et al. Chimeric antigen receptor T cells for sustained remissions in leukemia. New England Journal of Medicine. 2014;371(16):1507-17.
96. Turtle CJ, Hanafi LA, Berger C, Gooley TA, Cherian S, Hudecek M, et al. CD19 CAR-T cells of defined CD4+:CD8+ composition in adult B cell ALL patients. J Clin Invest. 2016;126(6):2123-38.
97. Pehlivan KC, Duncan BB, Lee DWJChmr. CAR-T Cell Therapy for acute lymphoblastic leukemia: transforming the treatment of relapsed and refractory disease. Current hematologic malignancy reports. 2018;13(5):396-406.
98. Rosenbaum LJNEJoM. Tragedy, perseverance, and chance—the story of CAR-T therapy. The New England journal of medicine. 2017;377(14):1313-5.
99. Susanibar Adaniya SP, Cohen AD, Garfall AL. Chimeric antigen receptor T cell immunotherapy for multiple myeloma: A review of current data and potential clinical applications. American journal of hematology. 2019.
100. Ruella M, Barrett DM, Kenderian SS, Shestova O, Hofmann TJ, Perazzelli J, et al. Dual CD19 and CD123 targeting prevents antigen-loss relapses after CD19-directed immunotherapies. J Clin Invest. 2016;126(10):3814-26.
101. Zah E, Lin MY, Silva-Benedict A, Jensen MC, Chen YY. T Cells Expressing CD19/CD20 Bispecific Chimeric Antigen Receptors Prevent Antigen Escape by Malignant B Cells. Cancer Immunol Res. 2016;4(6):498-508.

102. Martyniszyn A, Krahl A-C, Andre MC, Hombach AA, Abken HJHgt. CD20-CD19 bispecific CAR T cells for the treatment of B-cell malignancies. Human gene therapy. 2017;28(12):1147-57.
103. Fry TJ, Shah NN, Orentas RJ, Stetler-Stevenson M, Yuan CM, Ramakrishna S, et al. CD22-targeted CAR T cells induce remission in B-ALL that is naive or resistant to CD19-targeted CAR immunotherapy. nature medicine. 2018;24(1):20.
104. Park JR, Digiusto DL, Slovak M, Wright C, Naranjo A, Wagner J, et al. Adoptive transfer of chimeric antigen receptor re-directed cytolytic T lymphocyte clones in patients with neuroblastoma. Mol Ther. 2007;15(4):825-33.
105. Louis CU, Savoldo B, Dotti G, Pule M, Yvon E, Myers GD, et al. Antitumor activity and long-term fate of chimeric antigen receptor–positive T cells in patients with neuroblastoma. Blood. 2011;118(23):6050-6.
106. Ahmed N, Brawley VS, Hegde M, Robertson C, Ghazi A, Gerken C, et al. Human epidermal growth factor receptor 2 (HER2)–specific chimeric antigen receptor–modified T cells for the immunotherapy of HER2-positive sarcoma. Journal of clinical oncology : official journal of the American Society of Clinical Oncology. 2015;33(15):1688.
107. Katz SC, Burga RA, McCormack E, Wang LJ, Mooring W, Point GR, et al. Phase I hepatic immunotherapy for metastases study of intra-arterial chimeric antigen receptor–modified T-cell therapy for CEA+ liver metastases. Clin Cancer Res. 2015;21(14):3149-59.
108. Lee DW, Gardner R, Porter DL, Louis CU, Ahmed N, Jensen M, et al. Current concepts in the diagnosis and management of cytokine release syndrome. Blood. 2014;124(2):188-95.
109. Neelapu SS, Tummala S, Kebriaei P, Wierda W, Gutierrez C, Locke FL, et al. Chimeric antigen receptor T-cell therapy—assessment and management of toxicities. Nat Rev Clin Oncol. 2018;15(1):47.
110. Hay KA, Turtle CJJD. Chimeric antigen receptor (CAR) T cells: lessons learned from targeting of CD19 in B-cell malignancies. drugs. 2017;77(3):237-45.
111. Topp MS, Gokbuget N, Stein AS, Zugmaier G, O'Brien S, Bargou RC, et al. Safety and activity of blinatumomab for adult patients with relapsed or refractory B-precursor acute lymphoblastic leukaemia: a multicentre, single-arm, phase 2 study. The Lancet Oncology. 2015;16(1):57-66.
112. Norelli M, Camisa B, Barbiera G, Falcone L, Purevdorj A, Genua M, et al. Monocyte-derived IL-1 and IL-6 are differentially required for cytokine-release syndrome and neurotoxicity due to CAR T cells. nature medicine. 2018;24(6):739.
113. Namuduri M, Brentjens RJ. Medical management of side effects related to CAR T cell therapy in hematologic malignancies. expert reviews in hematology: Taylor & Francis; 2016.
114. Morgan RA, Yang JC, Kitano M, Dudley ME, Laurencot CM, Rosenberg SA. Case report of a serious adverse event following the

administration of T cells transduced with a chimeric antigen receptor recognizing ERBB2. Mol Ther. 2010;18(4):843-51.
115. Lamers CH, Sleijfer S, Vulto AG, Kruit WH, Kliffen M, Debets R, et al. Treatment of metastatic renal cell carcinoma with autologous T-lymphocytes genetically retargeted against carbonic anhydrase IX: first clinical experience. Journal of clinical oncology : official journal of the American Society of Clinical Oncology. 2006;24(13):e20-2.
116. Cameron BJ, Gerry AB, Dukes J, Harper JV, Kannan V, Bianchi FC, et al. Identification of a Titin-derived HLA-A1-presented peptide as a cross-reactive target for engineered MAGE A3-directed T cells. Science translational medicine. 2013;5(197):197ra03.
117. Neelapu SS, Tummala S, Kebriaei P, Wierda W, Locke FL, Lin Y, et al. Toxicity management after chimeric antigen receptor T cell therapy: one size does not fit'ALL'. nat Rev Clin Oncol. 2018;15(4):218.
118. Künkele A, Taraseviciute A, Finn LS, Johnson AJ, Berger C, Finney O, et al. Preclinical assessment of CD171-directed CAR T-cell adoptive therapy for childhood neuroblastoma: CE7 epitope target safety and product manufacturing feasibility. Clinical Cancer Research. 2017;23(2):466-77.
119. Straathof KC, Pulè MA, Yotnda P, Dotti G, Vanin EF, Brenner MK, et al. An inducible caspase 9 safety switch for T-cell therapy. Blood. 2005;105(11):4247-54.
120. Di Stasi A, Tey S-K, Dotti G, Fujita Y, Kennedy-Nasser A, Martinez C, et al. Inducible apoptosis as a safety switch for adoptive cell therapy. New England Journal of Medicine. 2011;365(18):1673-83.
121. Paszkiewicz PJ, Fräßle SP, Srivastava S, Sommermeyer D, Hudecek M, Drexler I, et al. Targeted antibody-mediated depletion of murine CD19 CAR T cells permanently reverses B cell aplasia. J Clin Invest. 2016;126(11):4262-72.
122. Philip B, Kokalaki E, Mekkaoui L, Thomas S, Straathof K, Flutter B, et al. A highly compact epitope-based marker/suicide gene for easier and safer T-cell therapy. Blood. 2014;124(8):1277-87.
123. Minagawa K, Jamil MO, Al-Obaidi M, Pereboeva L, Salzman D, Erba HP, et al. In Vitro Pre-Clinical Validation of Suicide Gene Modified Anti-CD33 Redirected Chimeric Antigen Receptor T-Cells for Acute Myeloid Leukemia. PLoS One. 2016;11(12):e0166891.
124. Zhou X, Dotti G, Krance RA, Martinez CA, Naik S, Kamble RT, et al. Inducible caspase-9 suicide gene controls adverse effects from alloreplete T cells after haploidentical stem cell transplantation. Blood. 2015;125(26):4103-13.
125. Gargett T, Brown MPJFip. The inducible caspase-9 suicide gene system as a “safety switch” to limit on-target, off-tumor toxicities of chimeric antigen receptor T cells. frontiers in pharmacology. 2014;5:235.
126. Sakemura R, Terakura S, Watanabe K, Julamanee J, Takagi E, Miyao K, et al. A Tet-On inducible system for controlling CD19-chimeric antigen receptor expression upon drug administration. cancer Immunol Res. 2016;4(8):658-68.

127. Roybal KT, Rupp LJ, Morsut L, Walker WJ, McNally KA, Park JS, et al. Precision tumor recognition by T cells with combinatorial antigen-sensing circuits. cell

2016;164(4):770-9.
128. Morsut L, Roybal KT, Xiong X, Gordley RM, Coyle SM, Thomson M, et al. Engineering customized cell sensing and response behaviors using synthetic notch receptors. cell. 2016;164(4):780-91.
129. Cartellieri M, Feldmann A, Koristka S, Arndt C, Loff S, Ehninger A, et al. Switching CAR T cells on and off: a novel modular platform for retargeting of T cells to AML blasts. Blood Cancer Journal. 2016;6(8):e458.
130. Loureiro L, Feldmann A, Bergmann R, Koristka S, Berndt N, Arndt C, et al. Development of a novel target module redirecting UniCAR T cells to Sialyl Tn-expressing tumor cells. blood Cancer Journal. 2018;8(9):81.
131. Darowski D, Kobold S, Jost C, Klein C, editors. Combining the best of two worlds: Highly flexible chimeric antigen receptor adaptor molecules (CAR-adaptors) for the recruitment of chimeric antigen receptor T cells. mAbs; 2019: Taylor & Francis.
132. Ajina A, Maher JJMct. Strategies to address chimeric antigen receptor tonic signaling. Mol Cancer Ther. 2018;17(9):1795-815.
133. Jackson HJ, Rafiq S, Brentjens RJ. Driving CAR T-cells forward. Nat Rev Clin Oncol. 2016;13(6):370-83.
134. Khalil DN, Smith EL, Brentjens RJ, Wolchok JD. The future of cancer treatment: immunomodulation, CARs and combination immunotherapy. Nat Rev Clin Oncol. 2016;13(5):273-90.
135. Kunert A, Chmielewski M, Wijers R, Berrevoets C, Abken H, Debets R. Intra-tumoral production of IL18, but not IL12, by TCR-engineered T cells is non-toxic and counteracts immune evasion of solid tumors. Oncoimmunology. 2017;7(1):e1378842.
136. Chmielewski M, Abken H. CAR T Cells Releasing IL-18 Convert to T-Bet(high) FoxO1(low) Effectors that Exhibit Augmented Activity against Advanced Solid Tumors. Cell reports. 2017;21(11):3205-19.
137. Hu B, Ren J, Luo Y, Keith B, Young RM, Scholler J, et al. Augmentation of Antitumor Immunity by Human and Mouse CAR T Cells Secreting IL-18. Cell reports. 2017;20(13):3025-33.
138. Jaspers JE, Brentjens RJ. Development of CAR T cells designed to improve antitumor efficacy and safety. Pharmacology & Therapeutics. 2017.
139. Kloss CC, Condomines M, Cartellieri M, Bachmann M, Sadelain M. Combinatorial antigen recognition with balanced signaling promotes selective tumor eradication by engineered T cells. Nature biotechnology. 2013;31(1):71-5.
140. Lee L, Draper B, Chaplin N, Philip B, Chin M, Galas-Filipowicz D, et al. An APRIL-based chimeric antigen receptor for dual targeting of BCMA and TACI in multiple myeloma. Blood. 2018;131(7):746-58.

141. Wilkie S, van Schalkwyk MC, Hobbs S, Davies DM, van der Stegen SJ, Pereira ACP, et al. Dual targeting of ErbB2 and MUC1 in breast cancer using chimeric antigen receptors engineered to provide complementary signaling. Journal of clinical immunology. 2012;32(5):1059-70.
142. Chinnasamy D, Tran E, Yu Z, Morgan RA, Restifo NP, Rosenberg SAJCr. Simultaneous targeting of tumor antigens and the tumor vasculature using T lymphocyte transfer synergize to induce regression of established tumors in mice. Cancer research. 2013;73(11):3371-80.
143. Grada Z, Hegde M, Byrd T, Shaffer DR, Ghazi A, Brawley VS, et al. TanCAR: a novel bispecific chimeric antigen receptor for cancer immunotherapy. mol ther. 2013;2:e105.
144. Choi BD, Yu X, Castano AP, Bouffard AA, Schmidts A, Larson RC, et al. CAR-T cells secreting BiTEs circumvent antigen escape without detectable toxicity. Nature biotechnology. 2019:1-10.
145. Harlin H, Meng Y, Peterson AC, Zha Y, Tretiakova M, Slingluff C, et al. Chemokine expression in melanoma metastases associated with CD8+ T-cell recruitment. Cancer research. 2009;69(7):3077-85.
146. Craddock JA, Lu A, Bear A, Pule M, Brenner MK, Rooney CM, et al. Enhanced tumor trafficking of GD2 chimeric antigen receptor T cells by expression of the chemokine receptor CCR2b. journal of immunotherapy. 2010;33(8):780.
147. Moon EK, Carpenito C, Sun J, Wang L-CS, Kapoor V, Predina J, et al. Expression of a functional CCR2 receptor enhances tumor localization and tumor eradication by retargeted human T cells expressing a mesothelin-specific chimeric antibody receptor. Clin Cancer Res. 2011;17(14):4719-30.
148. Moon E, editor Immunotherapy: Beyond Anti–PD-1 and Anti–PD-L1 Therapies. ASCO; 2016: American Society of Clinical Oncology.
149. Yong CS, Dardalhon V, Devaud C, Taylor N, Darcy PK, Kershaw MH. CAR T-cell therapy of solid tumors. Immunology and cell biology. 2017.
150. Gargett T, Yu W, Dotti G, Yvon ES, Christo SN, Hayball JD, et al. GD2-specific CAR T Cells Undergo Potent Activation and Deletion Following Antigen Encounter but can be Protected From Activation-induced Cell Death by PD-1 Blockade. Mol Ther. 2016;24(6):1135-49.
151. John LB, Devaud C, Duong CP, Yong CS, Beavis PA, Haynes NM, et al. Anti-PD-1 antibody therapy potently enhances the eradication of established tumors by gene-modified T cells. Clin Cancer Res. 2013;19(20):5636-46.
152. John LB, Kershaw MH, Darcy PK. Blockade of PD-1 immunosuppression boosts CAR T-cell therapy. Oncoimmunology. 2013;2(10):e26286.
153. Ren J, Liu X, Fang C, Jiang S, June CH, Zhao Y. Multiplex genome editing to generate universal CAR T cells resistant to PD1 inhibition. Clinical Cancer Research. 2017;23(9):2255-66.
154. Liu X, Ranganathan R, Jiang S, Fang C, Sun J, Kim S, et al. A Chimeric Switch-Receptor Targeting PD1 Augments the Efficacy of

Second-Generation CAR T Cells in Advanced Solid Tumors. Cancer research. 2016;76(6):1578-90.
155. Rupp LJ, Schumann K, Roybal KT, Gate RE, Chun JY, Lim WA, et al. CRISPR/Cas9-mediated PD-1 disruption enhances anti-tumor efficacy of human chimeric antigen receptor T cells. scientific reports. 2017;7(1):737.
156. Suarez ER, Chang D-K, Sun J, Sui J, Freeman GJ, Signoretti S, et al. Chimeric antigen receptor T cells secreting anti-PD-L1 antibodies more effectively regress renal cell carcinoma in a humanized mouse model. Oncotarget. 2016;7(23):34341.
157. Rafiq S, Yeku OO, Jackson HJ, Purdon TJ, van Leeuwen DG, Drakes DJ, et al. Targeted delivery of a PD-1-blocking scFv by CAR-T cells enhances anti-tumor efficacy in vivo. Nature biotechnology. 2018;36(9):847-56.
158. Brekke OH, Sandlie IJNrDd. Therapeutic antibodies for human diseases at the dawn of the twenty-first century. Biomolecules. 2003;2(1):52.
159. Ehrlich P. Collected studies on immunity: J. Wiley & sons; 1906.
160. Weiner LM, Surana R, Wang S. Monoclonal antibodies: versatile platforms for cancer immunotherapy. Nature Reviews Immunology. 2010;10(5):317.
161. Yakes FM, Chinratanalab W, Ritter CA, King W, Seelig S, Arteaga CL. Herceptin-induced inhibition of phosphatidylinositol-3 kinase and Akt Is required for antibody-mediated effects on p27, cyclin D1, and antitumor action. Cancer research. 2002;62(14):4132-41.
162. Scott AM, Wolchok JD, Old LJ. Antibody therapy of cancer. Nature reviews Cancer. 2012;12(4):278-87.
163. Hallek M, Fischer K, Fingerle-Rowson G, Fink AM, Busch R, Mayer J, et al. Addition of rituximab to fludarabine and cyclophosphamide in patients with chronic lymphocytic leukaemia: a randomised, open-label, phase 3 trial. Lancet (London, England). 2010;376(9747):1164-74.
164. Maloney DG, Grillo-López AJ, White CA, Bodkin D, Schilder RJ, Neidhart JA, et al. IDEC-C2B8 (Rituximab) anti-CD20 monoclonal antibody therapy in patients with relapsed low-grade non-Hodgkin's lymphoma. Blood. 1997;90(6):2188-95.
165. Coiffier B, Haioun C, Ketterer N, Engert Aa, Tilly H, Ma D, et al. Rituximab (anti-CD20 monoclonal antibody) for the treatment of patients with relapsing or refractory aggressive lymphoma: a multicenter phase II study. Blood. 1998;92(6):1927-32.
166. McLaughlin P, Grillo-López AJ, Link BK, Levy R, Czuczman MS, Williams ME, et al. Rituximab chimeric anti-CD20 monoclonal antibody therapy for relapsed indolent lymphoma: half of patients respond to a four-dose treatment program. Journal of clinical oncology : official journal of the American Society of Clinical Oncology. 1998;16(8):2825-33.
167. Czuczman MS, Grillo-Lopez A, White C, Saleh M, Gordon L, LoBuglio A, et al. Treatment of patients with low-grade B-cell

lymphoma with the combination of chimeric anti-CD20 monoclonal antibody and CHOP chemotherapy. Journal of clinical oncology : official journal of the American Society of Clinical Oncology. 1999;17(1):268-.
168. Vose J, Link B, Grossbard M, Czuczman M, Grillo-Lopez A, Gilman P, et al. Phase II study of rituximab in combination with CHOP chemotherapy in patients with previously untreated, aggressive non-Hodgkin's lymphoma. Journal of Clinical Oncology. 2001;19(2):389-97.
169. Coiffier B, Lepage E, Briere J, Herbrecht R, Tilly H, Bouabdallah R, et al. CHOP chemotherapy plus rituximab compared with CHOP alone in elderly patients with diffuse large-B-cell lymphoma. New England Journal of Medicine. 2002;346(4):235-42.
170. Beers SA, Glennie MJ, White AL. Influence of immunoglobulin isotype on therapeutic antibody function. Blood. 2016;127(9):1097-101.
171. DiLillo DJ, Ravetch JV. Fc-Receptor Interactions Regulate Both Cytotoxic and Immunomodulatory Therapeutic Antibody Effector Functions. Cancer Immunol Res. 2015;3(7):704-13.
172. Francisco JA, Cerveny CG, Meyer DL, Mixan BJ, Klussman K, Chace DF, et al. cAC10-vcMMAE, an anti-CD30-monomethyl auristatin E conjugate with potent and selective antitumor activity. Blood. 2003;102(4):1458-65.
173. Younes A, Bartlett NL, Leonard JP, Kennedy DA, Lynch CM, Sievers EL, et al. Brentuximab vedotin (SGN-35) for relapsed CD30-positive lymphomas. The New England journal of medicine. 2010;363(19):1812-21.
174. Younes A, Gopal AK, Smith SE, Ansell SM, Rosenblatt JD, Savage KJ, et al. Results of a pivotal phase II study of brentuximab vedotin for patients with relapsed or refractory Hodgkin's lymphoma. Journal of clinical oncology. 2012;30(18):2183.
175. Chames P, Van Regenmortel M, Weiss E, Baty DJBjop. Therapeutic antibodies: successes, limitations and hopes for the future. british journal of pharmacology. 2009;157(2):220-33.
176. Canevari S, Stoter G, Arienti F, Bolis G, Colnaghi MI, Di Re EM, et al. Regression of advanced ovarian carcinoma by intraperitoneal treatment with autologous T lymphocytes retargeted by a bispecific monoclonal antibody. J Natl Cancer Inst. 1995;87(19):1463-9.
177. Slaney CY, Wang P, Darcy PK, Kershaw MH. CARs versus biTEs: a comparison between T cell–redirection strategies for cancer treatment. Cancer discovery. 2018;8(8):924-34.
178. Le Jeune C, Thomas X. Potential for bispecific T-cell engagers: role of blinatumomab in acute lymphoblastic leukemia. Drug design, development and therapy. 2016;10:757-65.
179. Suryadevara CM, Gedeon PC, Sanchez-Perez L, Verla T, Alvarez-Breckenridge C, Choi BD, et al. Are BiTEs the "missing link" in cancer therapy? Oncoimmunology. 2015;4(6):e1008339.

180. Huehls AM, Coupet TA, Sentman CL. Bispecific T-cell engagers for cancer immunotherapy. Immunology and cell biology. 2015;93(3):290-6.
181. Queudeville M, Handgretinger R, Ebinger M. immunotargeting relapsed or refractory precursor B-cell acute lymphoblastic leukemia–role of blinatumomab. OncoTargets and therapy. 2017;10:3567.
182. Speck T, Heidbuechel JP, Veinalde R, Jaeger D, von Kalle C, Ball CR, et al. Targeted BiTE expression by an oncolytic vector augments therapeutic efficacy against solid tumors. Clin Cancer Res. 2018.
183. Mirzaei HR, Rodriguez A, Shepphird J, Brown CE, Badie B. Chimeric Antigen Receptors T Cell Therapy in Solid Tumor: Challenges and Clinical Applications. Frontiers in immunology. 2017;8:1850.
184. Gauthier J, Yakoub-Agha I. Chimeric antigen-receptor T-cell therapy for hematological malignancies and solid tumors: Clinical data to date, current limitations and perspectives. Current research in translational medicine. 2017;65(3):93-102.
185. Ahmed M, Cheng M, Cheung IY, Cheung NK. Human derived dimerization tag enhances tumor killing potency of a T-cell engaging bispecific antibody. Oncoimmunology. 2015;4(4):e989776.
186. Goebeler ME, Knop S, Viardot A, Kufer P, Topp MS, Einsele H, et al. Bispecific T-Cell Engager (BiTE) Antibody Construct Blinatumomab for the Treatment of Patients With Relapsed/Refractory Non-Hodgkin Lymphoma: Final Results From a Phase I Study. Journal of clinical oncology : official journal of the American Society of Clinical Oncology. 2016;34(10):1104-11.
187. Topp MS, Kufer P, Gokbuget N, Goebeler M, Klinger M, Neumann S, et al. Targeted therapy with the T-cell-engaging antibody blinatumomab of chemotherapy-refractory minimal residual disease in B-lineage acute lymphoblastic leukemia patients results in high response rate and prolonged leukemia-free survival. Journal of clinical oncology : official journal of the American Society of Clinical Oncology. 2011;29(18):2493-8.
188. Topp MS, Gokbuget N, Zugmaier G, Degenhard E, Goebeler ME, Klinger M, et al. Long-term follow-up of hematologic relapse-free survival in a phase 2 study of blinatumomab in patients with MRD in B-lineage ALL. Blood. 2012;120(26):5185-7.
189. von Stackelberg A, Locatelli F, Zugmaier G, Handgretinger R, Trippett TM, Rizzari C, et al. Phase I/Phase II Study of Blinatumomab in Pediatric Patients With Relapsed/Refractory Acute Lymphoblastic Leukemia. Journal of clinical oncology : official journal of the American Society of Clinical Oncology. 2016;34(36):4381-9.
190. Velasquez MP, Bonifant CL, Gottschalk S. Redirecting T cells to hematological malignancies with bispecific antibodies. Blood. 2018;131(1):30-8.
191. Goebeler ME, Bargou R. Blinatumomab: a CD19/CD3 bispecific T cell engager (BiTE) with unique anti-tumor efficacy. Leukemia & lymphoma. 2016;57(5):1021-32.

192. Pircher M, Schirrmann T, Petrausch U. T Cell Engineering. Immuno-Oncology. 42: Karger Publishers; 2015. p. 110-35.
193. Sakuishi K, Apetoh L, Sullivan JM, Blazar BR, Kuchroo VK, Anderson AC. Targeting Tim-3 and PD-1 pathways to reverse T cell exhaustion and restore anti-tumor immunity. Journal of Experimental Medicine. 2010:jem. 20100643.
194. Topalian SL, Taube JM, Anders RA, Pardoll DM. Mechanism-driven biomarkers to guide immune checkpoint blockade in cancer therapy. Nature Reviews Cancer. 2016;16(5):275.
195. Le Mercier I, Chen W, Lines JL, Day M, Li J, Sergent P, et al. VISTA regulates the development of protective antitumor immunity. Cancer research. 2014;74(7):1933-44.
196. Derré L, Rivals J-P, Jandus C, Pastor S, Rimoldi D, Romero P, et al. BTLA mediates inhibition of human tumor-specific CD8+ T cells that can be partially reversed by vaccination. J Clin Invest. 2010;120(1):157-67.
197. Sharma P, Allison JP. The future of immune checkpoint therapy. J Science. 2015;348(6230):56-61.
198. Hodi FS, O'Day SJ, McDermott DF, Weber RW, Sosman JA, Haanen JB, et al. Improved Survival with Ipilimumab in Patients with Metastatic Melanoma. New England Journal of Medicine. 2010;363(8):711-23.
199. Weber J. Immune checkpoint proteins: a new therapeutic paradigm for cancer--preclinical background: CTLA-4 and PD-1 blockade. Semin Oncol. 2010;37(5):430-9.
200. Lynch TJ, Bondarenko I, Luft A, Serwatowski P, Barlesi F, Chacko R, et al. Ipilimumab in combination with paclitaxel and carboplatin as first-line treatment in stage IIIB/IV non–small-cell lung cancer: results from a randomized, double-blind, multicenter phase II study. Journal of clinical oncology : official journal of the American Society of Clinical Oncology. 2012;30(17):2046-54.
201. Calabrò L, Morra A, Fonsatti E, Cutaia O, Amato G, Giannarelli D, et al. Tremelimumab for patients with chemotherapy-resistant advanced malignant mesothelioma: an open-label, single-arm, phase 2 trial. The Lancet. 2013;14(11):1104-11.
202. Postow MA, Callahan MK, Wolchok JDJJoco. Immune checkpoint blockade in cancer therapy. Journal of clinical oncology : official journal of the American Society of Clinical Oncology. 2015;33(17):1974.
203. Prieto PA, Yang JC, Sherry RM, Hughes MS, Kammula US, White DE, et al. CTLA-4 blockade with ipilimumab: long-term follow-up of 177 patients with metastatic melanoma. Clin Cancer Res. 2012;18(7):2039-47.
204. Carosella ED, Ploussard G, LeMaoult J, Desgrandchamps F. A Systematic Review of Immunotherapy in Urologic Cancer: Evolving Roles for Targeting of CTLA-4, PD-1/PD-L1, and HLA-G. Eur Urol. 2015;68(2):267-79.

205. Barber DL, Wherry EJ, Masopust D, Zhu B, Allison JP, Sharpe AH, et al. Restoring function in exhausted CD8 T cells during chronic viral infection. Nature. 2006;439(7077):682-7.
206. Abate-Daga D, Hanada K-i, Davis JL, Yang JC, Rosenberg SA, Morgan RA. Expression profiling of TCR-engineered T cells demonstrates over-expression of multiple inhibitory receptors in persisting lymphocytes. Blood. 2013:blood-2013-04-495531.
207. Kleffel S, Posch C, Barthel SR, Mueller H, Schlapbach C, Guenova E, et al. Melanoma Cell-Intrinsic PD-1 Receptor Functions Promote Tumor Growth. Cell. 2015;162(6):1242-56.
208. Sharpe AH, Pauken KEJNRI. The diverse functions of the PD1 inhibitory pathway. 2018;18(3):153.
209. Haile ST, Dalal SP, Clements V, Tamada K, Ostrand-Rosenberg S. Soluble CD80 restores T cell activation and overcomes tumor cell programmed death ligand 1–mediated immune suppression. The Journal of Immunology. 2013;191(5):2829-36.
210. Ma W, Gilligan BM, Yuan J, Li T. Current status and perspectives in translational biomarker research for PD-1/PD-L1 immune checkpoint blockade therapy. Journal of hematology & oncology. 2016;9(1):47.
211. Latchman Y, Wood CR, Chernova T, Chaudhary D, Borde M, Chernova I, et al. PD-L2 is a second ligand for PD-1 and inhibits T cell activation. Nature immunology. 2001;2(3):261-8.
212. Chemnitz JM, Parry RV, Nichols KE, June CH, Riley JLJTJoI. SHP-1 and SHP-2 associate with immunoreceptor tyrosine-based switch motif of programmed death 1 upon primary human T cell stimulation, but only receptor ligation prevents T cell activation. 2004;173(2):945-54.
213. Hui E, Cheung J, Zhu J, Su X, Taylor MJ, Wallweber HA, et al. T cell costimulatory receptor CD28 is a primary target for PD-1–mediated inhibition. 2017;355(6332):1428-33.
214. Karwacz K, Bricogne C, MacDonald D, Arce F, Bennett CL, Collins M, et al. PD‐L1 co‐stimulation contributes to ligand‐induced T cell receptor down‐modulation on CD8+ T cells. 2011;3(10):581-92.
215. Azuma M, Yssel H, Phillips JH, Spits H, Lanier LLJJoEM. Functional expression of B7/BB1 on activated T lymphocytes. 1993;177(3):845-50.
216. Verwilghen J, Lovis R, De Boer M, Linsley PS, Haines GK, Koch AE, et al. Expression of functional B7 and CTLA4 on rheumatoid synovial T cells. 1994;153(3):1378-85.
217. Butte MJ, Keir ME, Phamduy TB, Sharpe AH, Freeman GJJI. Programmed death-1 ligand 1 interacts specifically with the B7-1 costimulatory molecule to inhibit T cell responses. 2007;27(1):111-22.
218. Butte MJ, Pena-Cruz V, Kim M-J, Freeman GJ, Sharpe AHJMi. Interaction of human PD-L1 and B7-1. 2008;45(13):3567-72.

219. Gubin MM, Zhang X, Schuster H, Caron E, Ward JP, Noguchi T, et al. Checkpoint blockade cancer immunotherapy targets tumour-specific mutant antigens. Nature. 2014;515(7528):577-81.
220. Ahmadzadeh M, Johnson LA, Heemskerk B, Wunderlich JR, Dudley ME, White DE, et al. Tumor antigen–specific CD8 T cells infiltrating the tumor express high levels of PD-1 and are functionally impaired. Blood, The Journal of the American Society of Hematology. 2009;114(8):1537-44.
221. Schreiner J, Thommen DS, Herzig P, Bacac M, Klein C, Roller A, et al. Expression of inhibitory receptors on intratumoral T cells modulates the activity of a T cell-bispecific antibody targeting folate receptor. Oncoimmunology. 2016;5(2):e1062969.
222. Sakuishi K, Ngiow SF, Sullivan JM, Teng MW, Kuchroo VK, Smyth MJ, et al. TIM3+ FOXP3+ regulatory T cells are tissue-specific promoters of T-cell dysfunction in cancer. Oncoimmunology. 2013;2(4):e23849.
223. Matsuzaki J, Gnjatic S, Mhawech-Fauceglia P, Beck A, Miller A, Tsuji T, et al. Tumor-infiltrating NY-ESO-1–specific CD8+ T cells are negatively regulated by LAG-3 and PD-1 in human ovarian cancer. Proceedings of the National Academy of Sciences. 2010;107(17):7875-80.
224. Zhang Y, Kang S, Shen J, He J, Jiang L, Wang W, et al. Prognostic significance of programmed cell death 1 (PD-1) or PD-1 ligand 1 (PD-L1) expression in epithelial-originated cancer: a meta-analysis. Medicine. 2015;94(6):e515.
225. Daud AI, Loo K, Pauli ML, Sanchez-Rodriguez R, Sandoval PM, Taravati K, et al. Tumor immune profiling predicts response to anti–PD-1 therapy in human melanoma. 2016;126(9):3447-52.
226. Ribas A, Shin DS, Zaretsky J, Frederiksen J, Cornish A, Avramis E, et al. PD-1 blockade expands intratumoral memory T cells. 2016;4(3):194-203.
227. Mamalis A, Garcha M, Jagdeo J. Targeting the PD-1 pathway: a promising future for the treatment of melanoma. Archives of dermatological research. 2014;306(6):511-9.
228. Wagner LM, Adams VR. Targeting the PD-1 pathway in pediatric solid tumors and brain tumors. OncoTargets and therapy. 2017;10:2097-106.
229. Kelly K, Crowley J, Bunn Jr PA, Presant CA, Grevstad PK, Moinpour CM, et al. Randomized phase III trial of paclitaxel plus carboplatin versus vinorelbine plus cisplatin in the treatment of patients with advanced non–small-cell lung cancer: a Southwest Oncology Group trial. Journal of Clinical Oncology. 2001;19(13):3210-8.
230. Michot J, Bigenwald C, Champiat S, Collins M, Carbonnel F, Postel-Vinay S, et al. Immune-related adverse events with immune checkpoint blockade: a comprehensive review. European Journal of Cancer. 2016;54:139-48.

231. Squibb B-M. Yervoy (ipilimumab): Immune-mediated adverse reaction management guide. 2011.
232. Brahmer J, Reckamp KL, Baas P, Crinò L, Eberhardt WE, Poddubskaya E, et al. Nivolumab versus docetaxel in advanced squamous-cell non–small-cell lung cancer. New England Journal of Medicine. 2015;373(2):123-35.
233. Sukumar M, Kishton RJ, Restifo NP. Metabolic reprograming of anti-tumor immunity. Current Opinion in Immunology. 2017;46:14-22.
234. Newick K, O'Brien S, Moon E, Albelda SMJArom. CAR T cell therapy for solid tumors. 2017;68:139-52.
235. Finn OJ. Cancer immunology. New England Journal of Medicine. 2008;358(25):2704-15.
236. Palucka K, Banchereau J. Cancer immunotherapy via dendritic cells. Interaction of Immune and Cancer Cells: Springer; 2014. p. 75-89.
237. Jackson HJ, Brentjens RJJCd. Overcoming antigen escape with CAR T-cell therapy. 2015;5(12):1238-40.
238. Topalian SL, Hodi FS, Brahmer JR, Gettinger SN, Smith DC, McDermott DF, et al. Safety, activity, and immune correlates of anti–PD-1 antibody in cancer. New England Journal of Medicine. 2012;366(26):2443-54.
239. Tan Y, Trent J, Wilky B, Kerr D, Rosenberg A. Current status of immunotherapy for gastrointestinal stromal tumor. Cancer gene therapy. 2017;24(3):130-3.
240. Arina A, Schreiber K, Binder DC, Karrison TG, Liu RB, Schreiber H. Adoptively transferred immune T cells eradicate established tumors despite cancer-induced immune suppression. The Journal of Immunology. 2014;192(3):1286-93.
241. Rutkowski MR, Svoronos N, Perales-Puchalt A, Conejo-Garcia JR. Chapter Seven-The Tumor Macroenvironment: Cancer-Promoting Networks Beyond Tumor Beds. Advances in cancer research. 2015;128:235-62.
242. Rutkowski MR, Svoronos N, Perales-Puchalt A, Conejo-Garcia JR. The Tumor Macroenvironment: Cancer-Promoting Networks Beyond Tumor Beds. Adv Cancer Res. 2015;128:235-62.
243. Anders CK, Abramson V, Tan T, Dent R. The Evolution of Triple-Negative Breast Cancer: From Biology to Novel Therapeutics. American Society of Clinical Oncology educational book American Society of Clinical Oncology Annual Meeting. 2016;35:34-42.
244. Siegel RL, Miller KD, Jemal A. Cancer Statistics, 2017. CA: a cancer journal for clinicians. 2017;67(1):7-30.
245. Howlader N, Altekruse SF, Li CI, Chen VW, Clarke CA, Ries LA, et al. US incidence of breast cancer subtypes defined by joint hormone receptor and HER2 status. 2014;106(5).
246. Louie MC, Sevigny MBJAjocr. Steroid hormone receptors as prognostic markers in breast cancer. 2017;7(8):1617.

247. Dent R, Trudeau M, Pritchard KI, Hanna WM, Kahn HK, Sawka CA, et al. Triple-negative breast cancer: clinical features and patterns of recurrence. 2007;13(15):4429-34.
248. Dawson S, Provenzano E, Caldas CJEjoc. Triple negative breast cancers: clinical and prognostic implications. 2009;45:27-40.
249. Foulkes WD, Smith IE, Reis-Filho JSJNEjom. Triple-negative breast cancer. 2010;363(20):1938-48.
250. Lehmann BD, Bauer JA, Chen X, Sanders ME, Chakravarthy AB, Shyr Y, et al. Identification of human triple-negative breast cancer subtypes and preclinical models for selection of targeted therapies. 2011;121(7):2750-67.
251. Georgiannos SN, Renaut A, Goode AW, Sheaff MJS. The immunophenotype and activation status of the lymphocytic infiltrate in human breast cancers, the role of the major histocompatibility complex in cell-mediated immune mechanisms, and their association with prognostic indicators. 2003;134(5):827-34.
252. Varn FS, Andrews EH, Mullins DW, Cheng CJNc. Integrative analysis of breast cancer reveals prognostic haematopoietic activity and patient-specific immune response profiles. 2016;7:10248.
253. Mahmoud SM, Paish EC, Powe DG, Macmillan RD, Grainge MJ, Lee AH, et al. Tumor-infiltrating CD8+ lymphocytes predict clinical outcome in breast cancer. 2011;29(15):1949-55.
254. Milani A, Sangiolo D, Aglietta M, Valabrega GJBCT, Therapy. Recent advances in the development of breast cancer vaccines. 2014;6:159.
255. Nanda R, Chow LQ, Dees EC, Berger R, Gupta S, Geva R, et al. Pembrolizumab in Patients With Advanced Triple-Negative Breast Cancer: Phase Ib KEYNOTE-012 Study. Journal of clinical oncology : official journal of the American Society of Clinical Oncology. 2016;34(21):2460-7.
256. Burstein MD, Tsimelzon A, Poage GM, Covington KR, Contreras A, Fuqua SA, et al. Comprehensive genomic analysis identifies novel subtypes and targets of triple-negative breast cancer. 2015;21(7):1688-98.
257. Denkert C, Liedtke C, Tutt A, von Minckwitz G. Molecular alterations in triple-negative breast cancer-the road to new treatment strategies. Lancet (London, England). 2017;389(10087):2430-42.
258. Zhang S, Chen L, Cui B, Chuang H-Y, Yu J, Wang-Rodriguez J, et al. ROR1 is expressed in human breast cancer and associated with enhanced tumor-cell growth. PloS one. 2012;7(3):e31127.
259. Chien H-P, Ueng S-H, Chen S-C, Chang Y-S, Lin Y-C, Lo Y-F, et al. Expression of ROR1 has prognostic significance in triple negative breast cancer. Virchows Archiv. 2016;468(5):589-95.
260. Cui B, Zhang S, Chen L, Yu J, Widhopf GF, Fecteau J-F, et al. Targeting ROR1 inhibits epithelial–mesenchymal transition and metastasis. Cancer research. 2013;73(12):3649-60.
261. Bray F, Ferlay J, Soerjomataram I, Siegel RL, Torre LA, Jemal A. Global cancer statistics 2018: GLOBOCAN estimates of incidence and

mortality worldwide for 36 cancers in 185 countries. CA: a cancer journal for clinicians. 2018;68(6):394-424.
262. Jemal A, Bray F, Center MM, Ferlay J, Ward E, Forman D. Global cancer statistics. CA: a cancer journal for clinicians. 2011;61(2):69-90.
263. Field JK, Oudkerk M, Pedersen JH, Duffy SW. Prospects for population screening and diagnosis of lung cancer. The Lancet. 2013;382(9893):732-41.
264. Malvezzi M, Bertuccio P, Levi F, La Vecchia C, Negri E. European cancer mortality predictions for the year 2012. Annals of oncology. 2012;23(4):1044-52.
265. Reck M, Popat S, Reinmuth N, De Ruysscher D, Kerr K, Peters S. Metastatic non-small-cell lung cancer (NSCLC): ESMO Clinical Practice Guidelines for diagnosis, treatment and follow-up. Annals of oncology. 2014;25(suppl_3):iii27-iii39.
266. Toh C-K, Gao F, Lim W-T, Leong S-S, Fong K-W, Yap S-P, et al. Never-smokers with lung cancer: epidemiologic evidence of a distinct disease entity. Journal of clinical oncology. 2006;24(15):2245-51.
267. Kris MG, Johnson BE, Berry LD, Kwiatkowski DJ, Iafrate AJ, Wistuba II, et al. Using multiplexed assays of oncogenic drivers in lung cancers to select targeted drugs. Jama. 2014;311(19):1998-2006.
268. Kwak EL, Bang Y-J, Camidge DR, Shaw AT, Solomon B, Maki RG, et al. Anaplastic lymphoma kinase inhibition in non–small-cell lung cancer. New England Journal of Medicine. 2010;363(18):1693-703.
269. Kerr KM, Bubendorf L, Edelman MJ, Marchetti A, Mok T, Novello S, et al. Second ESMO consensus conference on lung cancer: pathology and molecular biomarkers for non-small-cell lung cancer. Annals of Oncology. 2014;25(9):1681-90.
270. Rotow J, Bivona TG. Understanding and targeting resistance mechanisms in NSCLC. Nature Reviews Cancer. 2017;17(11):637.
271. Asahina H, Yamazaki K, Kinoshita I, Sukoh N, Harada M, Yokouchi H, et al. A phase II trial of gefitinib as first-line therapy for advanced non-small cell lung cancer with epidermal growth factor receptor mutations. British journal of cancer. 2006;95(8):998.
272. Inoue A, Suzuki T, Fukuhara T, Maemondo M, Kimura Y, Morikawa N, et al. Prospective phase II study of gefitinib for chemotherapy-naive patients with advanced non-small-cell lung cancer with epidermal growth factor receptor gene mutations. Journal of clinical oncology : official journal of the American Society of Clinical Oncology. 2006;24(21):3340-6.
273. Tamura K, Okamoto I, Kashii T, Negoro S, Hirashima T, Kudoh S, et al. Multicentre prospective phase II trial of gefitinib for advanced non-small cell lung cancer with epidermal growth factor receptor mutations: results of the West Japan Thoracic Oncology Group trial (WJTOG0403). British journal of cancer. 2008;98(5):907.
274. Lee CK, Brown C, Gralla RJ, Hirsh V, Thongprasert S, Tsai C-M, et al. Impact of EGFR inhibitor in non–small cell lung cancer on

progression-free and overall survival: a meta-analysis. Journal of the National Cancer Institute. 2013;105(9):595-605.
275. Mok TS, Wu Y-L, Thongprasert S, Yang C-H, Chu D-T, Saijo N, et al. Gefitinib or carboplatin–paclitaxel in pulmonary adenocarcinoma. New England Journal of Medicine. 2009;361(10):947-57.
276. Turke AB, Zejnullahu K, Wu Y-L, Song Y, Dias-Santagata D, Lifshits E, et al. Preexistence and clonal selection of MET amplification in EGFR mutant NSCLC. Cancer cell. 2010;17(1):77-88.
277. Engelman JA, Zejnullahu K, Gale C-M, Lifshits E, Gonzales AJ, Shimamura T, et al. PF00299804, an irreversible pan-ERBB inhibitor, is effective in lung cancer models with EGFR and ERBB2 mutations that are resistant to gefitinib. Cancer research. 2007;67(24):11924-32.
278. Yoon SM, Shaikh T, Hallman M. Therapeutic management options for stage III non-small cell lung cancer. World journal of clinical oncology. 2017;8(1):1.
279. Bradley J, Hu C, Komaki R, Masters G, Blumenschein G, Schild S, et al. Long-term results of RTOG 0617: a randomized phase 3 comparison of standard dose versus high dose conformal chemoradiation therapy+/-cetuximab for stage III NSCLC. International Journal of Radiation Oncology• Biology• Physics. 2017;99(2):S105.
280. Antonia SJ, Villegas A, Daniel D, Vicente D, Murakami S, Hui R, et al. Overall survival with durvalumab after chemoradiotherapy in stage III NSCLC. New England Journal of Medicine. 2018;379(24):2342-50.
281. Rittmeyer A, Barlesi F, Waterkamp D, Park K, Ciardiello F, Von Pawel J, et al. Atezolizumab versus docetaxel in patients with previously treated non-small-cell lung cancer (OAK): a phase 3, open-label, multicentre randomised controlled trial. The Lancet. 2017;389(10066):255-65.
282. Liu SV, Camidge DR, Gettinger SN, Giaccone G, Heist RS, Hodi FS, et al. Atezolizumab (atezo) plus platinum-based chemotherapy (chemo) in non-small cell lung cancer (NSCLC): Update from a phase Ib study. American Society of Clinical Oncology; 2017.
283. Socinski MA, Jotte RM, Cappuzzo F, Orlandi F, Stroyakovskiy D, Nogami N, et al. Atezolizumab for first-line treatment of metastatic nonsquamous NSCLC. New England Journal of Medicine. 2018;378(24):2288-301.
284. Wang R-F, Wang HY. Immune targets and neoantigens for cancer immunotherapy and precision medicine. Cell research. 2017;27(1):11.
285. Novellino L, Castelli C, Parmiani G. A listing of human tumor antigens recognized by T cells: March 2004 update. Cancer Immunology, Immunotherapy. 2005;54(3):187-207.
286. Martincorena I, Campbell PJJS. Somatic mutation in cancer and normal cells. Science. 2015;349(6255):1483-9.

287. June CH, O'Connor RS, Kawalekar OU, Ghassemi S, Milone MC. CAR T cell immunotherapy for human cancer. Science. 2018;359(6382):1361-5.
288. Grupp SA, Kalos M, Barrett D, Aplenc R, Porter DL, Rheingold SR, et al. Chimeric antigen receptor–modified T cells for acute lymphoid leukemia. New England Journal of Medicine. 2013;368(16):1509-18.
289. Richman SA, Nunez-Cruz S, Moghimi B, Li LZ, Gershenson ZT, Mourelatos Z, et al. High-affinity GD2-specific CAR T cells induce fatal encephalitis in a preclinical neuroblastoma model. Cancer immunology research. 2018;6(1):36-46.
290. Parkhurst MR, Yang JC, Langan RC, Dudley ME, Nathan D-AN, Feldman SA, et al. T cells targeting carcinoembryonic antigen can mediate regression of metastatic colorectal cancer but induce severe transient colitis. Molecular Therapy. 2011;19(3):620-6.
291. Lamers CH, Sleijfer S, Van Steenbergen S, Van Elzakker P, Van Krimpen B, Groot C, et al. Treatment of metastatic renal cell carcinoma with CAIX CAR-engineered T cells: clinical evaluation and management of on-target toxicity. Molecular therapy. 2013;21(4):904-12.
292. O'Rourke DM, Nasrallah MP, Desai A, Melenhorst JJ, Mansfield K, Morrissette JJ, et al. A single dose of peripherally infused EGFRvIII-directed CAR T cells mediates antigen loss and induces adaptive resistance in patients with recurrent glioblastoma. Science translational medicine. 2017;9(399):eaaa0984.
293. Hinrichs CS, Restifo NP. Reassessing target antigens for adoptive T-cell therapy. Nature biotechnology. 2013;31(11):999.
294. Masiakowski P, Carroll RD. A novel family of cell surface receptors with tyrosine kinase-like domain. Journal of Biological Chemistry. 1992;267(36):26181-90.
295. Shabani M, Naseri J, Shokri F. Receptor tyrosine kinase-like orphan receptor 1: a novel target for cancer immunotherapy. Expert Opin Ther Targets. 2015;19(7):941-55.
296. Forrester W. The Ror receptor tyrosine kinase family. Cellular and molecular life sciences. 2002;59(1):83-96.
297. Matsuda T, Nomi M, Ikeya M, Kani S, Oishi I, Terashima T, et al. Expression of the receptor tyrosine kinase genes, Ror1 and Ror2, during mouse development. Mechanisms of development. 2001;105(1):153-6.
298. Green JL, Kuntz SG, Sternberg PW. Ror receptor tyrosine kinases: orphans no more. Trends in cell biology. 2008;18(11):536-44.
299. Zheng Y-Z, Ma R, Zhou J-K, Guo C-L, Wang Y-S, Li Z-G, et al. ROR1 is a novel prognostic biomarker in patients with lung adenocarcinoma. Scientific reports. 2016;6:36447.
300. Liu Y, Yang H, Chen T, Luo Y, Xu Z, Li Y, et al. Silencing of receptor tyrosine kinase ROR1 inhibits tumor-cell proliferation via PI3K/AKT/mTOR signaling pathway in lung adenocarcinoma. 2015;10(5):e0127092.

301. Yamaguchi T, Yanagisawa K, Sugiyama R, Hosono Y, Shimada Y, Arima C, et al. NKX2-1/TITF1/TTF-1-Induced ROR1 is required to sustain EGFR survival signaling in lung adenocarcinoma. Cancer cell. 2012;21(3):348-61.
302. DaneshManesh AH, Mikaelsson E, Jeddi‐Tehrani M, Bayat AA, Ghods R, Ostadkarampour M, et al. Ror1, a cell surface receptor tyrosine kinase is expressed in chronic lymphocytic leukemia and may serve as a putative target for therapy. International journal of cancer. 2008;123(5):1190-5.
303. Baskar S, Kwong KY, Hofer T, Levy JM, Kennedy MG, Lee E, et al. Unique cell surface expression of receptor tyrosine kinase ROR1 in human B-cell chronic lymphocytic leukemia. Clinical Cancer Research. 2008;14(2):396-404.
304. Shabani M, Omran HA, Jeddi-Tehrani M, Vossough P, Faranoush M, Sharifian RA, et al. Overexpression of orphan receptor tyrosine kinase Ror1 as a putative tumor-associated antigen in Iranian patients with acute lymphoblastic leukemia. Tumor Biology. 2007;28(6):318-26.
305. Zhang S, Chen L, Wang-Rodriguez J, Zhang L, Cui B, Frankel W, et al. The onco-embryonic antigen ROR1 is expressed by a variety of human cancers. The American journal of pathology. 2012;181(6):1903-10.
306. Balakrishnan A, Goodpaster T, Randolph-Habecker J, Hoffstrom BG, Jalikis FG, Koch LK, et al. Analysis of ROR1 protein expression in human cancer and normal tissues. Clinical Cancer Research. 2017;23(12):3061-71.
307. Zhang S, Cui B, Lai H, Liu G, Ghia EM, Widhopf GF, et al. Ovarian cancer stem cells express ROR1, which can be targeted for anti–cancer-stem-cell therapy. Proceedings of the National Academy of Sciences. 2014;111(48):17266-71.
308. Zhang S, Zhang H, Ghia EM, Huang J, Wu L, Zhang J, et al. Inhibition of chemotherapy resistant breast cancer stem cells by a ROR1 specific antibody. Proceedings of the National Academy of Sciences. 2019;116(4):1370-7.
309. Jung EH, Lee HN, Han GY, Kim MJ, Kim CWJCb, function. Targeting ROR1 inhibits the self‐renewal and invasive ability of glioblastoma stem cells. cell biochemistry and function. 2016;34(3):149-57.
310. Hudecek M, Schmitt TM, Baskar S, Lupo-Stanghellini MT, Nishida T, Yamamoto TN, et al. The B-cell tumor–associated antigen ROR1 can be targeted with T cells modified to express a ROR1-specific chimeric antigen receptor. Blood. 2010;116(22):4532-41.
311. Choi MY, Widhopf GF, 2nd, Wu CC, Cui B, Lao F, Sadarangani A, et al. Pre-clinical Specificity and Safety of UC-961, a First-In-Class Monoclonal Antibody Targeting ROR1. Clin Lymphoma Myeloma Leuk. 2015;15 Suppl:S167-9.

312. Uhlén M, Fagerberg L, Hallström BM, Lindskog C, Oksvold P, Mardinoglu A, et al. Tissue-based map of the human proteome. Science. 2015;347(6220):1260419.
313. Widhopf GF, Prussak CE, Wu CC, Sadarangani A, Zhang S, Lao F, et al. Cirmtuzumab vedotin (UC-961ADC3), an anti-ROR1-monomethyl auristatin E antibody-drug conjugate, is a potential treatment for ROR1-positive leukemia and solid tumors. Am Soc Hematology; 2013.
314. Mani R, Chiang C-L, Frissora FW, Yan R, Mo X, Baskar S, et al. ROR1-targeted delivery of OSU-2S, a nonimmunosuppressive FTY720 derivative, exerts potent cytotoxicity in mantle-cell lymphoma in vitro and in vivo. experimental hematology. 2015;43(9):770-4. e2.
315. Mani R, Mao Y, Frissora FW, Chiang C-L, Wang J, Zhao Y, et al. Tumor antigen ROR1 targeted drug delivery mediated selective leukemic but not normal B-cell cytotoxicity in chronic lymphocytic leukemia. Leukemia. 2015;29(2):346.
316. Daneshmanesh A, Hojjat-Farsangi M, Khan A, Jeddi-Tehrani M, Akhondi M, Bayat A, et al. Monoclonal antibodies against ROR1 induce apoptosis of chronic lymphocytic leukemia (CLL) cells. Leukemia. 2012;26(6):1348.
317. Daneshmanesh AH, Hojjat ‐ Farsangi M, Moshfegh A, Khan AS, Mikaelsson E, Österborg A, et al. The PI3K/AKT/mTOR pathway is involved in direct apoptosis of CLL cells induced by ROR1 monoclonal antibodies. British journal of haematology. 2015;169(3):455-8.
318. Yang J, Baskar S, Kwong KY, Kennedy MG, Wiestner A, Rader C. Therapeutic potential and challenges of targeting receptor tyrosine kinase ROR1 with monoclonal antibodies in B-cell malignancies. PloS one. 2011;6(6):e21018.
319. Berger C, Sommermeyer D, Hudecek M, Berger M, Balakrishnan A, Paszkiewicz PJ, et al. Safety of targeting ROR1 in primates with chimeric antigen receptor–modified T cells. cancer Immunol Res. 2015;3(2):206-16.
320. Elmacken M, Awasthi A, Ayello J, van de Ven C, Luo W, Liao Y, et al. ROR1 expressing neuroblastoma (NB), medulloblastoma (MB), and ewing's sarcoma (ES) can be effectively targeted with nk cells modified to express an anti ROR1 chimeric antigen receptor (CAR). Cytotherapy. 2015;17(6):S48.
321. Liu L, Sommermeyer D, Cabanov A, Kosasih P, Hill T, Riddell SR. Inclusion of Strep-tag II in design of antigen receptors for T-cell immunotherapy. Nature biotechnology. 2016;34(4):430-4.
322. Specht JM, Lee S, Turtle CJ, Berger C, Baladrishnan A, Srivastava S, et al. Abstract CT131: A phase I study of adoptive immunotherapy for advanced ROR1+ malignancies with defined subsets of autologous T cells expressing a ROR1-specific chimeric antigen receptor (ROR1-CAR). AACR; 2018.
323. Srivastava S, Salter AI, Liggitt D, Yechan-Gunja S, Sarvothama M, Cooper K, et al. Logic-Gated ROR1 Chimeric Antigen Receptor Expression Rescues T Cell-Mediated Toxicity to Normal Tissues and

Enables Selective Tumor Targeting. Cancer cell. 2019;35(3):489-503. e8.
324. Gohil SH, Paredes-Moscosso SR, Harrasser M, Vezzalini M, Scarpa A, Morris E, et al. An ROR1 bi-specific T-cell engager provides effective targeting and cytotoxicity against a range of solid tumors. Oncoimmunology. 2017;6(7):e1326437.
325. Gohil SH, Della Peruta M, Paredes-Moscosso SR, Harrasser M, Cheung GW-K, Davies DM, et al. Novel humanised ROR1 chimeric antigen receptors for the treatment of haematological malignancies. Am Soc Hematology; 2016.
326. Spits H, Hooijberg E. NFAT-controlled expression of GFP permits visualization and isolation of antigen-stimulated primary human T cells. Blood. 2000;96:459-66.
327. Shaner NC, Campbell RE, Steinbach PA, Giepmans BN, Palmer AE, Tsien RYJNb. Improved monomeric red, orange and yellow fluorescent proteins derived from Discosoma sp. red fluorescent protein. 2004;22(12):1567.
328. Zufferey R, Donello JE, Trono D, Hope TJJJov. Woodchuck hepatitis virus posttranscriptional regulatory element enhances expression of transgenes delivered by retroviral vectors. 1999;73(4):2886-92.
329. Gohil SH. Pre-clinical development of novel ROR1 chimeric antigen receptor T cells and bispecific T cell engagers: UCL (University College London); 2018.
330. Chmielewski M, Kopecky C, Hombach AA, Abken H. IL-12 release by engineered T cells expressing chimeric antigen receptors can effectively Muster an antigen-independent macrophage response on tumor cells that have shut down tumor antigen expression. Cancer research. 2011;71(17):5697-706.
331. Topalian SL, Hodi FS, Brahmer JR, Gettinger SN, Smith DC, McDermott DF, et al. Safety, activity, and immune correlates of anti–PD-1 antibody in cancer. 2012;366(26):2443-54.
332. Kourie HR, Klastersky JAJCoio. Side-effects of checkpoint inhibitor-based combination therapy. Current Opinion in Oncology. 2016;28(4):306-13.
333. Fessas P, Lee H, Ikemizu S, Janowitz T, editors. A molecular and preclinical comparison of the PD-1–targeted T-cell checkpoint inhibitors nivolumab and pembrolizumab. Seminars in oncology; 2017: Elsevier.
334. Hooijberg E, Bakker AQ, Ruizendaal JJ, Spits HJB. NFAT-controlled expression of GFP permits visualization and isolation of antigen-stimulated primary human T cells. 2000;96(2):459-66.
335. Yu X, Zhan X, D'costa J, Tanavde VM, Ye Z, Peng T, et al. Lentiviral vectors with two independent internal promoters transfer high-level expression of multiple transgenes to human hematopoietic stem-progenitor cells. Molecular Therapy. 2003;7(6):827-38.

336. Wolchok JD, Kluger H, Callahan MK, Postow MA, Rizvi NA, Lesokhin AM, et al. Nivolumab plus ipilimumab in advanced melanoma. New England Journal of Medicine. 2013;369(2):122-33.
337. Postow MA, Chesney J, Pavlick AC, Robert C, Grossmann K, McDermott D, et al. Nivolumab and ipilimumab versus ipilimumab in untreated melanoma. The New England journal of medicine. 2015;372(21):2006-17.
338. Robert C, Schachter J, Long GV, Arance A, Grob JJ, Mortier L, et al. Pembrolizumab versus ipilimumab in advanced melanoma. 2015;372(26):2521-32.
339. Brahmer J, Reckamp KL, Baas P, Crinò L, Eberhardt WE, Poddubskaya E, et al. Nivolumab versus docetaxel in advanced squamous-cell non–small-cell lung cancer. 2015;373(2):123-35.
340. Loi S, Schmid P, Aktan G, Karantza V, Salgado RJAoO. 4O Relationship between tumor infiltrating lymphocytes (TILs) and response to pembrolizumab (pembro)+ chemotherapy (CT) as neoadjuvant treatment (NAT) for triple-negative breast cancer (TNBC): Phase Ib KEYNOTE-173 trial. 2019;30(Supplement_3):mdz095. 03.
341. Kiesgen S, Chicaybam L, Chintala NK, Adusumilli PSJJoTO. Chimeric antigen receptor (CAR) T-cell therapy for thoracic malignancies. 2018;13(1):16-26.
342. Gong J, Chehrazi-Raffle A, Reddi S, Salgia R. Development of PD-1 and PD-L1 inhibitors as a form of cancer immunotherapy: a comprehensive review of registration trials and future considerations. Journal for immunotherapy of cancer. 2018;6(1):8.
343. Gargett T, Yu W, Dotti G, Yvon ES, Christo SN, Hayball JD, et al. GD2-specific CAR T cells undergo potent activation and deletion following antigen encounter but can be protected from activation-induced cell death by PD-1 blockade. 2016;24(6):1135-49.
344. Cherkassky L, Morello A, Villena-Vargas J, Feng Y, Dimitrov DS, Jones DR, et al. Human CAR T cells with cell-intrinsic PD-1 checkpoint blockade resist tumor-mediated inhibition. 2016;126(8):3130-44.
345. Li S, Siriwon N, Zhang X, Yang S, Jin T, He F, et al. Enhanced Cancer Immunotherapy by Chimeric Antigen Receptor-Modified T Cells Engineered to Secrete Checkpoint Inhibitors. Clinical cancer research : an official journal of the American Association for Cancer Research. 2017;23(22):6982-92.
346. Ribas A, Wolchok JDJS. Cancer immunotherapy using checkpoint blockade. Science. 2018;359(6382):1350-5.
347. Curtin J, Dane A, Swanson A, Alexander I, Ginn S. Bidirectional promoter interference between two widely used internal heterologous promoters in a late-generation lentiviral construct. Gene therapy. 2008;15(5):384.
348. Zufferey R, Dull T, Mandel RJ, Bukovsky A, Quiroz D, Naldini L, et al. Self-inactivating lentivirus vector for safe and efficient in vivo gene delivery. Journal of virology. 1998;72(12):9873-80.
349. Krupka C, Kufer P, Kischel R, Zugmaier G, Lichtenegger FS, Kohnke T, et al. Blockade of the PD-1/PD-L1 axis augments lysis of

AML cells by the CD33/CD3 BiTE antibody construct AMG 330: reversing a T-cell-induced immune escape mechanism. Leukemia. 2016;30(2):484-91.
350. Tanoue K, Rosewell Shaw A, Watanabe N, Porter C, Rana B, Gottschalk S, et al. Armed Oncolytic Adenovirus-Expressing PD-L1 Mini-Body Enhances Antitumor Effects of Chimeric Antigen Receptor T Cells in Solid Tumors. Cancer research. 2017;77(8):2040-51.
351. Mukherjee M, Mace EM, Carisey AF, Ahmed N, Orange JSJMT. Quantitative imaging approaches to study the CAR immunological synapse. Mol Ther. 2017;25(8):1757-68.
352. Heczey A, Louis CU, Savoldo B, Dakhova O, Durett A, Grilley B, et al. CAR T Cells Administered in Combination with Lymphodepletion and PD-1 Inhibition to Patients with Neuroblastoma. Molecular therapy : the journal of the American Society of Gene Therapy. 2017;25(9):2214-24.
353. Uchibori R, Teruya T, Ido H, Ohmine K, Sehara Y, Urabe M, et al. Functional Analysis of an Inducible Promoter Driven by Activation Signals from a Chimeric Antigen Receptor. Molecular Therapy-Oncolytics

2019;12:16-25.
354. Adams S, Goldstein LJ, Sparano JA, Demaria S, Badve SS. Tumor infiltrating lymphocytes (TILs) improve prognosis in patients with triple negative breast cancer (TNBC). Oncoimmunology. 2015;4(9):e985930.
355. Buisseret L, Garaud S, de Wind A, Van den Eynden G, Boisson A, Solinas C, et al. Tumor-infiltrating lymphocyte composition, organization and PD-1/PD-L1 expression are linked in breast cancer. Oncoimmunology. 2017;6(1):e1257452.
356. Wherry EJ. T cell exhaustion. Nature immunology. 2011;12(6):492-9.
357. Wherry EJ, Blattman JN, Murali-Krishna K, Van Der Most R, Ahmed R. Viral persistence alters CD8 T-cell immunodominance and tissue distribution and results in distinct stages of functional impairment. Journal of virology. 2003;77(8):4911-27.
358. Datar IJ, Sanmamed MF, Wang J, Henick BS, Choi J, Badri T, et al. Expression analysis and significance of PD-1, LAG-3 and TIM-3 in human non-small cell lung cancer using spatially-resolved and multiparametric single-cell analysis. Clin Cancer Res. 2019:clincanres. 4142.2018.
359. Tchou J, Zhao Y, Levine BL, Zhang PJ, Davis MM, Melenhorst JJ, et al. Safety and efficacy of intratumoral injections of chimeric antigen receptor (CAR) T cells in metastatic breast cancer. Cancer immunology research

2017;5(12):1152-61.
360. Nanda R, Chow LQ, Dees EC, Berger R, Gupta S, Geva R, et al. Pembrolizumab in patients with advanced triple-negative breast

cancer: phase Ib KEYNOTE-012 study. Journal of clinical oncology : official journal of the American Society of Clinical Oncology. 2016;34(21):2460-7.
361. Cyprian FS, Akhtar S, Gatalica Z, Vranic S. Targeted immunotherapy with a checkpoint inhibitor in combination with chemotherapy: A new clinical paradigm in the treatment of triple-negative breast cancer. Bosnian journal of basic medical sciences. 2019.
362. Iorns E, Drews-Elger K, Ward TM, Dean S, Clarke J, Berry D, et al. A new mouse model for the study of human breast cancer metastasis. PloS one. 2012;7(10):e47995.
363. Arlauckas SP, Garris CS, Kohler RH, Kitaoka M, Cuccarese MF, Yang KS, et al. In vivo imaging reveals a tumor-associated macrophage–mediated resistance pathway in anti–PD-1 therapy. Science translational medicine. 2017;9(389):eaal3604.
364. Balyasnikova IV, Wainwright DA, Solomaha E, Lee G, Han Y, Thaci B, et al. Characterization and immunotherapeutic implications for a novel antibody targeting interleukin (IL)-13 receptor alpha2. The Journal of biological chemistry. 2012;287(36):30215-27.
365. Gargett T, TRUONG N, EBERT LM, YU W, BROWN MPJC. Optimization of manufacturing conditions for chimeric antigen receptor T cells to favor cells with a central memory phenotype. Cytotherapy. 2019.
366. Guedan S, Posey Jr AD, Shaw C, Wing A, Da T, Patel PR, et al. Enhancing CAR T cell persistence through ICOS and 4-1BB costimulation. JCI insight. 2018;3(1).
367. Rafiq S, Yeku OO, Jackson HJ, Purdon TJ, van Leeuwen DG, Drakes DJ, et al. Targeted delivery of a PD-1-blocking scFv by CAR-T cells enhances anti-tumor efficacy in vivo. Nature biotechnology. 2018.
368. Yoda A, Oishi I, Minami Y. Expression and function of the Ror ‐ family receptor tyrosine kinases during development: lessons from genetic analyses of nematodes, mice, and humans. Journal of receptors

signal transduction

2003;23(1):1-15.
369. Srivastava S, Salter AI, Liggitt D, Yechan-Gunja S, Sarvothama M, Cooper K, et al. Logic-Gated ROR1 Chimeric Antigen Receptor Expression Rescues T Cell-Mediated Toxicity to Normal Tissues and Enables Selective Tumor Targeting. Cancer cell. 2019;35(3):489-503.e8.
370. Li S, Siriwon N, Zhang X, Yang S, Jin T, He F, et al. Enhanced cancer immunotherapy by chimeric antigen receptor–modified T cells engineered to secrete checkpoint inhibitors. Clin Cancer Res. 2017;23(22):6982-92.

371. Ahn E, Araki K, Hashimoto M, Li W, Riley JL, Cheung J, et al. Role of PD-1 during effector CD8 T cell differentiation. Proceedings of the National Academy of Sciences. 2018;115(18):4749-54.
372. Moon EK, Wang LC, Dolfi DV, Wilson CB, Ranganathan R, Sun J, et al. Multifactorial T-cell hypofunction that is reversible can limit the efficacy of chimeric antigen receptor-transduced human T cells in solid tumors. Clin Cancer Res. 2014;20(16):4262-73.
373. Choi MY, Widhopf II GF, Ghia EM, Kidwell RL, Hasan MK, Yu J, et al. Phase I trial: cirmtuzumab inhibits ROR1 signaling and stemness signatures in patients with chronic lymphocytic leukemia. cell stem cell. 2018;22(6):951-9. e3.
374. James SE, Greenberg PD, Jensen MC, Lin Y, Wang J, Till BG, et al. Antigen sensitivity of CD22-specific chimeric TCR is modulated by target epitope distance from the cell membrane. J Immunol. 2008;180(10):7028-38.
375. Hartmann J, Schüßler‐Lenz M, Bondanza A, Buchholz CJJEmm. Clinical development of CAR T cells—challenges and opportunities in translating innovative treatment concepts. EMBO. 2017;9(9):1183-97.
376. Wallstabe L, Göttlich C, Nelke LC, Kühnemundt J, Schwarz T, Nerreter T, et al. ROR1-CAR T-cells are effective against lung and breast cancer in advanced microphysiologic 3D tumor models. JCI insight. 2019.
377. van de Wetering M, Francies HE, Francis JM, Bounova G, Iorio F, Pronk A, et al. Prospective derivation of a living organoid biobank of colorectal cancer patients. Cell. 2015;161(4):933-45.
378. Lancaster MA, Knoblich JAJS. Organogenesis in a dish: modeling development and disease using organoid technologies. Science. 2014;345(6194):1247125.
379. Brooks DG, Ha S-J, Elsaesser H, Sharpe AH, Freeman GJ, Oldstone MB. IL-10 and PD-L1 operate through distinct pathways to suppress T-cell activity during persistent viral infection. Proceedings of the National Academy of Sciences. 2008;105(51):20428-33.
380. Li A, Walling J, Kotliarov Y, Center A, Steed ME, Ahn SJ, et al. Genomic changes and gene expression profiles reveal that established glioma cell lines are poorly representative of primary human gliomas. Molecular Cancer Research. 2008;6(1):21-30.
381. Dai X, Cheng H, Bai Z, Li J. Breast cancer cell line classification and its relevance with breast tumor subtyping. Journal of Cancer. 2017;8(16):3131.
382. Siolas D, Hannon GJ. Patient-derived tumor xenografts: transforming clinical samples into mouse models. Cancer research. 2013;73(17):5315-9.
383. Lin H, Wei S, Hurt EM, Green MD, Zhao L, Vatan L, et al. Host expression of PD-L1 determines efficacy of PD-L1 pathway blockade–mediated tumor regression. J Clin Invest. 2018;128(2):805-15.
384. Finger LR, Pu J, Wasserman R, Vibhakar R, Louie E, Hardy RR, et al. The human PD-1 gene: complete cDNA, genomic organization,

and developmentally regulated expression in B cell progenitors. gene. 1997;197(1-2):177-87.
385. James B Rottman KG, Brenna Daly, Holly M. Horton, Kevin M. Friedman, Molly Perkins, Shannon Grande, Claire J Rhodes, Richard A. Morgan and Christopher J. Horvath. ROR1-Directed Chimeric Antigen Receptor T Cell Recognition of Self-Antigen Is Associated with Acute Toxicity, T Cell Dysfunction, and Poor Tumor Control. Blood. 2017;130(Suppl 1):4550.
386. Pimentel H, Jarnagin H, Zong H, Todorov C, Ganley K, Eng F, et al. Preclinical safety, biodistribution, and tumor infiltration analysis of CAR T cell targets using in situ hybridization technology. AACR: AACR; 2019.
387. Specht J, Lee S, Turtle C, Berger C, Balakrishnan A, Srivastava S, et al. Abstract P2-09-13: A phase I study of adoptive immunotherapy for ROR1+ advanced triple negative breast cancer (TNBC) with defined subsets of autologous T cells expressing a ROR1-specific chimeric antigen receptor (ROR1-CAR). AACR; 2019.
388. Ying Z, Huang XF, Xiang X, Liu Y, Kang X, Song Y, et al. A safe and potent anti-CD19 CAR T cell therapy. Nature medicine. 2019:1.
389. Minn I, Huss DJ, Ahn H-H, Chinn TM, Park A, Jones J, et al. Imaging CAR T cell therapy with PSMA-targeted positron emission tomography. Science advances. 2019;5(7):eaaw5096.
390. Meir R, Shamalov K, Betzer O, Motiei M, Horovitz-Fried M, Yehuda R, et al. Nanomedicine for cancer immunotherapy: tracking cancer-specific T-cells in vivo with gold nanoparticles and CT imaging. ACS nano. 2015;9(6):6363-72.